# Environmental Risk Assessment Resulting from the Discharge of Scrubber Wash Water into a Marine Environment

## Port of Tubarão and Coastal Region / Espírito Santo (ES)

**TECHNICAL REPORT**

2024

**Prepared by:**
CLS Brasil

CLS Brasil
Rio Branco Av., 311/1205 - Center
20.040-009 - Rio de Janeiro - RJ
Tel./Fax + 55 21 2532.5666
clsbrasil.com

# Technical team

Ana Carolina Rochinha Boechat
Registration with the Class Council: Not applicable
Federal Technical Register of Environmental Defense Activities and Instruments: 4961307
Responsible for Section(s): Wash water dispersion modeling

Signature:

Gabriel Medeiros Zielinsky
Registration with the Class Council: Not applicable
Federal Technical Register of Environmental Defense Activities and Instruments: 8119469
Responsible for Section(s): Hydrodynamic modeling

Signature:

João Vitor Carvalho Deboni
Registration with the Class Council: Not applicable
Federal Technical Register of Environmental Defense Activities and Instruments: 8295668
Responsible for Section(s): Wash water dispersion modeling

Signature:

Leonardo Maturo Marques da Cruz
Registration with the Class Council: AOCEANO 1237
Federal Technical Register of Environmental Defense Activities and Instruments: 252527
Responsible for Section(s): Revision and Approval of the Report

Signature:

Luiza Peiter de Barros Barreto
Registration with the Class Council: Not applicable
Federal Technical Register of Environmental Defense Activities and Instruments: 7437543
Responsible for Section(s): Target Lipid Model (TLM); Wash water dispersion modeling

Signature:

Marcelo Montenegro Cabral
Registration with the Class Council: 2010110225 - CREA/RJ
Federal Technical Register of Environmental Defense Activities and Instruments: 5621594
Responsible for Section(s): Revision and Approval of the Report

Signature:

Paula Vieira Castellões

Registration with the Class Council: 29.526/02 - CRBio

Federal Technical Register of Environmental Defense Activities and Instruments: 216354

Responsible for Section(s): Literature review and secondary data analysis

Signature:

# Summary

# Executive Summary

The study summarized here aims to contribute to the current discussion on the impacts on port waters, coastal waters and offshore waters in general, resulting from the discharges of washing water from ship Exhaust Gas Cleaning Systems (EGCS*)*, known as Scrubbers.

The practice of using Scrubbers has been widely used to control sulfur oxides (SOx) levels in compliance with MARPOL regulation 14 (Annex VI of 2008), which limits the sulfur content in fuel oil used in ships from 3.5% to 0.5%. This regulation has been required by the IMO (*International Maritime Organization*) since January 2020.

In addition to SOx, Scrubbers also remove other harmful air emissions such as particulate matter (PM) and PAHs (Polycyclic Aromatic Hydrocarbons) from the exhaust. When an EGCS is operated in so-called open-*loop mode*, the scrubbing water is discharged into the sea, sometimes after filtration and buffering with seawater, known as EGSE (*Exhaust Gas Scrubber Effluent*).

At its seventy-eighth session, the Marine Environment Protection Committee approved the 2022 Guidelines for assessing the risks and impacts of discharge water from EGCS (MEPC.1/Circ.899). These guidelines recommend a methodology for evaluating its environmental risks and impacts. They aim to provide a unified scientific approach to risk assessment, enabling evidence-based decision-making and justification before implementing local restrictions on the use of EGCS.

Initially, considering these guidelines and local and regional conditions, CLS Brasil conducted an assessment of the potential impacts of Scrubber wash water discharge at sea for the Port of Tubarão/ES and its navigation route, Asia-Brazil, using numerical computer modeling (Vale & CLS Brasil, 2024). This study used data obtained by the characterization of Scrubber effluents (SGS, 2022), in addition to several secondary data sources for environmental characterization. In this work, two distinct aspects were focused on:

- Changes in water and sediment quality, with the MAMPEC model (DELTARES, 2016), evaluating changes in expected concentrations of PAHs (Polycyclic Aromatic Hydrocarbons) and metals;
- Changes in pH and alkalinity, with the AquaEnv model (Hofmann *et al.*, 2010).

In Vale & CLS Brasil (2024), no significant changes in water and sediment quality were predicted, taking as reference the quality standards established by CONAMA Resolutions No. 357/05 and No. 454/12, respectively. Regarding acidification, the simulations carried out with the AquaEnv model also indicated practically insignificant changes.

In turn, the present study represents an advance in studies already carried out. The potential impacts of the discharge of Scrubber wash water are predicted based on an environmental risk assessment that considers the potential toxicity of the effluent, not limited to selected substances. In this way, it is possible to carry out a comprehensive assessment of the whole effluent (WEA, *Whole Effluent Assessment,* OSPAR Commission, 2005) and not only the concentrations of known substances in the environment, listed in MEPC.259(68). This also includes the analysis of the toxic effects of unknown substances, in addition to the synergistic effects between all components of the effluent, according MEPC.1/Circ.899 guidelines.

To this end, the present study was based on the following steps:

- Literature review related to the discharge of wash water from Scrubbers into the marine environment;
- Analysis of secondary data on the ecotoxicity of EGSE in an open-loop system, as published in scientific articles and/or technical reports;
- Application of the Target Lipid Model (TLM) methodology to assess the toxic potential of Scrubber wash water;
- Definition of Predicted No-Effect Concentration (PNEC) for environmental risk assessment;
- Hydrodynamic computational modeling in the coastal region of the Port of Tubarão, with the Delft3D model (Deltares, 2021), and in the offshore region to characterize the navigation route, with ROMS (Regional Ocean Modeling System) (Haidvogel *et al.*, 2008).
- Computational modeling of wash water dispersion in a marine environment, using the DREAM (Dose-Related Exposure Assessment Model) model (Reed & Hetland, 2002), evaluating effluent dispersion both in the coastal region and in shipping routes.

The assessment of the toxicity of Scrubber wash water effluent is based on the Predicted No-Effect Concentration (PNEC). The PNEC is defined as the concentration below which no adverse effects on the aquatic environment are expected (ECHA, 2008).

To further assess the toxic potential of Scrubber wash water, the **Target Lipid Model (TLM)** modeling methodology was used. TLM is a Quantitative Structure-Activity Relationship (QSAR) mathematical model. These models are typically used to relate toxic effect levels to properties such as the octanol-water partition coefficient $K_{ow}$ (e.g., Mccarty & Mackay, 1993). TLM assesses the aqueous toxicity of Type 1 narcotics, which are nonpolar organic chemicals such as PAHs that are toxic through accumulation in the lipids of organisms, resulting in narcosis. As discussed in the scientific literature, chemical-based toxicity predictions, such as TLM, may overestimate cumulative risks when compared to results observed in empirical toxicity tests performed in the laboratory. The TLM was applied using as *input* data the concentrations of PAHs measured in 30 Scrubber wash water samples from 5 different vessels in Brazil and Singapore by SGS - Global Marine Services (SGS, 2022). The results of this application are expressed in toxic units (TU) and represent a metric to assess the variation in effluent toxicity at various engine power levels and locations where the samples were collected. Although not directly comparable with ecotoxicity data obtained in laboratory tests, the TU results obtained with the TLM serve as an assessment of the toxic potential of effluents. To assess the ecotoxicological effects, a risk concentration that protects 95% of the species from 7 different taxonomic groups was used, following the REACH (European Registration, Evaluation, Authorization and Restriction of Chemicals) guidelines. The low engine power data are associated with the berthing situation in ports, while the higher power data are associated with discharge situations along shipping routes. The effluents were analyzed for 11 PAHs, with results for acute and chronic toxicity. No evidence of acute toxic effects was found in any of the scenarios analyzed. In a low engine power situation, no potential chronic effect of the effluents was detected either. However, along the shipping route, four effluents showed evidence of chronic toxicity, suggesting a potential toxic effect of 50% on organisms in the vicinity of the discharge.

**To obtain PNEC values for the whole effluent**, we started from a compilation of secondary data on EGSE ecotoxicity results organized according to the trophic level of the test organism used. In the literature, there is a wide range of EGSE ecotoxicity test results available, and for this study, those that consolidate from median lethal concentration (when 50% of the tested organisms die in a given period) to sub-lethal effects were selected. The consolidation of results respected the premise considered most conservative, selecting the worst results among those analyzed, regardless of whether they were acute or chronic thresholds.

Among all the results compiled from the literature, the most critical EGSE concentration value that causes adverse effects in at least 10% of the tested population was 1%. The ecotoxicity results are expressed in effluent concentrations, while defining a PNEC requires conversion.

The reference PNEC for this study was calculated following the guidance of the European Chemicals Agency (ECHA) in Chapter 10 (Characterization of dose-response for environment) of the guidance document on information requirements and chemical safety assessment (ECHA, 2008). According to the ECHA document, since the conditions of laboratory test methods differ from natural conditions, it is considered more likely that ecosystems are more sensitive to chemicals than individual organisms in the laboratory. Therefore, test results are not used directly for risk assessment, and these should be assessed by extrapolating to natural conditions. In this work, the assessment factor method was used. The general principle of this method is that the toxic concentration results of the laboratory results are divided by an assessment factor suggested in the ECHA document. The scarcer the data, the higher the assessment factor. The PNEC is estimated by dividing the lowest toxic concentration value found by the indicated assessment factor. Following these guidelines, the lowest toxic concentration found, 1%, was divided by the assessment factor of 100. This value is recommended for the case of predicted concentration of no observed effect of long-term toxicity (e.g., EC10 or NOEC) of three freshwater or saltwater species (usually algae and/or crustaceans and/or fish) representing three trophic levels. Thus, **the reference PNEC adopted in this work was 0.01% (10,000-fold dilution).** The same value was used for the shipping route situations and for the situation of a ship berthed in port. It should be noted that this threshold is conservative, since it is a value derived from the most toxic concentration found.

The assessment of environmental risks is based on the PEC/PNEC ratio, where PEC (Predicted Environmental Concentration) is the concentration of the Scrubber wash water in the sea calculated after its dilution by the turbulent transport and dispersion processes. This type of assessment is valid for substances that cause effects through direct exposure through a dissolved or diluted phase in water. The methodology is used by SINTEF to characterize environmental risks in the DREAM model. This methodology assumes that if PEC=PNEC (or PEC/PNEC=1) the environmental risk is 5%, assuming that 5% of the species may be affected. This is based on species sensitivity distribution relationships with the PEC/PNEC ratio that can be found in scientific literature.

Scrubber wash water concentrations at sea, or PEC, were calculated through simulations of effluent dispersion at sea performed with DREAM, a model developed by SINTEF (http://www.sintef.no/) for calculating fluid transport at sea. The simulations considered hypothetical discharges inside the sheltered area and in two positions on the navigation route of the Port of Tubarão, Vitória-ES.

To obtain the currents inside the Port of Tubarão and surrounding areas, a **hydrodynamic modeling study was conducted** covering the region of Vitória and Espírito Santo Bay. For this purpose, the Delft3D model was used, an advanced tool for simulating multidimensional hydrodynamic flows and transport phenomena. The model was fed with bathymetric data obtained from nautical charts, tidal data from global tidal models, river flows obtained from databases of the Brazilian National Water Agency (ANA) and winds from the Brazilian National Institute of Meteorology (INMET). To properly represent various environmental conditions, a 1-year simulation period was defined (January to December 2012). The results indicated a predominance of currents forced by the tides, especially inside the estuaries and in the sheltered area of the Port of Vitória. Within the sheltered area of the port, the currents are very low, with values between 1 and 5 cm/s. This condition is quite unfavorable for the dispersion of pollutants discarded in this region, as they tend to remain in high concentrations, without mixing with the water surrounding the port.

To obtain the current regime in the offshore region, a hydrodynamic modeling study was used with the ROMS model. The model was configured to simulate the currents in the region over a 3-year period, between January 2012 and December 2014. The temporal extension was sufficient to reproduce the ocean circulation in the region, with the observation of the main features, such as the Brazil Current, and its spatiotemporal variations, considering seasonal changes, such as meanders and eddies. The results were validated with *in-situ* and remote sensing data. In the continental shelf region, the currents have a magnitude of up to 110 cm/s, while in the deeper ocean region, the currents have a magnitude of approximately 70 cm/s.

In the **simulations of dispersion of Scrubber wash water at sea,** for the coastal and offshore routes, discharges were considered with the vessel moving at a speed of 13.5 knots towards the port. For the discharge simulations at the Port of Tubarão, discharge in a fixed position for 15 uninterrupted days was considered, assuming that this would be the maximum stay of a ship in the port.

In the case of **discharges along shipping routes**, both in the coastal region and in the deeper region (offshore), concentrations of 0.01% (or PEC/PNEC=1 and environmental risk 5%) are associated with exposure times on the order of minutes and will possibly undergo dilution shortly after the ship passes. It is worth noting that in these simulations the effect of turbulence induced by the vessel's propeller and movement are not considered. Thus, it is possible to conclude that the chronic toxic effects and consequent environmental risks resulting from these discharges along shipping routes are practically non-existent.

For **discharges in the Port of Tubarão** region, simulations using the DREAM model indicated an environmental risk of 5% (i.e., 5% of species could be affected) at approximately 4 km from the discharge point. However, it is important to highlight that these conclusions stem from the fact that the same PNEC was applied to both the navigation route scenarios, with high engine power, and to a situation where a ship is berthed in the port. While the TLM model could calculate the potential toxic effect on effluents for different engine power levels, among the references considered for assessing the ecotoxicity of the whole effluent, no available results allowed for a direct comparison of effluent generated at different engine powers. Although conservative, it is crucial to note that considering a single PNEC for different engine powers is unrealistic, especially for a scenario where a ship is berthed at the port with minimal operation. Thus, it is understood that the area with significant environmental risks due to the toxicity of Scrubbers wash water may be much more restricted to the vicinity of ships berthed at the Port of Tubarão than the 4 km estimated in this study. Even considering the low toxicity of the effluent compared to the dilution capacity of the medium, there is concern about the bioaccumulation of contaminants, especially in the port region, if this effluent is discharged in the region. On coastal and offshore routes, this concern is considerably reduced. However, on these routes, the synergistic effect of vessel traffic must be considered. In any situation, the biodegradation capacity of this effluent must be clearly and thoroughly assessed, even to be able to consider or not the effects of bioaccumulation.

Finally, it is recommended that the decision to release or not the discharge of Scrubbers wash water in the port region be preceded by the implementation of an environmental characterization project to evaluate the region, especially the hydrocarbonoclastic biota. In addition, an environmental monitoring project should be implemented to evaluate the possible effects of these discharges. The results of the dispersion modeling of the plume obtained in this study can be used as a reference for the design of the sampling grid for this monitoring.

# 1. Introduction

This study aims to contribute to the current discussion on the impacts on the marine environment resulting from the discharge of washing water from ship exhaust gas cleaning systems (EGCS), known as Scrubbers.

To limit impacts, since January 2020, the IMO (International Maritime Organization) has required compliance with MARPOL regulation 14 (Annex VI, 2008). This regulation limits the sulfur content in ship fuel oil to 3.5% to 0.5%. The practice of using Scrubbers has been widely used as one of the options to control SOx emissions from vessels.

In addition to SOx, Scrubbers also remove other harmful air emissions from the exhaust, such as particulate matter (PM) and Polycyclic Aromatic Hydrocarbons (PAHs). When the EGCS is operated in open-loop mode, the wash water is discharged into the sea, sometimes after filtering and buffering with seawater.

At its seventy-eighth session, the Marine Environment Protection Committee approved the 2022 Guidelines for assessing the risks and impacts of discharge water from Exhaust Gas Cleaning Systems (MEPC.1/Circ.899). These guidelines recommend a methodology for evaluating the environmental risks and impacts of discharge water from Exhaust Gas Cleaning Systems (EGCS). They aim to provide a unified scientific approach to risk assessment, enabling evidence-based decision-making and justification before implementing local restrictions on the use of EGCS.

Initially, considering these guidelines and local and regional conditions, CLS Brasil conducted an assessment of the potential impacts of Scrubber wash water discharge at sea for the Port of Tubarão/ES and its navigation route, Asia-Brazil, using numerical computer modeling (Vale & CLS Brasil, 2024). This study used data obtained in SGS (2022), in addition to several secondary data sources for environmental characterization. In this work, two distinct aspects were focused on:

- Changes in water and sediment quality, with the MAMPEC model (DELTARES, 2016), evaluating changes in expected concentrations of PAHs and metals;
- Changes in pH and alkalinity, with the AquaEnv model (Hofmann *et al.*, 2010).

In the previous study, no significant changes in water and sediment quality were predicted, based on the standards established by CONAMA Resolutions No. 357/05 and No. 454/12, respectively. Regarding acidification, simulations conducted with the AquaENV model also indicated practically insignificant changes.

In this new study, the focus is on environmental risk assessment, considering the potential toxicity of the effluent in a comprehensive manner, without limiting it to specific substances. While the previous study focused on specific compounds, such as PAHs and metals, here a whole effluent assessment is carried out (*WEA*, according to the OSPAR Commission, 2005). With this expanded approach, the analysis of the toxic effects of unknown substances is also considered, as well as the synergistic effects between all components of the effluent, according to MEPC.1/Circ.899 guidelines.

The present study was based on the following steps:

- Literature review related to the discharge of wash water from Scrubbers into the marine environment;
- Analysis of secondary data on the ecotoxicity of EGSE in an open-loop system, as published in scientific articles and/or technical reports;
- Application of the Target Lipid Model (TLM) methodology to assess the toxic potential of Scrubber wash water;
- Definition of Predicted No-Effect Concentration (PNEC) for environmental risk assessment;
- Hydrodynamic computational modeling in the coastal region of the Port of Tubarão, with the Delft3D model (DELTARES, 2021), and in the offshore region to characterize the navigation route, with ROMS (Regional Ocean Modeling System) (Haidvogel *et al.*, 2008).
- Computational modeling of wash water dispersion in a marine environment, using the DREAM (Dose-Related Exposure Assessment Model) model (Reed & Hetland, 2002), evaluating effluent dispersion both in the coastal region and in shipping routes.

The study area was maintained in the Port of Tubarão, as defined in Vale & CLS Brasil (2024). Located on the southeast coast of Brazil, it is a port area with intense vessel traffic, covering important navigation routes for access to the port.

# 2. Effluent Ecotoxicity

To assess the ecotoxicity of the effluent (Exhaust Gas Scrubber Effluent, EGSE), meeting the project objectives, two different approaches were used: literature review and TLM (Target Lipid Model). Some general premises guided the selection of references and data to be considered.

It should be clarified that in the literature survey to define the state of the art and throughout the text of this report, only EGSE results of open-loop systems were considered, in accordance with the study's objective.

In this report, whenever possible, the analyses and considerations on the EGSE were carried out respecting the structure adopted in Vale & CLS Brasil (2024): low power (vessel moored in port), medium power (vessel on coastal shipping route), and high power (vessel on offshore shipping route). In cases where this subdivision was not possible, due to the lack of reference, for example, as a more conservative approach, the worst results among all those available in literature were considered. There are not many references that address the distinction between low and high engine power, although it is recognized that the composition of the effluent is directly related to engine power. Only the studies by Kamper *et al.* (2021) and Word *et al.* (2004), among those considered, highlighted the importance of this categorization. Among them, Word *et al.* (2024) stands out for adopting an approach more aligned with our categorization, evaluating samples they consider representative of port conditions (~50% engine power) and in open-sea transit (>70%). However, their definition of port conditions involves a considerably higher engine power (~50%), which differs from our port category, where minimal engine use is assumed.

The information available in the literature in reports and scientific papers on EGSE between 2005 and 2024 was collected, with presentation of chemical characterization (inlet water and effluent), comparisons of the effluent generated by different EGCS (Exhaust Gas Cleaning Systems*) models,* and assessments of the ecotoxicity of the effluent as a whole at different trophic levels, summarized in the following table (Table 1).

Table 1: Brief description of the references considered on open-loop EGCS, indicating those that present results of chemical characterization of EGSE and those that present results of ecotoxicological tests of EGSE. Source: CLS Brasil.

| References considered on EGCS open-loop and EGSE | | | | |
|---|---|---|---|---|
| # | reference (citation) | brief description of the content | chemical characterization of EGSE | ecotoxicity of EGSE |
| 1 | Hufnagl *et al.* (2005) | assessment of EGSE discharge on port ecosystems, without verification of adverse effects after periodic campaigns for one year and assessments that included bioaccumulation in mussels | X | X |
| 2 | Hansen (2012) | report on EGCS operating in different modes and characterizing the effluents generated and indicating special attention to PAHs | X | |
| 3 | Lange *et al.* (2015) | assessment of the impacts of EGSE discharge in ports and coastal waters, considering chemical composition, discussed in light of different regulatory instruments, mainly considering persistent pollutants | X | |
| 4 | Koski *et al.* (2017a) | publication warning of synergistic effects of EGSE discharge on plankton productivity and metal bioaccumulation, although dilution in the marine environment should be considered, extensive literature review on toxic effects of different compounds found in EGSE | X | X |
| 5 | Koski *et al.* (2017b) | evaluation of the ecotoxicity of EGSE in two species of planktonic copepods and concluding that the impact of EGSE discharge must be assessed on a case-by-case basis, since in certain places and situations it may be the last drop to induce an unfavorable change in the ecosystem | | X |
| 6 | Magnusson *et al.* (2018) | assessment of the environmental risks of EGSE discharge, concluding that the ecotoxicity of this effluent is the result of a "cocktail effect" and that it should not be assessed solely by prediction models based separately on the concentrations of the compounds found in the effluent | | X |
| 7 | Koyama *et al.* (2018) | report by the Japanese expert council concluding that the risks from EGSE discharge are negligible in the short and long term, although they are unacceptable for the water quality of coastal areas due to bioaccumulation | | X |
| 8 | Ytreberg *et al.* (2019) | assessment of the impact of EGSE discharge on Baltic Sea microplankton and involving a mesocosm experiment | X | X |
| 9 | Gadd *et al.* (2020) | risk assessment of EGSE discharge based on secondary data available in the literature, which provides excellent discussions on the topic and indicates more sensitive areas in New Zealand where discharge should be avoided | | |
| 10 | Teuchies *et al.* (2020) | publication in the journal Environmental Sciences Europe , which discusses concerns about the impacts of EGSE | X | |

References considered on EGCS open-loop and EGSE

| # | reference (citation) | brief description of the content | chemical characterization of EGSE | ecotoxicity of EGSE |
|---|---|---|---|---|
| | | discharge, discouraging disposal in coastal and estuarine waters | | |
| 11 | Schmolke *et al.* (2020) | assessment of the environmental risk of EGSE discharge from the combination of modeled data, concluding that in areas with low water exchange and high ship traffic there may be an accumulation of pollutants in the marine environment | X | |
| 12 | Eldridge *et al.* (2021) | critical review of the availability, reliability and ecological relevance of Arctic species toxicity tests for use in environmental risk assessment | | |
| 13 | Kamper *et al.* (2021) | assessment of the ecotoxicity and environmental risks of EGSE discharge of open-loop EGCS and concluding that it is an acceptable risk after evaluating the PEC/PNEC ratio | X | X |
| 14 | Thor *et al.* (2021) | evaluation of the ecotoxicological effects of EGSE, introducing the term “witches' cauldron” for the action of EGCS on the effluent, not only due to the synergy of the compounds, but also due to the generation of compounds about which we know very little | | X |
| 15 | Ytreberg *et al.* (2021a) | discussion about the valuation of the environmental impacts of ship emissions from a marine perspective | | |
| 16 | Ytreberg *et al.* (2021b) | assessment of the impact of EGSE discharge on a summer bloom event in the Baltic Sea, with regard to biological effects (e.g. microplankton species composition, biovolume and primary productivity) and chemical parameters | X | X |
| 17 | Martínez-López *et al.* (2022) | assessment of the environmental impact of EGSE discharge compared to atmospheric emissions, concluding that toxic atmospheric emissions were greater than those from EGSE discharge, and that the open-loop model presented lower risks to eutrophication due to $N_{tot}$ | X | |
| 18 | Picone *et al.* (2023) | assessment of the impact of EGSE on planktonic biological indicators, showing that it can have adverse effects on the entire life cycle of marine organisms, probably due to the synergy of the effluent components and discussing the sublethal effects that affect feeding of early life stages and reproductive success | X | X |
| 19 | Word *et al.* (2024) | assessment of the ecological risk of EGSE discharge using different methods, concluding that, contrary to what was predicted by the TLM model, ecotoxicological tests indicate minimal ecological risks, as predicted by the CORMIX and MAMPEC models | X | X |

These references, or part of them, served as a comparative and defining basis for the toxic effect of the different compounds present in the EGSE and the ecotoxicity of the whole effluent.

However, the chemical characterization of EGSE adopted in this report considers the primary data obtained in SGS (2022), both in Brazil and Singapore. Aiming at conservatism, the *open-loop* EGSE results obtained were considered, even though significant geographical differences were observed in the quality of the inlet water in the system, as shown in the following graphs. In Figure 1, the blue bars represent the range of variation of the inlet water quality results, by engine power, or as a whole (considering minimum, median and maximum of all data).

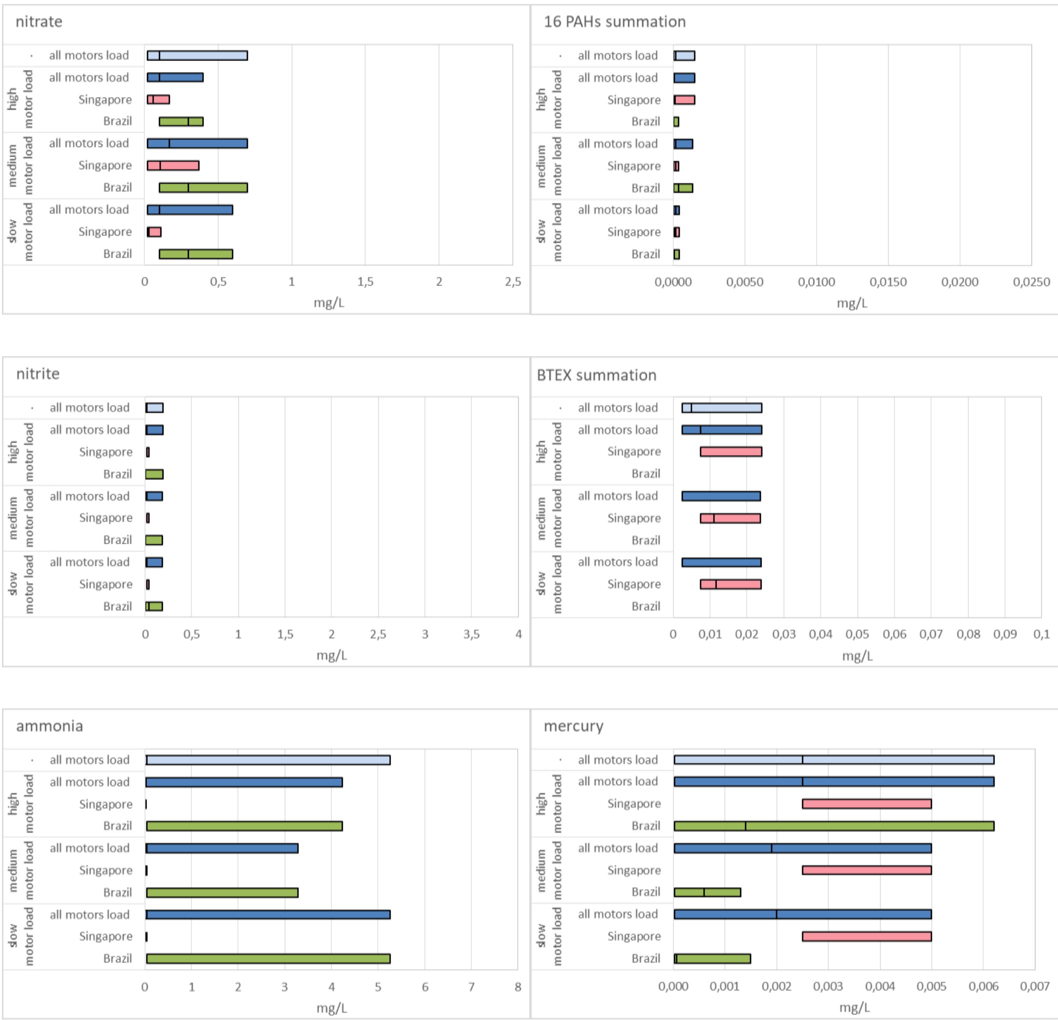


Figure 1: Range of variation of inlet water quality results, by engine power, or as a whole (considering minimum, median and maximum of all data), enabling comparisons between data obtained in Brazil and Singapore. Source: CLS Brasil.

The use of the Target Lipid Model (TLM) adds a new perspective to the assessment of the ecotoxicity of EGSE effluent. Its objective is to characterize the toxicity of the effluent itself, using mathematical modeling that considers its composition. This method allows not only to measure the toxicity of the effluent, but also to identify the most ecologically harmful chemical compounds at the time of discharge, without considering interactions with seawater, such as dilution and dispersion, and only the chemical properties of the compounds.

Thor *et al.* (2020) describe the interaction of Polycyclic Aromatic Hydrocarbons (PAHs) in the effluent as highly toxic, referring to this mixture as a "witch's cauldron", not only due to the synergy of the compounds, but also due to the generation of compounds about which we know very little. In the literature, this synergistic effect of the chemical composition of the EGCE is also known as the "cocktail effect" (Magnusson *et al.*, 2018). These interactions depend on several factors, including the nature of the fuel, the lubricant used, the combustion process and the composition of the inlet water in the EGCS system (Teuchies *et al.*, 2020). Due to this, Magnusson *et al.* (2018) conclude that environmental risks should not be assessed only by predictive models based separately on the concentrations of the compounds found in the effluent, but also on the ecotoxicity of the whole effluent, which justifies the use of the two different approaches adopted in this study.

Since the TLM is a toxicological model, one of its variables depends on laboratory tests with the effluent on organisms from different taxonomic groups. However, in the absence of data on the effects of effluent on organisms, adaptations and simplifications were necessary, complemented by a bibliographic survey. The application of the TLM in the evaluation of EGSE is still limited, with the main reference for this study being the work of Word *et al.* (2024), already briefly described and yet to be detailed.

With the support of bibliographic research, we seek to measure the toxicity of effluent discharged into the marine environment, considering both existing records and the sample characterization methodology, providing subsidies for a careful evaluation of the toxic effect of EGSE.

## 2.1. TLM (Target Lipid Model)

To quantify the potential ecological risks of Scrubbers wash water, an analysis of the toxicity of the concentrations of Polycyclic Aromatic Hydrocarbons (PAHs) present in the wash water was conducted. For this purpose, the TLM (Target Lipid Model) method was used, a toxicity model based on sample composition, which will be presented in greater detail below.

### 2.1.1 Model Description

The TLM is a mathematical model of the QSAR (Quantitative Structure-Activity Relationship) type used to evaluate the aqueous toxicity of Type 1 narcotics, which are nonpolar organic chemicals – such as PAHs – whose mode of toxicity comes from their accumulation in the lipids of organisms, resulting in narcosis. Developed by Di Toro *et al*. (2000), the TLM assumes that the target lipid is the site of toxic action in the organism causing the acute effect of narcosis. The methodology developed by the authors allows the estimation of the toxicity of Type I narcotics based on their degree of solubility in lipid or water, expressed by the octanol-water partition coefficient, log(Kow). The octanol-water partition coefficient, or log(Kow), is an indicator of the relationship between lipophilicity (soluble in water) and hydrophilicity (soluble in water) of a chemical compound. Compounds with higher log(Kow) are more soluble in fat, and those with lower log(Kow) are more soluble in water. Di Toro *et al.* (2000) showed that it is possible to estimate toxicity due to the correlation between the exposure concentration of a chemical product necessary to induce an effect (in this case the LC50, the concentration causing 50% mortality of the organisms) and the log(Kow). The relationship between the two is linearly inverse and is the same for all species. This relationship was initially proven through a database of 156 chemicals and 33 species. In Figure 2, a portion of the results obtained is shown, where the same slope of the line between log(CL50) and log(Kow) is observed for all the species tested.

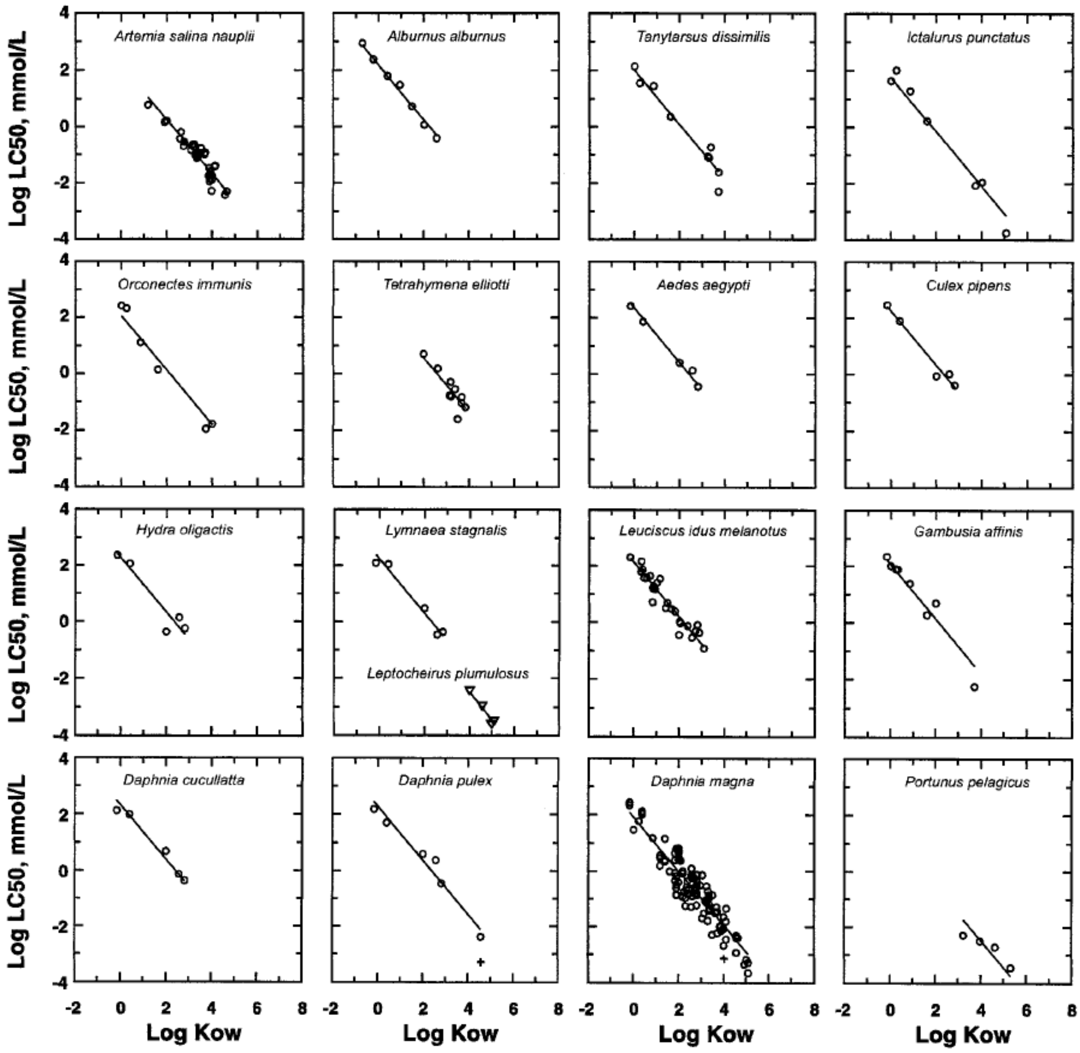


Figure 2: Relationship between log(CL50) and log(Kow) for different species. The lines have a constant slope of -0.970 and the y-intercept varies for each species. Source: Di Toro *et al.* (2000).

From this relationship, when log(Kow) = 0, the aqueous concentration is equal to the LC50 (intercept on the y-axis). This point is the Critical Target Lipid Body Burden (CTLBB). The CTLBB is the critical chemical concentration in the body's lipids required to achieve the observed effect (lethal or chronic) and is variable by species and chemical compound.

The TLM has been validated for both individual components and hydrocarbon mixtures (Grath *et al.al*. 2005). Updates include the inclusion of heterocyclic compounds (Grath *et al*., 2021) and other sensitive species (Grath *et al*., 2018) in the toxicity database, resulting in a current database of over 240 chemicals and 79 species from 8 taxonomic groups and adjusted fixed values.

In the method, toxicity is predicted for each PAH individually, according to the Equation 1 and Equation 2 presented below. The Equation 1 derives the acute aquatic critical concentration (LC50) of the compound, in this case, the PAH.

Equation 1: TLM equation that predicts the acute aquatic effect concentration (LC50).

$$\log(C^*_{L50}) = m\log(K_{ow}) + \log(C^*_{TLBB}) + \Delta c$$

where

- **Acute aqueous concentration ($C^*_{L50}$):** concentration causing 50% mortality in organisms (mmol/L);
- **Narcosis slope (m):** slope of the linear relationship between log(LC50) and log(Kow) and has a universal value equal to -0.94;
- **Octanol-water partition coefficient ($K_{ow}$):** indicates the relationship between the lipophilicity (lipid-soluble) and hydrophilicity (water-soluble) of the compound;
- **Target body lipid load ( $C^*_{TLBB}$):** chemical concentration in the body lipid required to achieve the observed effect (variable by species) (µmol/$g_{octanol}$);
- **Correction factor (Δc):** correction factor required for some classes of chemicals (mmol/L), specifically for monocyclic aromatic (-0.025), polycyclic aromatic (-0.364) and heterocyclic (-0.472) hydrocarbons (Grath *et al.* 2021).

Using the result of Equation 1, the Toxic Unit (TU) is calculated for each PAH. The TU is a metric for evaluating toxicity and consists of dividing the concentration of the compound in the effluent ($C_{measured}$ ; mmol/L) by the result of $C^*_{L50}$ obtained in the TLM, as shown in Equation 2.

Equation 2: Threshold predicted by TLM.

$$TU(individual) = \frac{C_{measured}}{TLM_{limit}}$$

To obtain the total TU of the effluent, the sum of the TU of each compound (Equation 3) is calculated, providing a metric for the exposure of the mixture.

Equation 3: TLM total toxic unit of the mixture.

$$TU(total) = \sum TU$$

The following applies:

→ If **TU ≥ 1, the mixture is considered toxic.**

Specifically:

- TU = 1, a 50% effect of the effluent on the organisms is expected
- TU = 2 is an indication that the substance is 2x more toxic than the safe threshold (and so on).

It is worth noting that a TU = 2 does not mean that the effluent will cause twice as much toxicity in organisms, as this depends on the organism's response curve to the dose.

However, these steps calculate the acute lethal concentration values in water. To obtain the chronic values, it is necessary to use an acute to chronic ratio factor, known as *the* Acute to Chronic Ratio (ACR). This number is usually obtained by analyzing pairs of acute and chronic laboratory data from different species on different chemicals. The geometric mean is calculated from the distribution of these values. Using data from 6 species and 20 chemicals, Di Toro *et al.* (2000) concluded that the ACR is independent of the chemical and species, since it does not show an apparent trend with the partition coefficient. Therefore, a single value can be applied to all species and chemicals.

It is worth highlighting some points regarding the use of TLM. Firstly, when applying the addition of effective concentrations (or individual TU), TLM assumes that each PAH acts independently, providing a super-conservative approach to the results obtained, since it disregards any interaction between the compounds that could result in a decrease in their concentration. Following this logic, dispersion and weathering processes are also disregarded.

Nevertheless, in the global context, TLM is widely used to predict the toxicity of petroleum components, such as hydrocarbons. Defined as one of the tools in the environmental risk assessment methodology, TLM is adopted by the US EPA (United States Environmental Protection Agency) and the ECHA (European Chemical Agency). Its structure was implemented in the PetroRisk and PetroTox models by Concawe, developed to assess the aquatic risk of petroleum-derived substances based on the substance composition.

Recently, the TLM has also been applied to assess the toxicity of Scrubbers wash water. In the study "Pudget Sound Exhaust Gas Cleaning System (EGCS) Washwater Ecological Risk Assessment" by Word *et al.* (2024), the model was one of the main tools to predict the toxicity of polycyclic aromatic hydrocarbons present in water from the discharge of EGCS from ships operating in Pudget Sound, located in Washington/United States. Although some pollutants exceeded environmental standards, the rapid dilution of the wastewater and empirical toxicity tests suggest a minimal ecological risk in the evaluated area.

Furthermore, the results obtained by the TLM are used to calculate the Predicted Non-Effect Concentration (PNEC), the concentration below which unacceptable effects on organisms are not expected. In practice, this concentration corresponds to the dilution to which the effluent must be subjected so that it does not present toxic effects to the environment.

### 2.1.2 Input Data

Within the scope of this study, the methodology was applied to 16 PAHs, identified by the US EPA as major pollutants. According to the MEPC 259 guidelines (68), these 16 PAHs are those that should be evaluated regarding monitoring the water quality of the discharge of Scrubbers wash water. A more explicit list of PAHs can be found in MEPC 340 (77). The composition of PAHs in the water may be related to the type of vessel engine, location, power, among others. Therefore, data from samples obtained by SGS-Global Marine Services were used to characterize Scrubbers effluents on 5 vessels in Brazil and Singapore (SGS, 2022). The characterization included 30 water samples at the equipment inlet and 30 EGCS discharge samples after gas scrubbing at three different engine power stages of the vessels (high, medium and low). Each vessel underwent 6 different tests, in 3 power stages and in 2 different locations. A total of 59 parameters were analyzed, generating 3,934 data. According to the study, around 64% of this total were levels below the minimum threshold of quantification of the analytical method adopted.

For the TLM, the output measurements of all vessels and powers were considered. Since the objective of applying this methodology is to characterize the effluent discharged by the *Scrubbers*, the samples were treated separately.

In total, **24 scenarios** were obtained:

→ 8 vessels (NSU C – Brazil and Singapore; YUAN HUA HAI – Brazil and Singapore; SOHAR MAX – Brazil and Singapore; ORE AMAZONAS and SOLAR FRONTIER); and

→ 3 powers (high, medium and low).

The nomenclature and designation given to the different powers is based on the characterization presented in Vale & CLS Brasil (2024):

→ Offshore Route (High Power): associated with Output 2 data,

→ Coastal Route (Medium Power): associated with Output 4 data; and

→ Port (Low Power): associated with Output 6 data.

### 2.1.3 Coefficients

As demonstrated in item 2.1.1, by Equation 1 to Equation 3, the TLM requires chemical and toxicological information for each PAH as input data. The values used and their justifications will be explained below.

To calculate the lethal concentration (Equation 1) of each hydrocarbon, three parameters are required: the partition coefficient (log(Kow)), the $C^{*}_{TLBB}$ and Δc.

The partition coefficient was obtained using the Epi Suite TM software version 4.11 (US Environmental Protection Agency, 2018; Meylan & Howard, 1999), which contains a revised database of more than 40,000 substances. The partition coefficients, along with the CAS number and molar mass of each substance are presented in Table 2. The CAS number (CAS-nr) is a unique number assigned to chemical substances by the US Chemical Abstracts Service (CAS). This way, each substance can be unambiguously identified by the scientific community. The molar mass, in turn, represents the mass in grams of a compound, and was used to convert the concentration of the samples from $g/m^3$ to $mol/m^3$.

Table 2: List of simulated PAHs and their respective parameters required for modeling. Kow = Octanol-water partition coefficient.

| PAH | CAS-nr | log(Kow) | Molar mass [g/mol] |
|---|---|---|---|
| Acenaphthene | 83-32-9 | 3.92 | 154.21 |
| Acenaphthylene | 208-96-8 | 3.94 | 152.20 |
| Anthracene | 120-12-7 | 4.45 | 178.20 |
| Benzo[a]anthracene 1.92E-06 | 56-55-3 | 5.76 | 228.29 |
| Benzo[a]pyrene | 50-32-8 | 6.13 | 252.30 |
| Benzo[b]fluoranthene | 205-99-2 | 5.78 | 252.30 |
| Benzo[g,h,i]perylene | 191-24-2 | 6.22 | 276.33 |
| Benzo[k]fluoranthene | 207-08-9 | 6.11 | 252.30 |
| Chrysene | 218-01-9 | 5.81 | 228.30 |
| Dibenzo[a,h]anthracene | 53-70-3 | 6.50 | 278.35 |
| Phenanthrene | 85-01-8 | 4.46 | 178.20 |
| Fluoranthene | 206-44-0 | 5.16 | 202.26 |
| Fluorene | 86-73-7 | 4.18 | 166.20 |
| Indeno[1,2,3,c,d]pyrene | 193-39-5 | 6.50 | 276.33 |
| Naphthalene | 91-20-3 | 3.30 | 128.19 |
| Pyrene | 129-00-0 | 4.88 | 202.30 |

The remaining values – m, Δc and CTLBB – were taken from the most recent model calibrations, presented in Grath *et al.* (2018) and Grath *et al.* (2021).

As demonstrated previously, the slope of narcosis (m) is the same for all species and substances, and therefore the universal value of -0.94 was used.

The chemical correction value (Δc) of -0.364 for polycyclic aromatic hydrocarbons was taken from Grath *et al.* (2021), who sought to calibrate and validate the TLM for the inclusion of other types of hydrocarbons. This same value was used for PAHs in Word *et al.* (2024).

For the $C^*_{TLBB}$, the chemical concentration in the lipids of each organism necessary to obtain an acute effect, it was decided to use a single value known as HC5. HC5 is defined as the risk concentration that protects 95% of the species and is calculated considering different CTLBB values, normally from different taxonomic groups (Grath *et al.*, 2018). Thus, it takes into account the diversity of species exposed to the same substance in the environment, bringing a conservative approach to the assessment of aquatic toxicity. Grath *et al.* (2018) present an expanded application of TLM to predict aquatic toxicity of hydrocarbons and derive hazard concentrations (HC5). In this study, the authors recalibrated the TLM, enhancing the acute and chronic toxicity databases to include a greater diversity of taxonomic groups and species, resulting in revised CTLBB and ACR values aligned with the European Union Registration, Evaluation, Authorization and Restriction of Chemicals (REACH) guidelines *for* species sensitivity distributions in petroleum substance risk assessments. In total, 1097 acute toxicity values from 79 species were considered, including hydrocarbons and non-hydrocarbons. Species were separated into 8 taxonomic groups that follow the REACH guidelines, specified in Table 3.

Table 3: Taxonomic groups considered for calculating the risk concentration (HC5). Taken from Grath *et al.* 2018.

| Category |
|---|
| Fish (*salmonids, minnows, bluegill, sunfish, channel catfish*) |
| Second family of the Chordata phylum (fish, amphibians, etc.) |
| Crustaceans (cladocerans, copepods, ostracods, isopods, amphipods, crayfish, etc.) |
| Insects (fly, dragonfly, mosquito, etc.) |
| A family in a phylum other than Arthropoda or Chordata (e.g. Rotifera, Annelida, Mollusca etc.) |
| A family in any insect order or phylum not yet represented |
| Algae |
| Aquatic plants |

Chronic CTLBB ranged from approximately 0.36 to 137 $\mu mol/g_{octanol}$, with a geometric mean of 11.7 $\mu mol/g_{octanol}$.

From the new results obtained with the TLM, the authors calculated HC5 values applicable for use in risk assessments. These HC5 values were validated with an independent set of 106 chronic observations of hydrocarbons in aquatic plants, invertebrates and fish. Of the set, only 7.5% of the values were below the HC5, suggesting that the calculated HC5 does not underestimate the chronic toxicity of individual hydrocarbons.

One of the results of the work was the derivation of chronic harmful concentrations for 5% of the species as a function of the partition coefficient, separated by type of hydrocarbon. The results obtained for PAHs are presented in Table 4.

Table 4: Chronic hazardous concentration for 5% of species, HC5 (µmol/L). Taken from Grath *et al.* 2018.

| Log(Kow) | $HC5_{Chronic}$ - PAH |
|---|---|
| 2 | 4.81 |
| 2.5 | 1.70 |
| 3 | 0.599 |
| 3.5 | 0.211 |
| 4 | 0.0746 |
| 4.5 | 0.0263 |
| 5 | 0.0093 |
| 5.5 | 0.0033 |
| 6 | 0.012 |
| 6.5 | 0.004 |

Based on these data, an interpolation was performed to obtain the HC5 values of the PAHs used in this study as a function of log(Kow) (Figure 3). This value protects 95% of the species, which adds conservatism to the approach. In the absence of specific ecotoxicological tests for the effluent discharged from Scrubbers (SGS, 2021) in different taxonomic groups, it is considered that the use of a single value extracted from the literature, which covers several species, is the most appropriate choice.

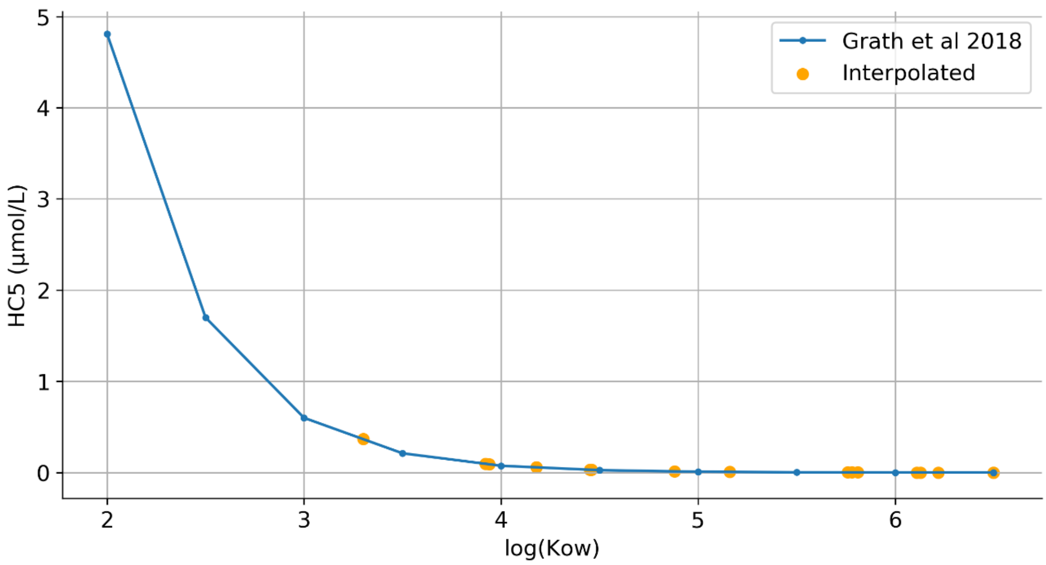


Figure 3: Chronic risk concentration curve as a function of the partition coefficient (in blue) and the interpolated values (orange points).

The HC5 value obtained in Grath *et al.* (2018) is related to the chronic effect, and the TLM calculates the LC50, which is the acute effect. For the conversion from acute to chronic, an ACR of 5.2 was used;

that is, the chronic value multiplied by 5.2 results in the acute value, since the concentration to generate an acute effect is usually higher. The ACR of 5.2 was taken from the same study and meets almost all REACH requirements, derived from a database of 20 different species representing seven of the eight taxonomic groups required by REACH and including cyanobacteria (Grath *et al.*, 2018). This same ACR value was also adopted in Word *et al.* (2024).

Through ACR, it was possible to convert the interpolated chronic HC5 values from Grath *et al.* (2018) to acute HC5 in µmol/L. Finally, acute HC5 was converted to $\mu mol/g_{octanol}$ (model unit), according to Equation 4.

Equation 4: Calculation of conversion of risk concentration (HC5) from µmol/L to $\mu mol/g_{octanol}$.

$$HC5(\mu mol/g_{octanol}) = \frac{Kow \times HC5\ (\mu mol/L)}{820}$$

where 820 g/L is the density of octanol.

The chronic values (in µmol/L) and acute values (in µmol/L and µmol/goctanol) for each compound are presented Table 5. In Figure 4, the partition coefficient and the acute HC5 (in µmol/L and µmol/goctanol) for each compound are shown.

Table 5: Octanol-water partition coefficient and chronic (µmol/L) and acute (µmol/L and µmol/goctanol) hazardous concentration for 5% of the species (HC5) for PAHs, resulting from interpolation.

| Compound | Log(Kow) | Interpolated $HC5_{Chronic}$ [µmol/L] | Interpolated $HC5_{Acute}$ [µmol/L] | Interpolated $HC5_{Acute}$ [µmol/$g_{octanol}$] |
|---|---|---|---|---|
| Naphthalene | 3.30 | 0.3666 | 1.9061 | 4.6380 |
| Acenaphthene | 3.92 | 0.9642 | 0.5014 | 5.0860 |
| Acenaphthylene | 3.94 | 0.0910 | 0.4730 | 5.0243 |
| Fluorene | 4.18 | 0.0572 | 0.2975 | 5.4913 |
| Anthracene | 4.45 | 0.0311 | 0.1619 | 5.5638 |
| Phenanthrene | 4.46 | 0.0302 | 0.1569 | 5.5167 |
| Pyrene | 4.88 | 0.0134 | 0.0696 | 6.4364 |
| Fluoranthene | 5.16 | 0.0074 | 0.0384 | 6.7647 |
| Benzo[a]anthracene 1.92E-06 | 5.76 | 0.0022 | 0.0115 | 8.0573 |
| Benzo[b]fluoranthene | 5.78 | 0.0021 | 0.0110 | 8.1160 |
| Chrysene | 5.81 | 0.0020 | 0.0104 | 8.1806 |
| Benzo[k]fluoranthene | 6.11 | 0.0010 | 0.0053 | 8.3655 |
| Benzo[a]pyrene | 6.13 | 0.0010 | 0.0052 | 8.4860 |
| Benzo[g,h,i]perylene | 6.22 | 0.0008 | 0.0044 | 8.9245 |
| Dibenzo[a,h]anthracene | 6.50 | 0.0004 | 0.0021 | 8.0214 |
| Ideno[1,2,3,c,d]pyrene | 6.50 | 0.0004 | 0.0021 | 8.0214 |

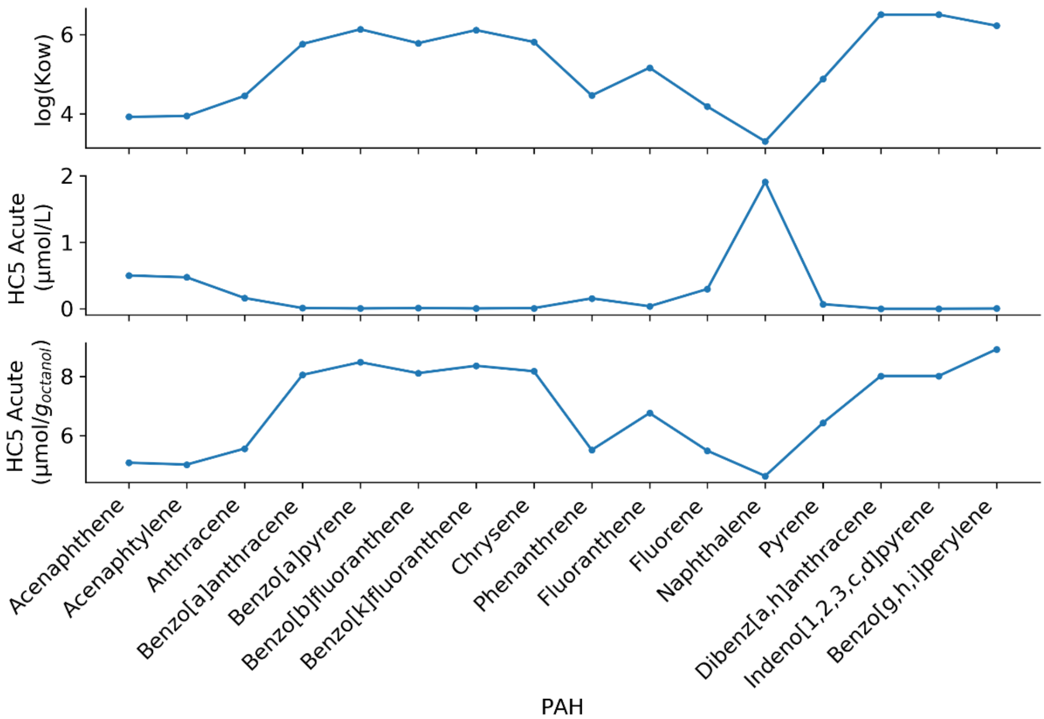


Figure 4: Octanol-water partition coefficient (log(Kow)) (upper panel), risk concentration (HC5, µmol/L) (middle panel) and risk concentration (HC5, µmol/$g_{octanol}$) (lower panel) of the 16 selected PAHs.

However, it is important to note that for some higher molecular weight PAHs, bioavailability is limited due to their reduced water solubility. Redman *et al.* (2014) demonstrated that there was no toxicity observed when log(Kow) was greater than or approximately 6, indicating a lack of bioavailability. This threshold is due to the solubility limits for aquatic toxicity, both for individual narcotic chemicals and for complex hydrocarbon mixtures, whose aqueous solubilities are insufficient to reach the critical lipid load (CTLBB) required to elicit an adverse effect (Grath *et al.*, 2014). This led to the empirical modification of the TLM, restricting log(Kow) to > 6 (Redman *et al.*, 2012).

For these reasons, it was decided to discard PAHs with partition coefficients ≥ 6, which are benzo[a]pyrene, benzo[k]fluoranthene, benzo[g,h,i]perylene, dibenzo[a,h]anthracene and indeno[1,2,3,c,d]pyrene.

In addition to the chemical and ecotoxicological properties, to calculate the TU (Equation 2), the concentration value of the compound in the effluent is required. As mentioned previously, the concentrations were taken from SGS (2022), which derived in 24 scenarios: 8 vessels (NSU C – Brazil and Singapore; YUAN HUA HAI – Brazil and Singapore; SOHAR MAX – Brazil and Singapore; ORE AMAZONAS and SOLAR FRONTIER) and 3 powers (high, medium and low). The concentration data of the samples collected at low power (berthed in port), medium (coastal shipping route) and high (offshore shipping route) of the 11 PAHs are presented in Table 6 to Table 8.

Table 6: Concentration (g/m³) of each vessel in the port scenario (low power).

| PAH | NSU C BR | NSU C SG | ORE AMAZONAS SG | SOHAR MAX BR | SOHAR MAX SG | SOLAR FRONTIER SG | YUAN HUA HAI BR | YUAN HUA HAI SG |
|---|---|---|---|---|---|---|---|---|
| Acenaphthene | 2.5e-6 | 6.0e-5 | 3.0e-5 | 2.0e-5 | 4.0e-5 | 2.0e-5 | 3.0e-5 | 8.0e-5 |
| Acenaphthylene | 2.5e-6 | 5.0e-5 | 5.0e-6 | 2.0e-5 | 5.0e-6 | 2.0e-5 | 4.0e-5 | 7.0e-5 |
| Anthracene | 2.5e-6 | 1.0e-5 | 5.0e-6 | 2.5e-5 | 5.0e-6 | 1.0e-5 | 2.5e-6 | 2.0e-5 |
| Benzo[a] anthracene | 2.5e-6 | 1.0e-5 | 1.0e-5 | 1.0e-5 | 1.0e-5 | 1.0e-5 | 2.5e-6 | 2.0e-5 |
| Benzo[b] fluoranthene | 2.5e-6 | 1.0e-5 | 5.0e-6 | 1.0e-5 | 5.0e-6 | 5.0e-6 | 2.5e-6 | 1.0e-5 |
| Chrysene | 2.5e-6 | 5.0e-5 | 4.0e-5 | 2.5e-5 | 3.0e-5 | 1.0e-5 | 1.0e-5 | 3.0e-5 |
| Phenanthrene | 2.5e-6 | 4.2e-4 | 2.5e-4 | 2.3e-4 | 3.3e-4 | 2.1e-4 | 6.0e-5 | 7.3e-4 |
| Fluoranthene | 2.5e-6 | 4.0e-5 | 2.0e-5 | 2.5e-5 | 2.0e-5 | 2.0e-5 | 2.0e-5 | 6.0e-5 |
| Fluorene | 2.5e-6 | 6.6e-4 | 7.0e-5 | 1.0e-4 | 8.0e-5 | 7.0e-5 | 2.5e-6 | 3.4e-4 |
| Naphthalene | 2.5e-6 | 1.53e-2 | 3.9e-4 | 1.2e-4 | 2.4e-4 | 1.1e-4 | 1.3e-4 | 7.7e-4 |
| Pyrene | 2.5e-6 | 5.0e-5 | 4.0e-5 | 8.0e-5 | 6.0e-5 | 4.0e-5 | 4.0e-5 | 1.0e-4 |

Table 7: Concentration (g/m³) of each vessel in the coastal route scenario (medium power).

| PAH | NSU C BR | NSU C SG | ORE AMAZONAS SG | SOHAR MAX BR | SOHAR MAX SG | SOLAR FRONTIER SG | YUAN HUA HAI BR | YUAN HUA HAI SG |
|---|---|---|---|---|---|---|---|---|
| Acenaphthene | 2.5e-6 | 1.2e-4 | 2.0e-5 | 7e-5 | 2.6e-4 | 6e-5 | 2.5e-6 | 6.0e-5 |
| Acenaphthylene | 2.5e-6 | 8.0e-5 | 5.0e-6 | 6.0e-5 | 4.0e-5 | 2.0e-5 | 2.5e-6 | 2.0e-5 |
| Anthracene | 2.5e-6 | 1.0e-5 | 5.0e-6 | 1.5e-4 | 4.0e-5 | 2.0e-5 | 2.5e-6 | 3.0e-5 |
| Benzo[a] anthracene | 2.5e-6 | 1.0e-5 | 5.0e-6 | 2.0e-5 | 1.4e-4 | 1.0e-5 | 2.5e-6 | 2e-5 |
| Benzo[b] fluoranthene | 2.5e-6 | 1.0e-5 | 5.0e-6 | 1.0e-5 | 6.0e-5 | 1.0e-5 | 2.5e-6 | 2.0e-5 |
| Chrysene | 2.5e-6 | 4.0e-5 | 3.0e-5 | 1.0e-5 | 3.5e-4 | 4.0e-5 | 2.0e-5 | 1.0e-4 |
| Phenanthrene | 3.0e-5 | 9.9e-4 | 2.2e-4 | 1.23e-3 | 1.8e-3 | 1.23e-3 | 3.1e-4 | 5.8e-4 |
| Fluoranthene | 2.5e-6 | 5.0e-5 | 2.0e-5 | 9.0e-5 | 1.0e-4 | 5.0e-5 | 3.0e-5 | 7.0e-5 |
| Fluorene | 4.0e-5 | 1.03e-3 | 6.0e-5 | 3.6e-4 | 3.6e-4 | 3.3e-4 | 9.0e-5 | 1.9e-4 |
| Naphthalene | 2.05e-3 | 2.1e-2 | 3.6e-4 | 1.9e-3 | 5.8e-4 | 4.7e-4 | 2.2e-4 | 3.7e-4 |
| Pyrene | 1.0e-5 | 3.0e-5 | 3.0e-5 | 1.5e-4 | 4.2e-4 | 4.0e-5 | 3.0e-5 | 1.0e-4 |

Table 8: Concentration (g/m³) of each vessel in the offshore route scenario (high power).

| PAH | NSU C BR | NSU C SG | ORE AMAZONAS SG | SOHAR MAX BR | SOHAR MAX SG | SOLAR FRONTIER SG | YUAN HUA HAI BR | YUAN HUA HAI SG |
|---|---|---|---|---|---|---|---|---|
| Acenaphthene | 2.5e-6 | 8.0e-5 | 3.0e-5 | 6.0e-5 | 2.0e-4 | 5.0e-5 | 2.5e-6 | 4.0e-5 |
| Acenaphthylene | 2.5e-6 | 4.0e-5 | 5.0e-6 | 5.0e-5 | 3.0e-5 | 2.0e-5 | 2.5e-6 | 1.0e-5 |
| Anthracene | 2.5e-6 | 1.0e-5 | 5.0e-6 | 2.1e-4 | 4.0e-5 | 1.0e-5 | 2.5e-6 | 2.0e-5 |
| Benzo[a] anthracene | 2.5e-6 | 1.0e-5 | 1.0e-5 | 3.0e-5 | 1.0e-4 | 1.0e-5 | 2.5e-6 | 2.0e-5 |
| Benzo[b] fluoranthene | 2.5e-6 | 1.0e-5 | 5.0e-6 | 1.0e-5 | 3.0e-5 | 1.0e-5 | 2.5e-6 | 1.0e-5 |
| Chrysene | 2.5e-6 | 1.0e-5 | 6.0e-5 | 2.1e-4 | 2.0e-4 | 2.0e-5 | 7.0e-5 | 2.0e-5 |
| Phenanthrene | 1.0e-5 | 4.8e-4 | 2.7e-4 | 1.69e-3 | 1.14e-3 | 1.02e-3 | 4.8e-4 | 2.1e-4 |
| Fluoranthene | 2.5e-6 | 2.0e-5 | 3.0e-5 | 1.4e-4 | 8.0e-5 | 3.0e-5 | 8.0e-5 | 2.0e-5 |
| Fluorene | 2.5e-6 | 4.4e-4 | 7.0e-5 | 4.9e-4 | 2.6e-4 | 1.9e-4 | 1.2e-4 | 1.1e-4 |
| Naphthalene | 1.0e-5 | 8.55e-3 | 4.2e-4 | 1.48e-3 | 5.0e-4 | 3.3e-4 | 3.4e-4 | 4.1e-4 |
| Pyrene | 2.5e-6 | 2.0e-5 | 4.0e-5 | 1.7e-4 | 2.6e-4 | 4.0e-5 | 1.1e-4 | 3.0e-5 |

A summary of the parameters used for the TLM is presented in Table 9.

Table 9: Summary of TLM input data.

| Variable | Value |
|---|---|
| $m$ | -0.94 |
| Δc | -0.364 |
| $HC5\ agudo\ (C^{*}_{TLBB})$ | Table 5 |
| ACR | 5.2 |
| Amount of simulated PAHs | 11 |
| Number of scenarios | 24 |
| Concentrations | Table 6, Table 7 and Table 8 |

### 2.1.4 Results

The results obtained were divided into ports and shipping routes (coastal and offshore), in Brazil and Singapore. Following the necessary configurations for the TLM, presented in item 2.1.1, 11 PAHs from 24 effluents were evaluated. For each scenario, the concentrations were varied, as shown in Table 6 to Table 8.

The first step of the TLM consists of calculating the acute LC50 of the chemical (Equation 1). In this part, there is no differentiation between the scenarios, since the inputs refer to the properties of each compound and its effects on the target lipid of the organisms.

In Figure 5, the LC50 results obtained reflect the HC5 values that were used as input data, which in turn are influenced by the partition coefficient. It is possible to observe that the compounds with the highest partition coefficient result in lower lethal concentrations, since high coefficients indicate that these compounds are more soluble in lipids and, consequently, more sensitive to organisms. Examples are chrysene, benzo[b]fluoranthene and benzo[a]anthracene, with acute lethal concentrations of 2.792 µg/L; 3.266 µg/L; and 3.064 µg/L, respectively. The highest value, 203.324 µg/L, was obtained with naphthalene, which means that the species considered in the protective concentration (HC5) will have a lethal effect with a very high concentration of the compound.

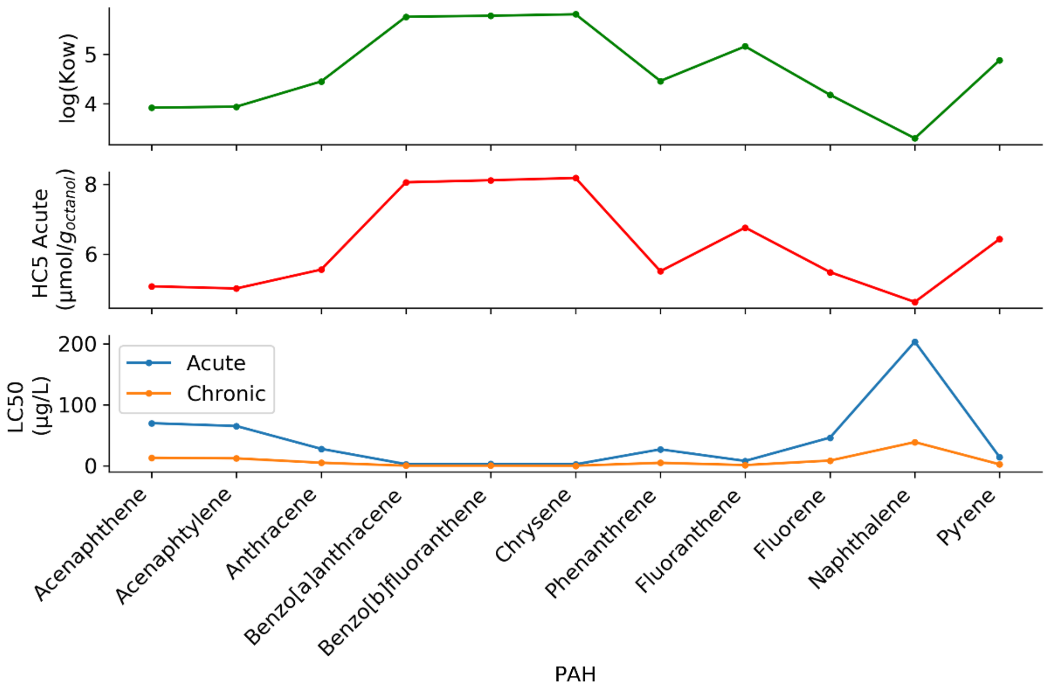


Figure 5: Octanol-water partition coefficient (upper panel), acute risk concentration (middle panel), and chronic and acute LC50 (lower panel) of each modeled compound.

From the LC50 values it is possible to derive the chronic concentration (EC50) using the ACR factor of 5.2. The results obtained are presented in Table 10.

Table 10: LC50 (acute, µg/L) and EC50 (chronic, µg/L) of each compound.

| PAH | CL50 | EC50 |
|---|---|---|
| Acenaphthene | 70.095 | 13.480 |
| Acenaphthylene | 65.448 | 12.586 |
| Anthracene | 28.137 | 5.411 |
| Benzo[a] anthracene | 3.064 | 0.589 |
| Benzo[b] fluoranthene | 3.266 | 0.628 |
| Chrysene | 2.792 | 0.537 |
| Phenanthrene | 27.302 | 5.250 |
| Fluoranthene | 8.351 | 1.606 |
| Fluorene | 46.463 | 8.935 |
| Naphthalene | 203.324 | 39.101 |
| Pyrene | 14.569 | 2.802 |

When comparing the acute lethal value obtained with the concentrations measured in the discharge, shown in Figure 6, it is possible to observe that no concentration exceeds the lethal concentration resulting from the TLM. Since the TU is the normalization of the concentration by the LC50, observing this relationship for each PAH gives indications of which samples are potentially toxic.

A TU greater than 1 suggests a potential toxic effect of organisms exposed to effluent discharged into Scrubbers wash water.

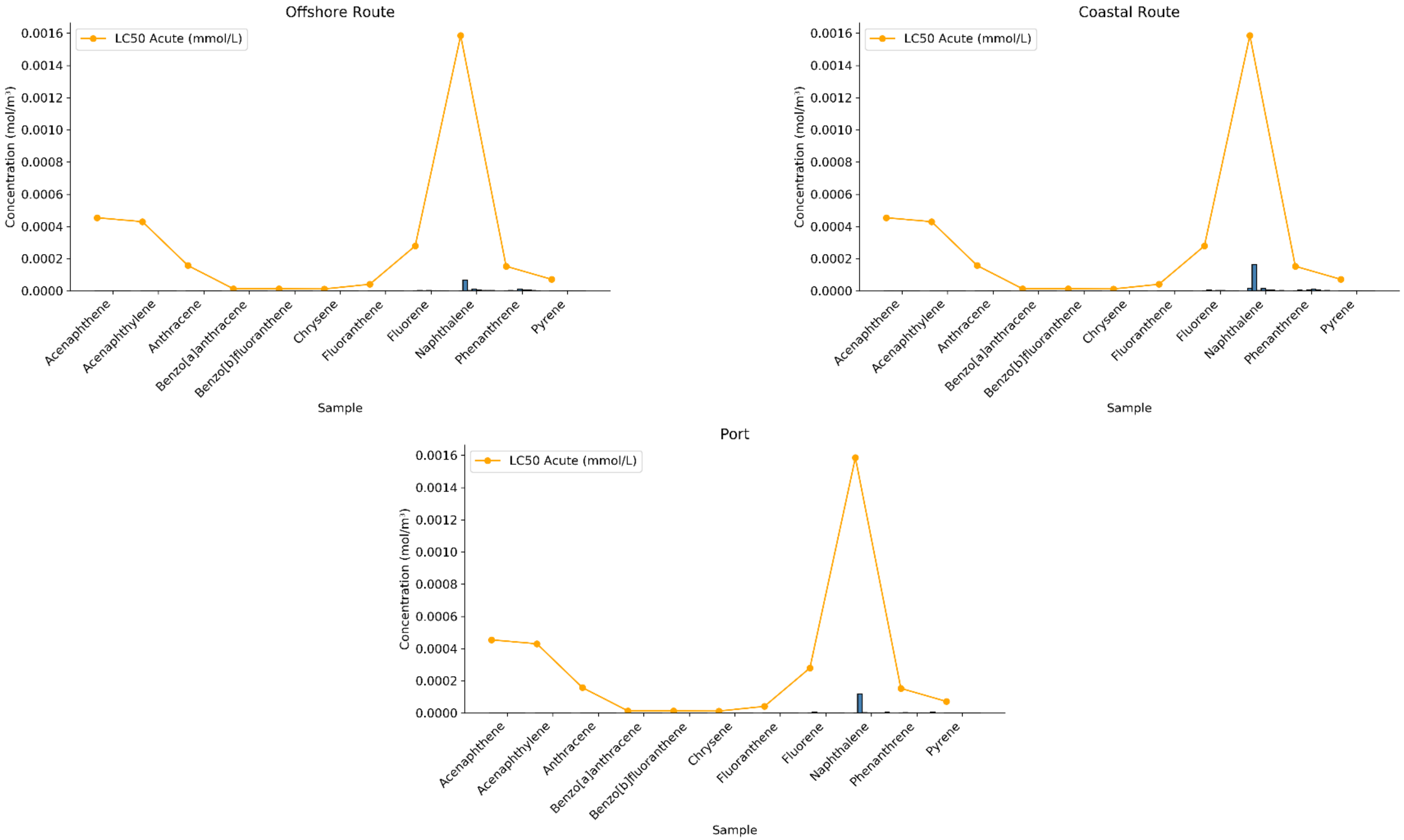


Figure 6: Concentration (in mol/m³) and acute LC50 (mmol/L) of each compound modeled in the offshore route (top left), coastal route (top right) and in port (bottom).

It is important to note that the toxic units were based on the 5th percentile, representing concentrations below which effects are highly unlikely and not concentrations at which effects may occur. Although the 5th percentile threshold can be exceeded without noticeable ecological effects, it is used as a conservative criterion to ensure the safety of exposed organisms (if the concentration is not exceeded) and to identify contaminants of potential concern in risk assessments. These assumptions are extremely conservative in the context of Scrubbers wash water discharge, since the protective concentration assumes continuous exposure of organisms over a long period and disregards natural dispersion and degradation processes, which eventually decrease concentrations in the environment.

That said, Figure 7, Figure 8 and Figure 9 show the output concentration measured in SGS (2022) (mol/m³) and the toxic unit of each PAH according to the vessel and power (offshore, coastal and port). Individually, none of the samples obtained TU equal to or greater than 1. It is possible to observe that the chemicals with a higher partition coefficient, and consequently lower LC50, resulted in higher TUs, such as chrysene and benzo[a]anthracene. Naphthalene and phenanthrene were also highlighted, as their sampled concentrations are higher.

Among the three potencies (low – port; medium – coastal route; high – offshore route), the highest toxicities were obtained in the coastal route, followed by the offshore route for the mentioned compounds. In the port, the TUs were much lower, with a peak for naphthalene of 0.07. In the vessels, the maximum was observed in the vessel SOHAR MAX SG with a TU for chrysene of 0.13 in the coastal route.

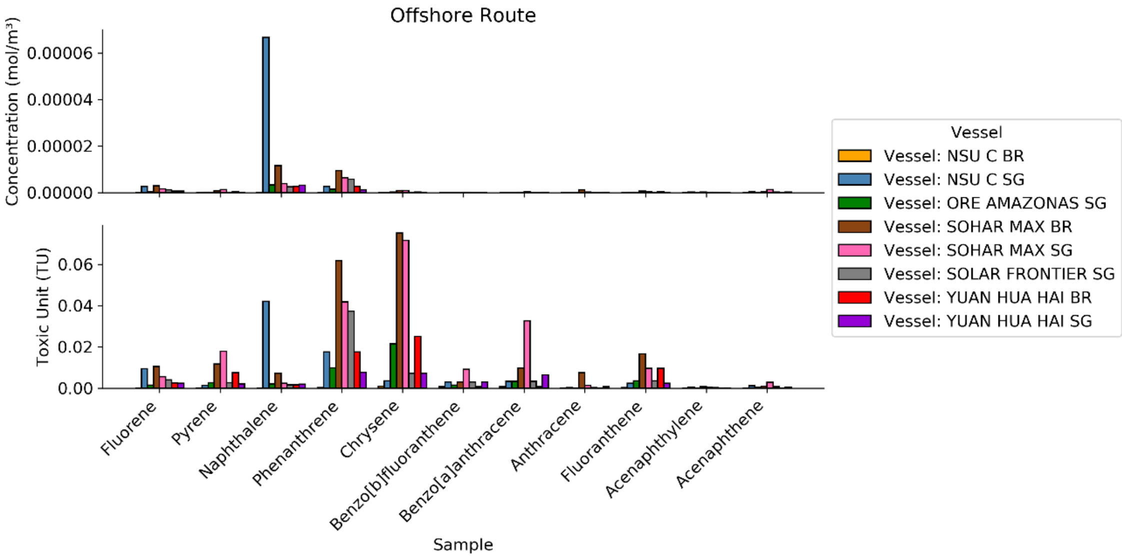


Figure 7: Concentration (mol/m³) (upper panel) and acute toxic unit (lower panel) of each modeled compound and each ship in the offshore route scenario.

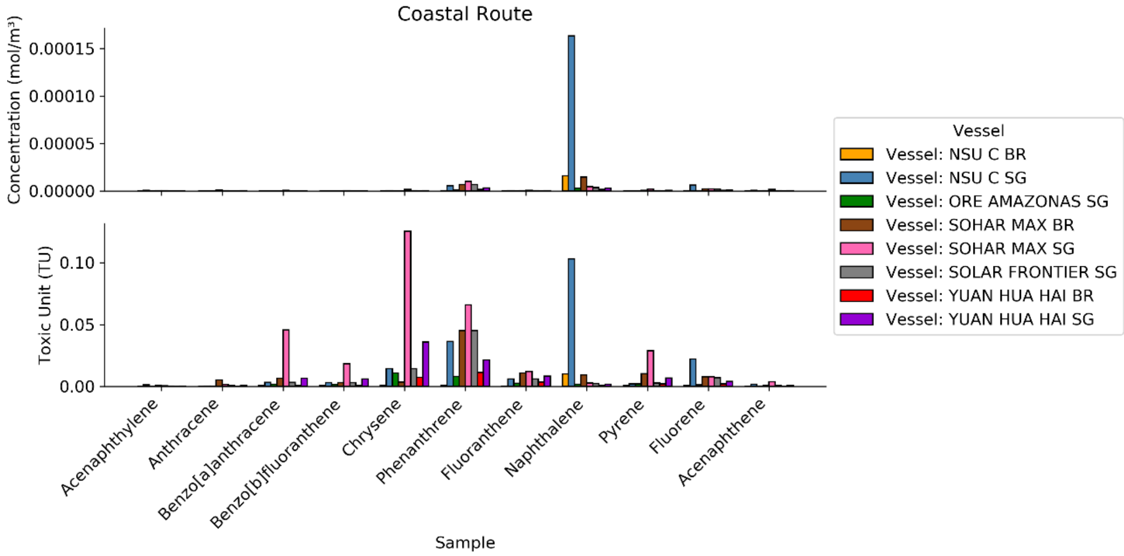


Figure 8: Concentration (mol/m³) (upper panel) and acute toxic unit (lower panel) of each modeled compound and each ship in the coastal route scenario.

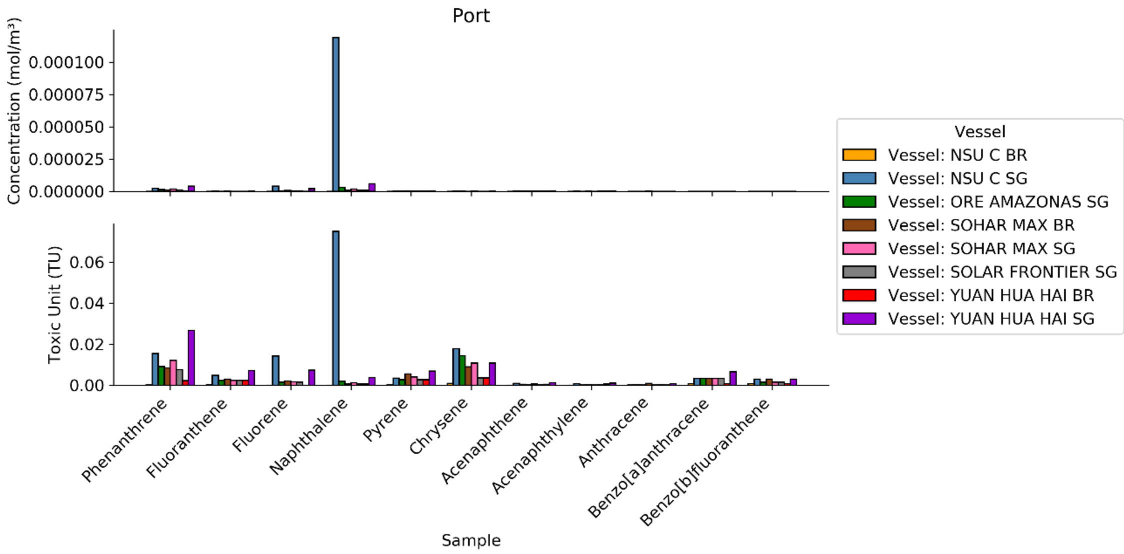


Figure 9: Concentration (mol/m³) (upper panel) and acute toxic unit (lower panel) of each modeled compound and each ship in the port scenario.

The sum of the TUs of the 11 PAHs in each effluent discharged by the Scrubbers wash water is presented in Figure 10 and Table 11.

The toxicity assessment with the TLM resulted in TUs between 0.004 and 0.313, indicating that the disposal of the 24 effluents will not potentially cause acute toxic effects on organisms. However, for the chronic effect, 4 effluents discharged in the navigation routes obtained values above 1 and are therefore potentially toxic. The effluents were from the scenarios SOHAR MAX SG – coastal route

(1.625); SOHAR MAX BR – offshore route (1.068); SOHAR MAX SG – offshore route (1.016) and NSU C SG – coastal route (1.006).

It is worth noting that these acute and chronic thresholds are conservative values of concentrations that would affect the most sensitive species.

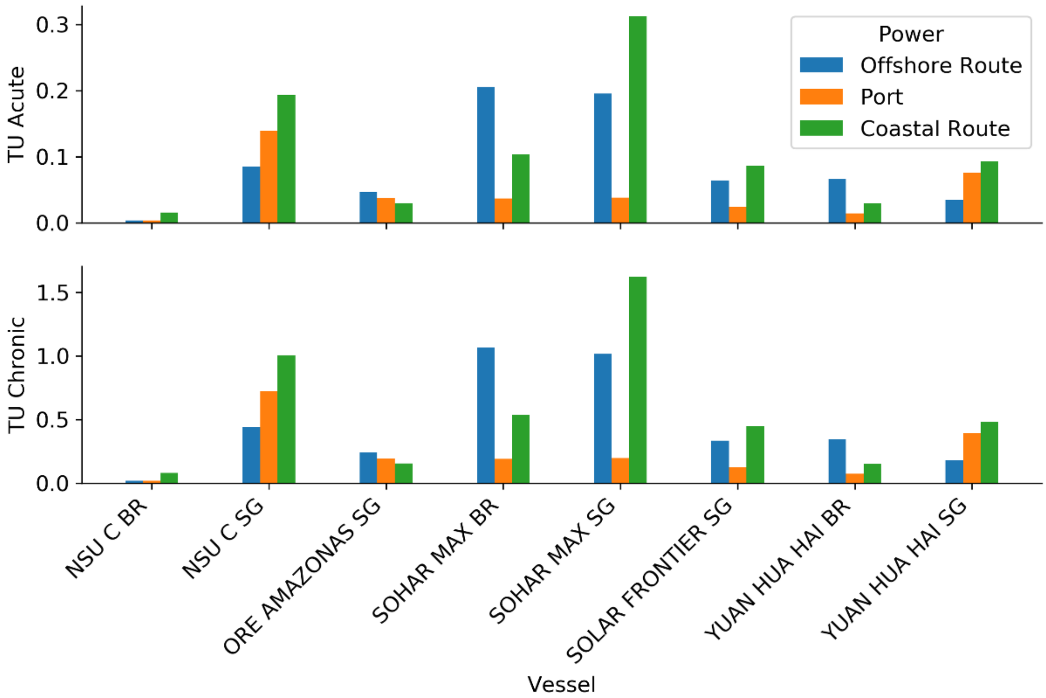


Figure 10: Acute (upper panel) and chronic (lower panel) toxic unit (TU) of effluents from 8 vessels in the offshore, coastal and port shipping route resulting from TLM.

Table 11: Acute and chronic toxic unit (UT) obtained for the Offshore Route (high power), Coastal Route (medium power) and Port Route (high power). Values with TU > 1 are highlighted in red.

| Effluent | Acute TU | Chronic TU |
|---|---|---|
| OFFSHORE ROUTE (HIGH POWER) | | |
| NSU C BR | 0.004 | 0.019 |
| NSU C SG | 0.085 | 0.441 |
| ORE AMAZONAS SG | 0.047 | 0.243 |
| SOHAR MAX BR | 0.205 | 1.068 |
| SOHAR MAX SG | 0.195 | 1.016 |
| SOLAR FRONTIER SG | 0.064 | 0.334 |
| YUAN HUA HAI BR | 0.066 | 0.342 |
| YUAN HUA HAI SG | 0.035 | 0.181 |
| COASTAL ROUTE (MEDIUM POWER) | | |
| NSU C BR | 0.016 | 0.081 |
| NSU C SG | 0.194 | 1.006 |
| ORE AMAZONAS SG | 0.030 | 0.156 |
| SOHAR MAX BR | 0.104 | 0.539 |
| SOHAR MAX SG | 0.313 | 1.625 |
| SOLAR FRONTIER SG | 0.086 | 0.446 |
| YUAN HUA HAI BR | 0.029 | 0.150 |
| YUAN HUA HAI SG | 0.093 | 0.484 |
| PORT (LOW POWER) | | |
| NSU C BR | 0.004 | 0.017 |
| NSU C SG | 0.139 | 0.723 |
| ORE AMAZONAS SG | 0.038 | 0.195 |
| SOHAR MAX BR | 0.036 | 0.189 |
| SOHAR MAX SG | 0.038 | 0.200 |
| SOLAR FRONTIER SG | 0.024 | 0.126 |
| YUAN HUA HAI BR | 0.014 | 0.074 |
| YUAN HUA HAI SG | 0.075 | 0.391 |

Analyzing the modeled compounds, from Figure 11 to Figure 13, the results are presented in percentage related to the total TU (100%) of the effluents, for each vessel and power. The figures show the proportion (in %) of each simulated PAH in the TU resulting from the effluent.

For all modeled scenarios, chrysene, benzo[a]anthracene and benzo[b]fluoranthene, compounds that have a greater affinity for the body's lipids, make a significant contribution, reaching contributions of 46% of chrysene on the offshore route of the vessel ORE AMAZONAS SG and 40% on the coastal route of the vessel SOHAR MAX SG. The compounds naphthalene and phenanthrene also resulted in significant shares.

In the vessels NSU C BR and NSU C SG, the total toxicity is predominantly contributed by naphthalene, with 64% and 53%, respectively, for the coastal route (Figure 11).

Phenanthrene was the largest contributor in the vessels SOLAR FRONTIER SG (58% on the offshore route, 53% on the coastal route and 39% in port) and SOHAR MAX BR (43% on the coastal route) (Figure 11 and Figure 12).

Therefore, of the 4 effluents that presented potential toxic effects, 3 are mainly due to the effects of chrysene and phenanthrene, while for the vessel NSU C SG, naphthalene and phenanthrene mainly contribute.

A highlight for the same compounds was also found in Vale & CLS Brasil (2024), in the simulations carried out with MAMPEC. In the study, the compounds naphthalene followed by phenanthrene stood out in the Port of Tubarão, while in the navigation route the maximum values were obtained for phenanthrene followed by naphthalene and fluorene.

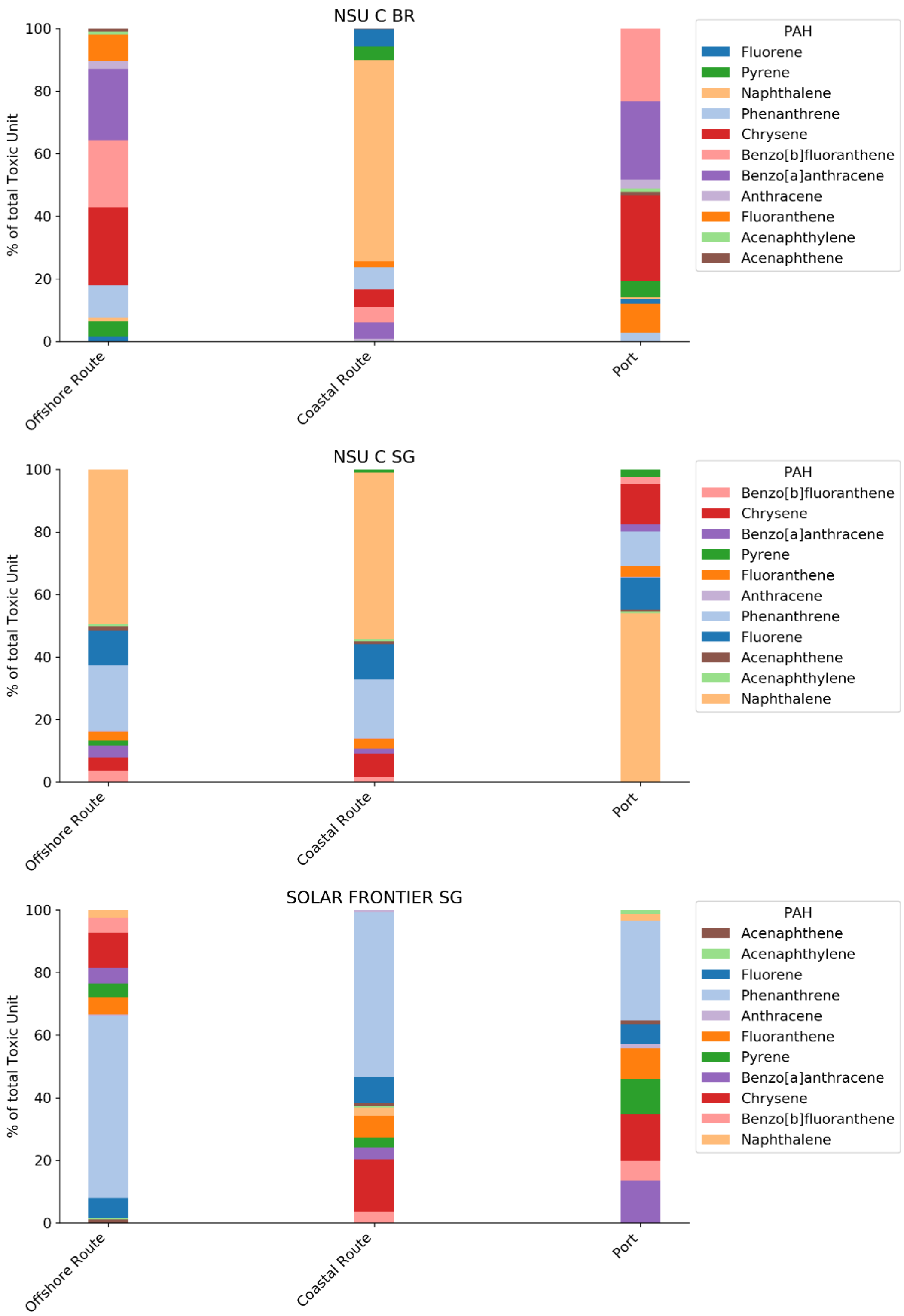


Figure 11: % of modeled compounds in the total acute toxic unit of effluents from vessels NSU C BR (upper figure), NSU C SG (middle figure) and SOLAR FRONTIER SG (lower figure).

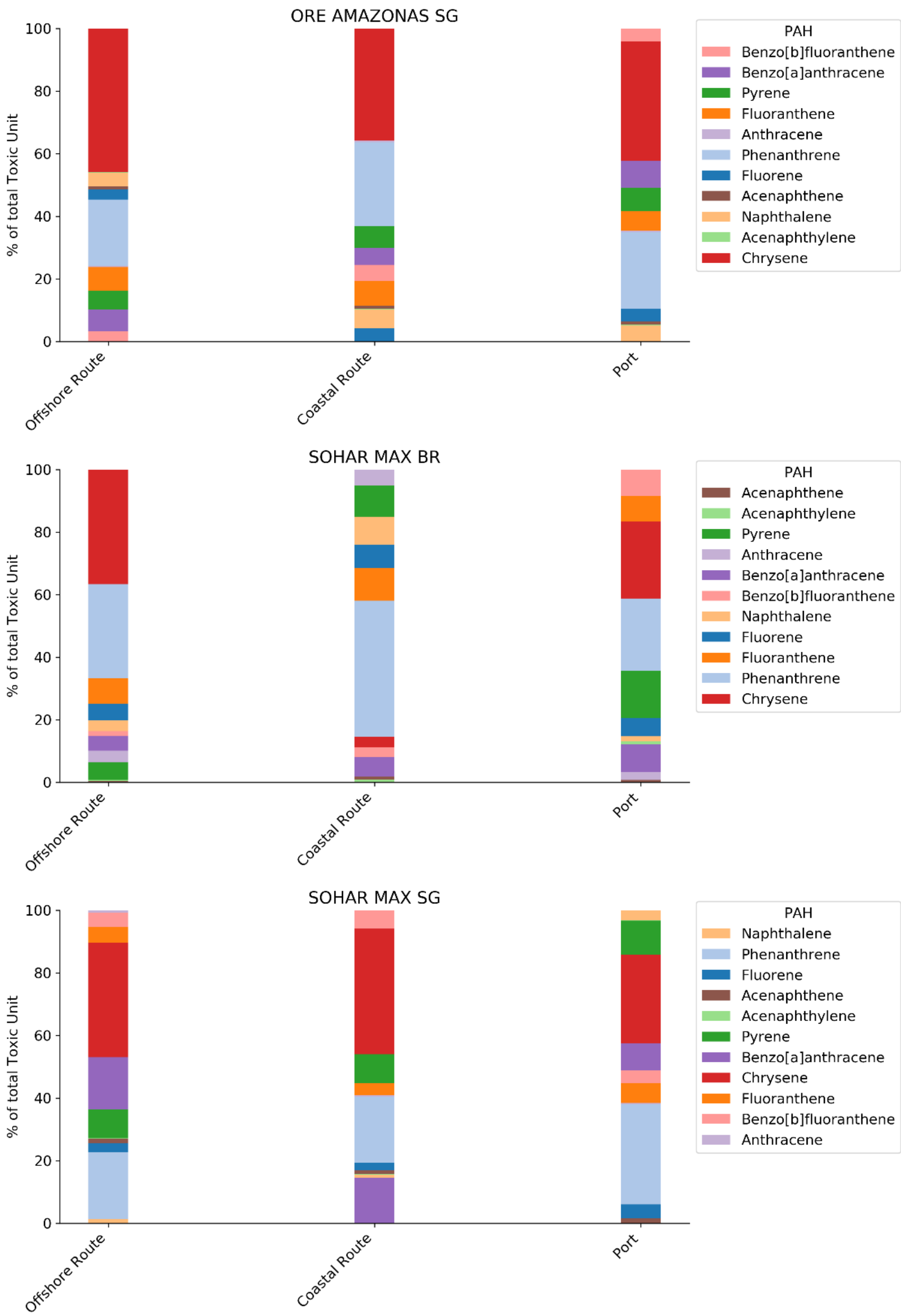


Figure 12: % of modeled compounds in the total acute toxic unit of effluents from vessels ORE AMAZONAS SG (upper figure), SOHAR MAX BR (middle figure) and SOHAR MAX SG (lower figure).

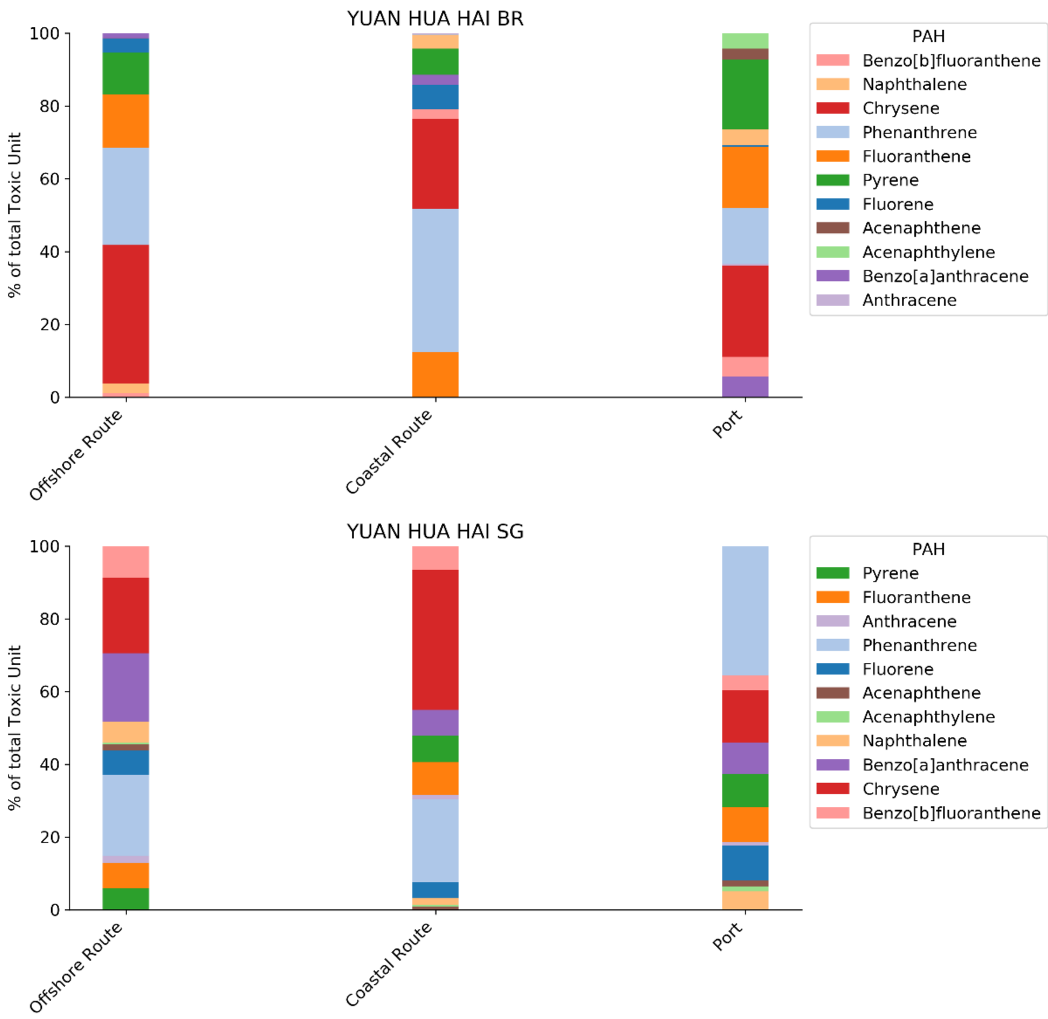


Figure 13: % of modeled compounds in the total acute toxic unit of effluents from vessels YUAN HUA HAI BR (upper figure) and YUAN HUA HAI SG (lower figure).

In Word *et. al.* (2024), higher values were found when compared to this study, with chronic TU between 2.8 and 16. However, the authors considered a greater quantity and variety of hydrocarbons in the TU calculation. Despite this, the conclusions indicate that the results obtained with the TLM are very conservative, since when compared with the results obtained in the laboratory, the TLM predicts a higher effluent toxicity than that obtained in the laboratory analyses, which verify a slightly toxic substance, with TU below 5.

### 2.1.5 Comparison of Results

Using the CL50 and EC50 results obtained in the TLM, the TU of the simulated effluent with MAMPEC were calculated in Vale & CLS Brasil (2024). For this, instead of using the concentration measured in SGS (2022) in Equation 2, the results of the maximum total concentration in the water column of the 11 PAHs modeled with the TLM were used. Table 12 presents the results of the sums obtained for the port, coastal route, and offshore areas.

Table 12: Acute and chronic toxic unit (TU) obtained for the Offshore *Route* (high power), Coastal (medium power) and Port (high power) with data resulting from MAMPEC.

| Effluent | Acute UT | Chronic UT |
|---|---|---|
| MAMPEC – Port | 3.50E-05 | 1.82E-04 |
| MAMPEC – Coastal Route | 8.48E-08 | 4.41E-07 |
| MAMPEC – Offshore Route | 3.46E-08 | 1.80E-07 |

The values obtained were significantly lower than the TU of the effluent at the vessel outlet (Table 11), suggesting that the effluent loses its toxicity quickly when dispersed in the water column. Furthermore, unlike the measurements performed, the highest values were observed in the Port scenario. However, based on the results used from MAMPEC, the discharge does not present a toxic risk.

### 2.1.6 Critical evaluation

The TLM adopts a very conservative approach since it assumes that each PAH acts independently, which translates into the addition of individual TUs, disregarding possible interactions between the compounds that would decrease their concentrations in the aquatic environment. The model also disregards important processes such as dispersion and weathering, which also result in decreased toxicity.

Another relevant point is the use of HC5, which represents a conservative concentration, below which toxic effects are highly unlikely. This criterion is adopted to ensure the safety of exposed organisms, as long as the concentration of the contaminant is not exceeded. However, it is not uncommon for a 5th percentile threshold to be exceeded without any noticeable ecological effect, as the threshold does not represent the concentration at which effects are likely to occur (WORD *et al.*, 2024). Furthermore, the values tested to obtain HC5 were not derived from tests performed with the effluent discarded from the Scrubbers at an exposure time close to reality and may be considering a longer exposure time of the organism to the compounds. These values were used because they represent the estimate closest to reality in this study.

These considerations suggest that chemically-based toxicity predictions, such as those used in the TLM, may overestimate cumulative risks when compared to results observed in empirical toxicity tests performed in the laboratory. There are several reasons that explain these discrepancies. First, there is uncertainty associated with the characterization of the toxicity assessments used to predict model results. Second, environmental fate processes, such as dispersion and degradation, may reduce the exposure of organisms under laboratory and field conditions, resulting in lower observed toxicity. Finally, the TLM model may overestimate interactions between effluent constituents, since it assumes additivity of response, which is not always the case.

Furthermore, due to the limitations of the model, 5 PAHs were discarded in the modeling, which evidently contribute and increase the toxicity of the effluent. Other PAHs and compounds, such as monocyclic and heterocyclic hydrocarbons, would also increase toxicity.

These factors highlight the need to consider the limitations of TLM when assessing the ecological risks associated with complex chemical mixtures, such as those present in discharged EGCS effluents.

## 2.2. Literature Review and Secondary Data Analysis

Eldridge *et al.* (2021) considers, based on several authors, that **Environmental Risk Assessments (ERA)** depend on peer-reviewed ecotoxicological literature to assist in regulatory decision-making, and a critical issue for this is the reliability of data reporting, which hinders, or even prevents, the absorption of data. The choice of relevant test organisms and endpoints (specific measures used to assess the ecotoxicity of a substance) contributes to the effectiveness of the ERA process, as do high-quality data and effective reporting, which reduce uncertainty around the potential for effects and give risk assessors greater confidence in their decisions and recommendations. In addition to assessing data quality, a reasonable and neutral interpretation of the results is crucial to ensure credibility in the scientific and public spheres (Brain & Hanson, 2021). Ecological analyses of various *endpoints* are relevant, from individual mortality to non-lethal effects at the population level, allowing assessments between trophic levels. The most important thing in these state-of-the-art surveys is transparency and clear identification of the origin of the data (references in the literature), its methodological and geographic scope.

In this study, the assessment of the state of the art regarding the ecotoxicity of EGSE generated by open-loop EGCS was restricted to results with planktonic test organisms representing different trophic levels (from bacterioplankton to ichthyoplankton, and from producers to tertiary consumers), identified below (Table 13). There was no geographical restriction on the origin of the effluents or test organisms; on the contrary, it was decided to be as comprehensive as possible.

According to Koski *et al.* (2017a), the productivity of an aquatic ecosystem depends on the productivity and efficiency of trophic transfer at the base of the food web. Thus, the negative effects of EGSE on plankton, for example, can have significant consequences for the structure of the food web and the overall functioning of the ecosystem. For ecotoxicity tests, it is essential to choose more sensitive organisms. Sensitive organisms act as early indicators of contamination and help characterize the level of ecological risk associated with the EGSE discharge (Koyama *et al.*, 2018). If these organisms are impacted, there is a high probability that other more resilient organisms will also be affected to some degree. The difference in the size of the organisms, in turn, is a determining factor for the organism's reaction to exposure (Thor *et al.*, 2021).

Table 13: Identification of the test organisms used to evaluate the ecotoxicity of EGSE on the different trophic levels of the planktonic food chain considering the selected references. Source: compiled by CLS Brasil.

| Origin of secondary ecotoxicity data of open-loop EGCS considered, by test organism | | | | |
|---|---|---|---|---|
| test organism | common name | category | trophic level | reference |
| *Allivibrio fischeri* | bacterium | bacterioplankton | producer | Hunfnagl *et al.* (2005) and Piconi *et al.* (2023) |
| *Nodularia spumigena* | cyanobacteria | bacterioplankton | producer | Ytreberg *et al.* (2019) |
| *Dunaliella tertiolecta* | green algae | phytoplankton | producer | Piconi *et al.* (2023) |
| *Melosira arctica* | diatom | meroplankton | producer | Ytreberg *et al.* (2019) |
| *Phaeodactylum tricornutum* | diatom | phytoplankton | producer | Piconi *et al.* (2023) |
| *Skeletonema costatum* | diatom | phytoplankton | producer | Koyama *et al.* (2018) and Word *et al.* (2024) |
| *Skeletonema* sp. | diatom | phytoplankton | producer | Kamper *et al.* (2021) |
| *Americamysis bahia* | mysid (crustacean) | zooplankton | $1^{st}$ consumer | Word *et al.* (2024) |
| *Artemia salina* | artemia (crustacean) | zooplankton | $1^{st}/2^{nd}$ consumer | Hunfnagl *et al.* (2005) |
| *Acartia tonsa* | copepod (crustacean) | zooplankton | $1^{st}/2^{nd}$ consumer | Koski *et al.* (2017a, b), Kamper *et al.* (2021) and Piconi *et al.* (2023) |
| *Temora longicornis* | copepod (crustacean) | zooplankton | $1^{st}/2^{nd}$ consumer | Koski *et al.* (2017b) |
| *Calanus helgolandicus* | copepod (crustacean) | zooplankton | $1^{st}/2^{nd}$ consumer | Magnusson *et al.* (2018) and Thor *et al.* (2021) |
| *Dicentrarchus labrax* | fish (European seabass) | ichthyoplankton | $2^{nd}/3^{rd}$ consumer | Kamper *et al.* (2021) |
| *Menidia beryllina* | inland silverside | ichthyoplankton | $2^{nd}/3^{rd}$ consumer | Word *et al.* (2024) |
| *Oryzias javanicus* | Javanese rice-fish | ichthyoplankton | $2^{nd}/3^{rd}$ consumer | Koyama *et al.* (2018) |

*Allivibrio fischeri* are marine bacteria that luminesce as a natural part of their metabolism. When exposed to a toxic substance, the bacteria's respiratory process is interrupted, reducing light output. This change can be used to calculate a percentage of inhibition of *Allivibrio fischeri* that directly correlates with toxicity. According to Viegas (2021), assessing the environmental risks of pollutant disposal on single-celled organisms is of utmost importance when it comes to ecotoxicity. Because they are organisms that occupy the base of the food chain in nature, when exposed to effluent, they can serve as a source of contamination for other organisms. According to Kamper *et al.* (2021) and Word *et al.* (2024), the assessment of ecotoxicity in terms of growth inhibition, in the case of phytoplankton, even allows quantifying trophic magnification based on the amount of biomass, that is, the potential risks to the transfer of energy between trophic levels.

Copepods are the main link in the food web between phytoplankton and fish, and play a large role in ocean biogeochemistry (including carbon sequestration) by contributing to vertical export through the production of fecal pellets and by contributing to nutrient remineralization through excretion and sloppy feeding Worden *et al.* (2015 *apud* Koski *et al.,* 2017b).

Experiments conducted under controlled conditions using laboratory-grown organisms may never capture the complex interactions of natural ecosystems. However, as pointed out by Koski *et al.* (2017b), they have the advantage of reducing the variability caused by different test organisms (e.g., previous feeding conditions and age of the organisms, which would introduce a disturbance factor in experiments where the interest is to estimate the effect of a pollutant). In parallel, mesocosm experiments allow the evaluation of the specific composition, photosynthetic activity and cellular biovolume of microplankton when exposed to different concentrations of EGSE, for example, as performed by Ytreberg *et al.* (2019 and 2021b).

The taxonomic details of each test organism, for which ecotoxicological assays with EGSE have available results in the selected literature, are presented in Table 14, along with considerations regarding their general use in ecotoxicity tests. In the literature, there is a wide range of EGSE ecotoxicity test results available, with different *endpoints.* In addition to those that evaluate lethality caused by EGSE, many other sub-lethal tests (bioluminescence (microtox), larval growth or development, feeding, egg production, egg hatching success, and fecal pellet production) have been performed (Table 15), both acute and sub-chronic and chronic (which refers to the duration of the test).

The results presented consolidate results from median lethal concentration (when 50% of the tested organisms die in a specific period), to sub-lethal effects tested, with perception in at least 10% of the organisms tested in the test period (both acute and sub-chronic and chronic).

It should be noted that, as previously discussed, the available results in the literature did not allow for categorization within the structure adopted for the TLM: low power (vessel berthed at port), medium power (vessel on the coastal navigation route), and high power (vessel on the offshore navigation route). Therefore, in line with the conservative approach adopted throughout the report, the presented results comprehensively consolidate different engine power levels at the time of effluent generation.

Table 14: Identification, taxonomy and considerations on the test organisms used in the ecotoxicity tests compiled from the literature for EGSE of *open-loop EGCS*. Source: CLS Brasil.

| Organisms used in effluent ecotoxicity tests \| EGCS open-loop | | | | |
|---|---|---|---|---|
| test organism | Class | Order/Family | species | considerations |
| 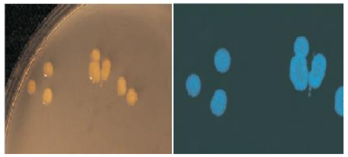 | Gammaproteobacteria | Order Vibrionales | *Allivibrio fischeri* (Beijerinck, 1889) Urbanczyk *et al.* (2007) | globally distributed, non-pathogenic, bioluminescent marine bacteria, sensitive to the toxicity of contaminants at trace (µg/L) and ultra-trace (ng/L) concentrations, expressed by the reduction/inhibition of its bioluminescence |
|  | Cyanophyceae | Order Nostocales | *Nodularia spumigena* Mertens ex Bornet & Flahault 1888 | species of toxic filamentous cyanobacteria, being the first species recognized forming aquatic blooms that cause disease and death in animals in brackish environments, for example, the Baltic Sea, with ecotoxicity evaluated in terms of photosynthetic activity and primary productivity |
|  | Chlorophyceae | Order Chlamydomonadales | *Dunaliella tertiolecta* Butcher 1959 | marine unicellular green algae used for ecotoxicity tests verified for inhibition of population growth and lethality |
|  | Coscinodiscophyceae | Order Melosirales | *Melosira arctica* Dickie 1852 | species of diatom considered meroplankton, as it remains floating freely like plankton during a certain phase of its life cycle, used in ecotoxicity tests to assess the impact of contaminants on Arctic ecosystems in terms of primary productivity |

Organisms used in effluent ecotoxicity tests | EGCS open-loop

| test organism | Class | Order/Family | species | considerations |
|---|---|---|---|---|
| 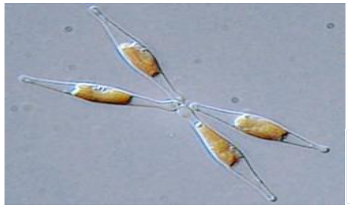 | Bacillariophyceae | Order Naviculales | *Phaeodactylum tricornutum* Bohlin, 1897 | marine unicellular algae that can be presented in different morphotypes (fusiform, triradiate and oval), used for ecotoxicity tests verified for inhibition of population growth and lethality |
| 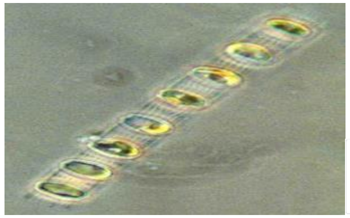 | Bacillariophyceae | Order Thalassiosirales | *Skeletonema costatum* (Greville) Cleve, 1873 | single-celled marine algae that forms chains, used for ecotoxicity tests, checking for inhibition of population growth and lethality |
|  | Branchiopoda | Order Anostraca | *Artemia salina* (Linnaeus, 1758) | planktonic marine microcrustacean used as a reliable, fast, low-cost and easy-to-handle test organism, used for ecotoxicity tests verified for the lethality of nauplii (juveniles) |
|  | Malacostraca | Order Mysida | *Americamysis bahia* (Molenock, 1969) | also referred to as *Mysidopsis bahia*, is a planktonic marine crustacean widely used as a test organism due to its ease of cultivation, used for ecotoxicity tests verified for the lethality of juveniles |

Organisms used in effluent ecotoxicity tests | EGCS open-loop

| test organism | Class | Order/Family | species | considerations |
|---|---|---|---|---|
| 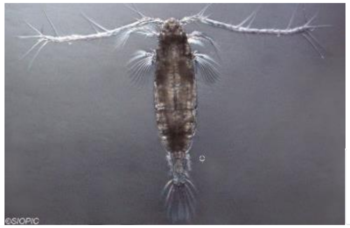 | Copepod | Order Calanoida | *Acartia tonsa* Dana, 1849-1852 | marine copepod widely distributed throughout the world, in some locations considered an invasive species, generally used for ecotoxicity tests verified for lethality in adults (but also for larval development, feeding, egg production, success in egg hatching and production of fecal pellets) |
|  | Copepod | Order Calanoida | *Temona longicornis* (Müller OF, 1785) | omnivorous marine copepod, widely distributed in the North Atlantic, generally used for ecotoxicity tests checking for lethality in juveniles and adults (but also feeding, egg production, egg hatching success and fecal pellet production) |
|  | Copepod | Order Calanoida | *Calanus helgolandicus* (Claus, 1863) | marine copepod widely distributed in the North Atlantic, key to assessing the planktonic trophic chain, from producers to higher levels, used for ecotoxicity tests verified for adult lethality |
|  | Teleostei | Family Moronidae | *Dicentrarchus labrax* (Linnaeus, 1758) | also mentioned as *Dicentrarchus excentricus,* European seabass, a very sensitive species for evaluating erythrocyte genotoxicity and biotransformation responses to polynuclear aromatic hydrocarbons (PAHs), used in tests with juveniles, regarding lethality and growth |

| Organisms used in effluent ecotoxicity tests \| EGCS open-loop | | | | |
|---|---|---|---|---|
| test organism | Class | Order/Family | species | considerations |
|  | Teleostei | Family Atherinopsidae | *Menidia beryllina* (Cope, 1867) | inland silverside, a species easily cultivated in the laboratory with induced spawning, very well distributed in North America (Atlantic) in varied habitats, basis in the diet of many species of larger fish of commercial interest, used for ecotoxicity tests verified in terms of lethality and larval growth |
|  | Teleostei | Family Adrianichthyidae | *Oryzias javanicus* (Bleeker, 1854) | Javanese rice-fish, a small tropical marine species from East Asia and the Indian Ocean, considered an excellent ecotoxicological experimental organism to assess lethality against various sources of pollution and the effects of global climate change on the ocean |

Table 15: Results of ecotoxicity tests compiled from the literature for open-loop *Scrubbers* effluent (ESGC), generalized and organized by test organism. Source: CLS Brasil.

**Summary of ecotoxicity results of EGSE generated by open-loop EGCS selected from the literature** (EGSE concentrations that affect between 10 and 50% of the tested population, in a given time, among acute and chronic tests; NT = non-toxic)

| test organism | Reference | Lethality | bioluminescence | larval growth or development | productivity primary and photosynthetic activity | feeding | egg production | successful hatching of eggs | production of fecal pellets |
|---|---|---|---|---|---|---|---|---|---|
| *Allivibrio fischeri* | Hunfnagl *et al.* (2005) | | NT | | | | | | |
| *Allivibrio fischeri* | Piconi *et al.* (2023) | | 18 - 41% | | | | | | |
| *Nodularia spumigena* | Ytreberg *et al.* (2019) | | | | 3.5 - 38.9% | | | | |
| *Dunaliella tertiolecta* | Piconi *et al.* (2023) | | | NT - 10% | | | | | |
| *Melosira arctica* | Ytreberg *et al.* (2019) | | | | 5.5 - 26.9% | | | | |
| *Phaeodactylum tricornutum* | Piconi *et al.* (2023) | | | NT - 15% | | | | | |
| *Skeletonema costatum* | Koyama *et al.* (2018) | | | 48 - 50% | | | | | |
| *Skeletonema costatum* | Word *et al.* (2024) | | | >100 % | | | | | |
| *Skeletonema* sp. | Kamper *et al.* (2021) | | | >91 % | | | | | |
| *Artemia salina* | Hunfnagl *et al.* (2005) | NT | | | | | | | |
| *Americamysis bahia* | Word *et al.* (2024) | >100 % | | | | | | | |
| *Acartia tonsa* | Koski *et al.* (2017a) | 10% | | | | 70% | 14 - 18% | 77 - 85% | 10% |
| *Acartia tonsa* | Koski *et al.* (2017b) | 10% | | | | 10 - 32% | | | |
| *Acartia tonsa* | Kamper *et al.* (2021) | >100 % | | 20 - 54% | | | | 80% | |
| *Acartia tonsa* | Piconi et al. (2023) | 5 - 19% | | 1.1 - 1.5% | | | | 7 - 30% | |
| *Temora longicornis* | Koski *et al.* (2017b) | 10% | | | | | | | |
| *Calanus helgolandicus* | Magnusson *et al.* (2018) | 1% | | 5% | | 1% | | | |
| *Calanus helgolandicus* | Thor *et al.* (2021) | 10.52% | | | | | | | |
| *Dicentrarchus labrax* | Kamper *et al.* (2021) | >91 % | | | | | | | |
| *Menidia beryllina* | Word *et al.* (2024) | 21,8 - >100% | | | | | | | |
| *Oryzias javanicus* | Koyama *et al.* (2018) | 35 - 100% | | | | | | | |

Among all the results compiled from the literature, and aiming at a more conservative approach, the final value considers the worst results of all of them (the lowest concentration reported in the literature), corresponding to **adverse effects** in at least 10% of the tested populations, caused by a **concentration of 1% EGSE.** The impact of EGSE discharge, although at a low concentration, was considered by Picone *et al.* (2023) as potentially critical, as it affects a crucial component of the marine food web (larval development of *Acartia tonsa*), possibly leading to losses throughout the food web due to resource restriction for planktivorous invertebrates and fish in their larval stages.

According to Gadd *et al.* (2020), several risk assessments regarding EGSE discharge are found in the literature, with mixed conclusions. Although EGSE dilution is expected to occur soon after disposal, exposure concentrations may be relevant in shipping routes. Effects in shipping routes and coastal waters were generally predicted to be low; however, effects in ports remain an area of uncertainty and potential concern due to lower contaminant dispersion and higher background concentrations of contaminants from other sources.

Coastal waters are particularly vulnerable to EGSE discharges due to high vessel traffic and high biodiversity (Picone *et al.*, 2023). Furthermore, the most significant impact is expected on planktonic organisms regardless of whether they spend all or part of their life cycle in the water column (Thor *et al.*, 2021). Marine plankton can be severely affected by EGSE discharges, and lethal and sublethal effects have been reported in copepods and microalgae (Koski *et al.*, 2017a; Thor *et al.*, 2021; Ytreberg *et al.*, 2019, 2021a, 2021b). Since the productivity of aquatic ecosystems can be highly dependent on the lower trophic levels according to bottom-up ecosystem regulation (Aebischer et al., 1990; Irigoien et al., 2004), adverse effects on plankton may have substantial consequences for the functioning of the entire ecosystem.

Even considering the low toxicity of the effluent compared to the dilution capacity of the medium, there is concern about the bioaccumulation of contaminants, especially in the port region, if this effluent is discharged in the region. On coastal and offshore *routes*, this concern is considerably reduced. However, on these routes, the synergistic effect of vessel traffic must be considered. In any situation, however, the biodegradation capacity of this effluent must be clearly and thoroughly assessed, even to be able to consider, or not, the effects of bioaccumulation.

If the idea of allowing the EGSE discharge in coastal regions and ports in Brazil is to be considered, a careful assessment should be carried out, also considering the benthic biota and all ecosystem interactions, not only with the EGSE to be discarded, but also with all other substances that may reach that ecosystem from any other source. In certain locations and/or situations, the EGSE discharge may be the last drop to induce an unfavorable change in the ecosystem, not only due to its chemical composition, but also due to bioaccumulation (Koski *et al.*, 2017a,b; Koyama *et al., 2018).* It is recommended that the decision whether or not to allow the discharge of *Scrubbers* wash water in port regions be localized and preceded by the implementation of an environmental characterization project to assess the region (mainly the hydrocarbonoclastic biota) and the implementation of an environmental monitoring project to continuously assess the possible effects of these discharges.

Additionally, the assessment of effluent ecotoxicity, while adhering to the engine power categorization adopted for the TLM evaluation, should consider representative organisms from at least three different levels. This is necessary because the TLM analysis clearly indicated that engine power influences the composition of the generated effluent, and therefore, its ecotoxicity.

## 2.3. Definition of Ecotoxicity Threshold

As described in the previous item (item 2.2 - Literature Review and Secondary Data Analysis), among all the results compiled from the literature, the most critical EGSE concentration value that causes adverse effects, in at least 10% of the population tested, was 1%.

However, for risk assessment, it is recommended that acute or chronic thresholds be converted to PNEC (Predicted No-Effect Concentration). This conversion was performed following the guidance of the ECHA (European Chemicals Agency) in Chapter 10 (Characterization of the dose-response for the environment) of the guidance document on information requirements and chemical safety assessment (ECHA, 2008). According to the ECHA document, since the conditions of laboratory test methods differ from natural conditions, it is considered more likely that ecosystems are more sensitive to chemicals than individual organisms in the laboratory. Therefore, test results are not used directly for risk assessment, and these should be assessed by extrapolating to natural conditions. This conversion is done based on an assessment factor, depending on whether it is a short-term threshold (acute threshold) or a long-term threshold (chronic threshold). Furthermore, the scarcer the data, the higher this assessment factor will be. Table 16 presents the assessment factors suggested by ECHA (2008).

Since 1% is a long-term (chronic) threshold, the evaluation factor used in this study was 100. This value is recommended for the case of predicted concentration of no observed effect of long-term toxicity (e.g., EC10 or NOEC) of three freshwater or saltwater species (usually algae and/or crustaceans and/or fish) representing three trophic levels. EC10 (Effective Concentration for 10%) is the concentration of a substance that causes an adverse effect in 10% of a test population or reduces a specific biological response (such as growth, reproduction, or survival rate) by 10%. NOEC (No Observed Effect Concentration) is the maximum concentration of a tested substance at which no statistically significant adverse effect is observed compared to the control group. In other words, it is the highest concentration at which no negative impact on the organism or ecosystem studied is detected.

Thus, the lowest toxic concentration value found, 1%, was divided by the evaluation factor of 100, generating **a PNEC of 0.01% (dilution factor of 10,000 times).** It should be noted that this threshold is conservative, since it is a value derived from the most toxic concentration found among all those reported in the selected literature.

This threshold is in the same order of magnitude as the results obtained by the TLM method. In the TLM, the LC50 values (lethal concentration for 50% of organisms) are obtained for each of the simulated PAHs, representing the short-term toxicity threshold. According to the ECHA (2008) guidelines and as implemented in other studies, such as Grath *et al.* (2014), the PNEC calculation is performed by dividing the lowest LC50 value found by the assessment factor, which varies depending on the number of trophic levels evaluated. For this study, a factor of 10,000 (more conservative) is considered appropriate, as recommended for a dataset with the lowest short-term (LC50) value from freshwater or marine representatives of three taxonomic groups (algae, crustaceans, and fish) across three trophic levels. Based on this approach, the PNEC obtained for the chemical compound with the lowest LC50, chrysene, is 0.0002792 µg/L, equivalent to 0.01% (a dilution factor of 10,000 times).

Table 16: Proposed assessment factors to derive the PNEC in marine (saltwater) environments depending on different data sets. Source: Adapted from ECHA (2008).

| Dataset | Assessment factor |
|---|---|
| Lowest short-term value (LC50) of freshwater or saltwater representatives of three taxonomic groups (algae, crustaceans and fish) from three trophic levels | 10,000 |
| Lowest short-term value (LC50) of freshwater or saltwater representatives of three taxonomic groups (algae, crustaceans, and fish) from three trophic levels + two additional marine taxonomic groups (e.g. echinoderms, molluscs) | 1,000 |
| A long-term result (e.g. EC10 or NOEC) (from studies of reproduction of freshwater or saltwater crustaceans or growth of fish) | 1,000 |
| Two long-term outcomes (e.g. EC10 or NOEC) of freshwater or saltwater species representing two trophic levels (algae and/or crustaceans and/or fish) | 500 |
| Lowest long-term outcome value (e.g. EC10 or NOEC) of three freshwater or saltwater species (typically algae and/or crustaceans and/or fish) representing three trophic levels | 100 |
| Two long-term results (e.g. EC10 or NOEC) from freshwater or saltwater species representing two trophic levels (algae and/or crustaceans and/or fish) + one long-term result from an additional marine taxonomic group (e.g. echinoderms, molluscs) | 50 |
| Lowest long-term outcome value (e.g. EC10 or NOEC) of three freshwater or saltwater species (typically algae and/or crustaceans and/or fish) representing three trophic levels + two long-term outcomes from additional marine taxonomic groups (e.g. echinoderms, molluscs) | 10 |

# 3. Hydrodynamic Modeling

To meet the objectives of this study and support the dispersion modeling (item 4), hydrodynamic numerical modeling of the area of interest was performed. Considering the different scales and phenomena involved, two distinct hydrodynamic models were used:

- **Coastal simulation**: covering the region of the Port of Tubarão and its surroundings (item 3.1); and
- **Offshore simulation**: covering the continental shelf area and the oceanic region furthest from the coast (item 3.2).

Numerical models are tools that aim to represent the dynamics and processes involved in the object of study through mathematical equations and parameterizations. Thus, models generate results that are approximations of the real state and have limitations and errors inherent to the method (e.g. truncation error, approximation error and parameterization of non-resolvable physical processes). All these sources contribute to divergences between the real and simulated state of the ocean. However, these two models allow a detailed analysis of the hydrodynamic characteristics at specific scales, contributing to a significantly more accurate representation of the dispersion processes in the study area.

## 3.1. Port of Tubarão

For the hydrodynamic simulation in the region of the Port of Tubarão and the Bay of Vitória, in Espírito Santo, the Delft3D model (DELTARES, 2021) was used, an advanced tool for simulating multidimensional hydrodynamic flows and transport phenomena.

Additional details on coastal hydrodynamic modeling and its results are available in ANNEX I, and a brief context will be given here.

The model has a high-resolution numerical grid that covers the river and estuarine region, incorporating bathymetric data extracted from Nautical Charts maintained by the Directorate of Hydrography and Navigation (DHN). The model domain is shown in Figure 14.

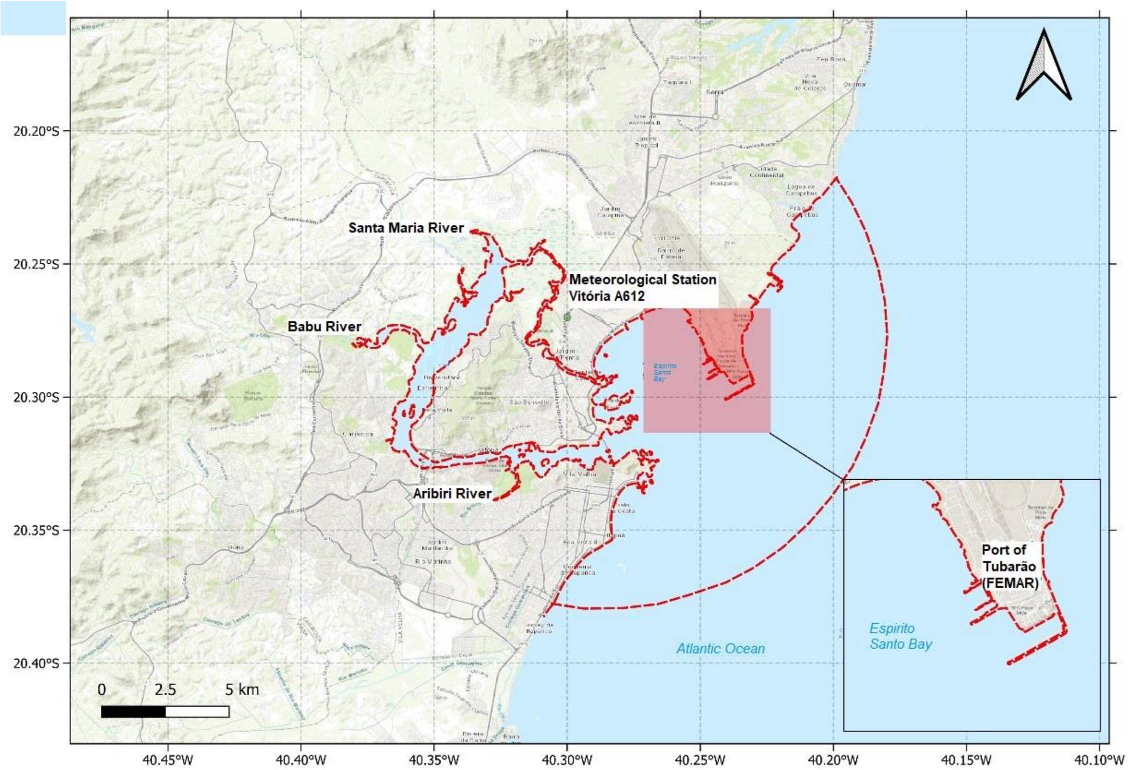


Figure 14: Domain of hydrodynamic modeling performed with DELFT3D for the Port of Tubarão and surroundings.

To adequately represent the diverse environmental conditions, the simulation period covered 1 full year, from January to December 2012.

When creating a simulation in a limited area of the ocean, one of the most important factors is the appropriate choice of boundary conditions to be used. This choice must be made with great care, since the results will be a consequence of the conditions chosen, i.e., the information contained in the boundaries must have at least some adherences to reality so that it is possible to represent the phenomena of interest within the simulation domain. Therefore, for the boundary conditions of coastal hydrodynamic modeling, the following were used:

- **Tide:** astronomical tide series from the global tidal model TPXO9.v5 atlas;
- **Wind:** wind data from the National Institute of Meteorology (INMET);
- **River:** river flows from hydrological data maintained by the National Water Agency (ANA); and
- **Temperature and salinity:** data from the hydrodynamic model developed by CLS Brasil (presented in item 3.2).

The coastal simulation allowed the detailing of the currents inside the Port of Tubarão and the region of Vitória Bay. The results showed that the currents are predominantly influenced by the tides, especially inside the estuaries and in the protected area of the Port of Vitória. Inside the sheltered area of the port, the current velocities are very low, varying between 1 and 5 cm/s, unfavorable conditions for the dispersion of pollutants.

## 3.2. Navigation Routes

For hydrodynamic simulations in the offshore region, the Regional Ocean Modeling System - ROMS (Haidvogel *et al., 2008)* was used. ROMS is a free-surface ocean model, with terrain-following coordinates and primitive equations, classified as state-of-the-art in hydrodynamic modeling.

The hydrodynamic model used in this study contains current data for the region between January 2012 and December 2014, covering three base years. The temporal extent is sufficiently long to accurately reproduce the ocean circulation in the studied region, with observation of the main features (e.g., the Brazil Current) and their space-time variations, considering seasonal changes (e.g., meanders and vortices). The results of this model have been used by CLS Brasil in various licensing processes in recent years (i.e., CLS Brasil, 2022a; CLS Brasil 2022b), providing forces for pollutant modeling studies, such as oil, gravel, production water, among others.

Regarding spatial extent, a numerical grid was designed (Figure 15), extending from 39° S to 14° S, and 60° W to 25° W. The grid domain covers the Brazilian east coast from the state of Bahia to the end of Rio Grande do Sul. Furthermore, it extends even further south, ending just after the city of Mar del Plata, in Argentina. The grid encompasses the continental shelf, the slope and part of the adjacent ocean basins.

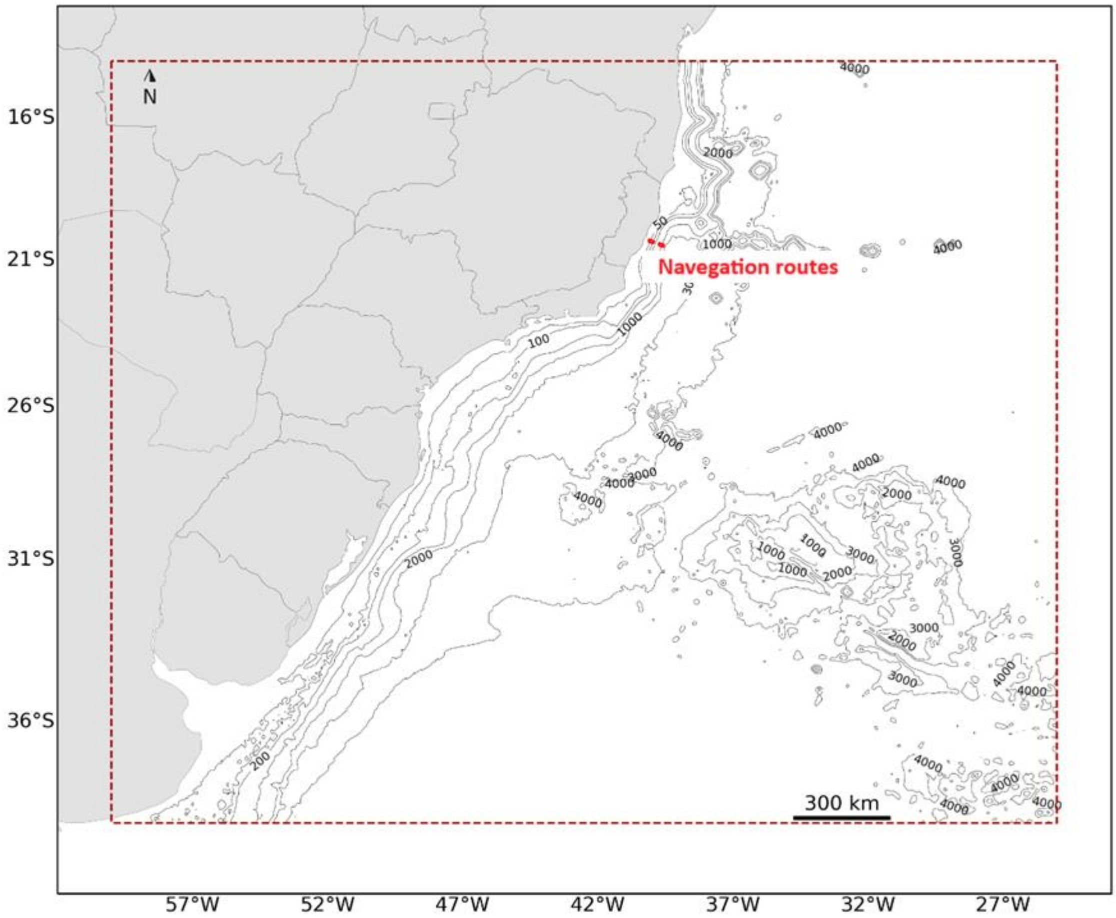


Figure 15: Modeling region conducted with ROMS. The dotted red polygon represents the limits of the hydrodynamic model grid and the navigation routes are marked in solid red.

The grid resolution is 1/16° (~6 km) and was chosen both to ensure satisfactory reproduction of the main bathymetric and coastline features and to allow for compatible computational performance. This choice resulted in a grid with 254,694 points at each horizontal level (sigma layer), with 30 vertical levels (sigma layers).

For the boundary conditions, it was decided to use results from global models, since it is impossible to have time series collected *in situ* of all meteorological and oceanographic parameters necessary for modeling along the entire boundary. By using these results in regional models, the focus is on the regions of interest, refining details such as the coastline, bathymetry, tide propagation, among others.

As initial and boundary conditions for the ocean forecasting system in the study region, data on temperature, salinity, sea surface height, and currents from the Mercator Global Analysis were used. This project provides, on a weekly basis, the results of the global ocean analysis and forecast for a 14-day period, with a spatial resolution of 1/12° and a temporal resolution of 24 hours. The global ocean model used in Mercator is NEMO (Nucleus for European Models of the Ocean), forced by atmospheric fields obtained from the ECMWF Analysis (European Center for Medium-Range Weather Forecasts).

NEMO assimilates current, surface height and SST data obtained from satellites, in addition to temperature and salinity data obtained *in situ,* which undergo careful quality control (Larnicol *et al*., 2006).

The model was initialized with the Mercator simulation results, interpolated to the spatial resolution (vertical and horizontal) of the grid used in ROMS, which is considered a nesting of models. In this case, the regional model for the simulated region (ROMS) is being nested in a global model (Mercator) in offline mode, that is, the boundary conditions used in the smaller area and higher resolution model were extracted from a larger area and lower resolution model previously run.

In addition to the initial boundary condition, other boundary conditions are required and have been used. These are:

→ **Bottom boundary condition:** result of cubic interpolation of information from digitalized nautical charts (DHN) and the global Earth surface relief model ETOPO 1 (Amante & Eakins, 2009). ETOPO1 is a global Earth surface relief model with spatial resolution of 1 arc minute, which integrates ocean topography and bathymetry.

→ **Surface boundary conditions** (ocean/atmosphere interface fluxes): data on zonal and meridional wind components, air temperature, atmospheric pressure, relative humidity, precipitation rate, and shortwave and longwave radiation were obtained through the ERA5 project, the latest generation of the ECMWF (European Centre for Medium-Range Forecasts) Reanalysis. ERA5 is the first product to be deployed as an operational service and has an hourly temporal and spatial resolution of 31 km at 137 atmospheric levels, from the surface to 0.01 hPa.

→ **Lateral boundary condition:** for the closed boundary (to the west), velocities tangential to the boundary were used, which could be different from zero, and for the three open boundaries (north, east and south), the results of temperature, salinity, sea surface height and daily currents from the Mercator were used. The Mercator has a spatial resolution of 1/12° and its results were interpolated in vertical sections located at the edges of the model.

→ **Tide:** harmonic constants from the global tidal model TPXO8 (Egbert; Erofeeva, 2002). This model has a resolution of 1/30° and uses data from the TOPEX/POSEIDON altimetric satellite as the primary source for assimilation.

The results show that the circulation patterns in the oceanic region and on the continental shelf follow those described in the literature, with good representation in the monthly mean fields. On the continental shelf, the currents present southwesterly flow between September and February and are less intense, with flow inversion in June and July, due to the Coastal Current.

The Brazil Current is observed at depths below the surface in the Santos and Pelotas basins, with a characteristic southwesterly flow. In the Campos Basin, mesoscale eddies mask the position of the Brazil Current, but southerly flow is evident down to 250 m depth. This range increases gradually with latitude.

In the Santos Basin, the Brazil Current presents intense meandering after the break of the coastline, with influences up to 500 meters deep at certain latitudes. The behavior of the current, with greater intensities at the surface and gradual reduction up to the shear zone with the Intermediate Boundary Current, is also in agreement with what is expected in the literature.

The currents reach magnitudes of up to 110 cm/s, while in the deepest oceanic region, they have magnitudes of approximately 70 cm/s.

During the evaluation of the representativeness of the hydrodynamic model, several parameters were used, such as tidal oscillation, surface temperature and currents (surface and deep) to be validated with *in-situ data* and remote sensing, both punctually and spatially. The quantitative differences found are within an acceptable range (e.g.: <13 cm in the tide; 0.2°C in the SST; 0.05 m/s in the surface currents). For example, Figure 16 shows the comparison of the tidal elevation calculated by the numerical model at the grid point closest to the station with data from the Vitória-ES tide gauge station for the entire modeling period. Statistically, the mean absolute error was 0.1 m with a Pearson linear correlation coefficient of 0.93. Although the tides simulated by the hydrodynamic model presented a slight underestimation of the amplitudes, it is noted that they were well represented from a statistical point of view.

Although some analyses indicate an underestimation of currents in specific situations, in general, statistical analyses of the distributions show an oscillating behavior of overestimation-underestimation. It is concluded that the model can represent the main phenomena of the region, such as the flow of the Brazil Current and the formation of meanders and vortices, both in space and in time.

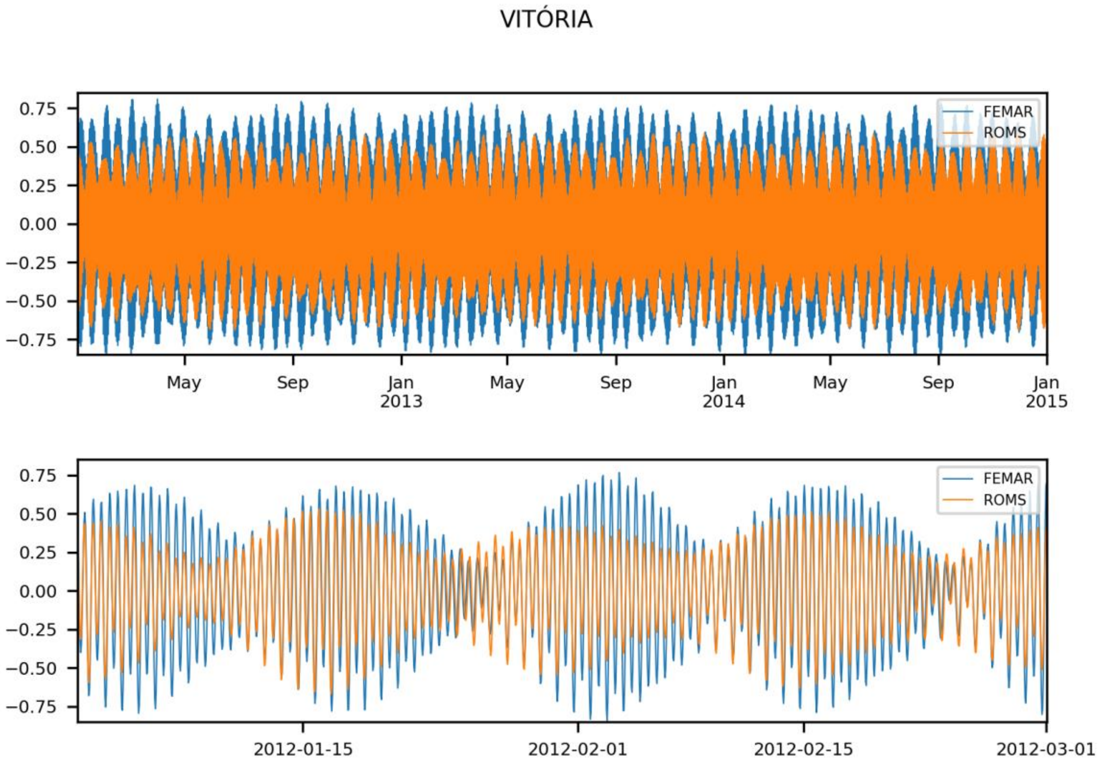


Figure 16: Comparison for the Vitória station – ES. Reconstituted series from FEMAR (blue) and the ROMS model (orange), for the entire period (above) and in zoom (below).

# 4. Wash Water Dispersion Modeling

This item describes the results obtained in the numerical modeling of the dispersion of Scrubbers wash water, both for the Port of Tubarão and for coastal and offshore shipping routes. The choice of these locations followed the same pattern proposed in Vale & CLS Brasil (2024), in which other simulations were carried out using the MAMPEC model – to evaluate changes in water and sediment quality – and AquaEnv – to evaluate changes in pH and alkalinity. The areas cover both the sheltered area situation (with vessels berthed in the port) and the situation of vessels in transit (shipping routes).

Figure 17 shows the location of the areas considered, as well as the washing water discharge points, justified in the following item (4.1 - Characteristics of the Discharges).

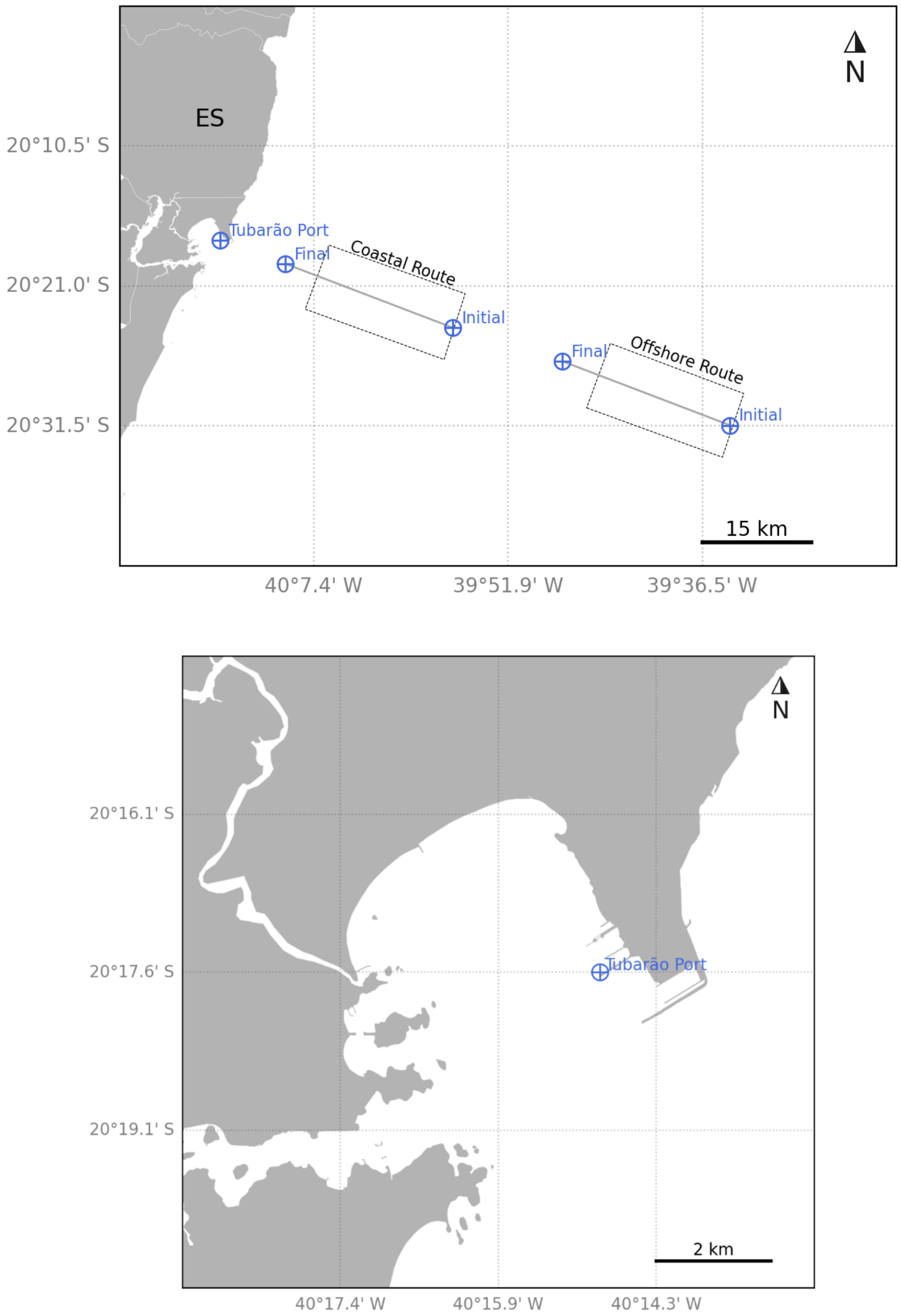


Figure 17: Location of the Port of Tubarão and the coastal and offshore navigation routes considered in this study. The lower map provides a focus on the Port of Tubarão.

## 4.1. Characteristics of the Discharges

The discharge points considered in the simulations are presented in Figure 17. Table 17 presents the coordinates and depth of the discharge points. Two discharge approaches were used:

- In the Port of Tubarão, a fixed discharge was considered, to simulate the vessel berthed in the port; and
- While on the shipping routes, mobile sources were considered, to simulate the vessel moving along the coastal and offshore routes.

Table 17: Geographic coordinates (WGS84 *Datum*) and local depth of the simulated points.

| Point | Latitude | Longitude | Local depth (m) |
|---|---|---|---|
| Port of Tubarão (fixed point) | 20°17'33.155''S | 40°14'50.305''W | 10 |
| Coastal Route (initial coordinate) | 20°24'08,208''S | 39°56'17.405''W | 53 |
| Offshore Route (initial coordinate) | 20°31'27.390''S | 39°34'13.998''W | 1,901 |

To represent situations analogous to reality, these areas are related to different engine powers of the vessels, namely:

- Port of Tubarão: located in the Port of Tubarão, in Vitória/ES, and its surroundings. Considers the situation of the lowest possible power of the ships;
- Coastal navigation route: located on the continental shelf, in a shallower water depth, and at distances of less than 24 nautical miles. Considers an intermediate power of the ships;
- Offshore navigation route: located in the oceanic region, in a deeper water depth, with distances greater than 24 nautical miles. Considers the maximum power of the ships.

Information from Vale & CLS Brasil (2024) was used to determine the discharge flow rate ($V_{AD}$). Equation 5 provides the formula for calculating the flow rate.

Equation 5: Calculation of discharge flow rate ($m^3/h$).

$$V_{AD} = P_{vessels} * V_{scrubber}$$

Where

$V_{AD}$ is the discharge water flow rate ($m^3/h$)

$P_{vessels}$ is the power of the vessels (MW)

$V_{scrubber}$ is the flow rate of open-loop Scrubbers per energy produced ($m^3/MWh$)

The Scrubbers' flow rate per energy produced was estimated at 90 $m^3$/MWh, as indicated in OSPAR (2022) and referenced in DHI (2021). The vessels' power values were calculated in Vale & CLS Brasil (2024) for each vessel code.

Table 18 presents the engine power and the flow rate for each vessel code for the Port of Tubarão, the coastal route and the offshore route. For the modeling, it was decided to use the maximum discharge flow rate in each power scenario (values highlighted).

Table 18: Engine power (MW), Scrubbers flow rate ($m^3$/MWh), and daily discharge water flow rate ($m^3$/day) for each vessel code at the Port of Tubarão, on the coastal navigation route, and the offshore navigation route. The maximum flow rate used in the modeling is highlighted in bold. Source: Adapted from Vale & CLS Brasil (2024).

| Code | $P_{vessels}$ (MW) | $V_{scrubber}$ ($m^3$/MWh) | $V_{AD}$ ($m^3$/day) |
|---|---|---|---|
| Port of Tubarão | | | |
| A | 0.60 | 90 | **1,296.0** |
| B | 0.60 | 90 | **1,296.0** |
| C | 0.60 | 90 | **1,296.0** |
| Coastal Route | | | |
| A | 15.20 | 90 | **32,832.0** |
| B | 15.20 | 90 | **32,832.0** |
| C | 7.85 | 90 | 16,956.0 |
| Offshore Route | | | |
| A | 19.07 | 90 | **41,191.2** |
| B | 19.00 | 90 | 41,040.0 |
| C | 14.60 | 90 | 31,536.0 |

For all scenarios, a 5 m deep discharge was stipulated, following a vertical downward orientation (180°) and a 40 cm discharge diameter. For the discharge scenario at the Port of Tubarão, the discharge time considered was 15 days from a fixed source, while in the navigation route scenarios, the discharge time was 1 hour from a mobile source. For these moving discharges, a vessel speed of 13.5 knots was considered – the reference value for navigation routes adopted in Vale & CLS Brasil (2024) – with a direction oriented towards the port of Tubarão (Figure 17), specifically 291° (NW).

It is estimated that more than 90% of the effluent characteristic of *Scrubbers* wash water is composed of seawater. Therefore, it is reasonable to assume that its density will be very close to that of seawater. For each scenario and location, the density of seawater at the surface was calculated and considered as the effluent density in the modeling, to coincide with the density entered in the respective simulation. For this estimate, the temperature and salinity profiles presented in item 4.3.4 (Salinity and Sea Temperature) were considered; the densities obtained are also presented in this item, specifically in Table 36.

Table 19 presents a summary of the main discharge parameters considered in the modeling.

Table 19: Main characteristics of discharges.

| Parameter | | Value | Unit |
|---|---|---|---|
| Depth of discharge | | 5 | m |
| Discharge angle | | vertical down | - |
| Discharge diameter | | 40 | cm |
| Discharge type | Port of Tubarão | fixed | - |
| | Navigation routes | mobile | |
| Discharge flow rate | Port of Tubarão | 1,296.0 | $m^3$/day |
| | Coastal navigation route | 32,832.0 | |
| | Offshore shipping route | 41,191.2 | |
| Discharge duration | Port of Tubarão | 15 | days |
| | Navigation routes | 1 | h |

## 4.2. Modeling Strategies

### 4.2.1 Dispersion Model

DREAM (Dose-Related Exposure Assessment Model) is a three-dimensional Lagrangian particle model developed to assess the consequences of the discharge of various types of effluents into the marine environment. It has a dynamically coupled near-field model, allowing the representation of substances on the water surface, dissolved in the water column, in droplets, or solid particles dispersed in the water column.

The near-field (or dynamic phase) is divided into the jet phase and dynamic collapse phase. The jet phase corresponds to the initial dilution of the plume, where the forces of momentum and the dynamic effects of local currents result in rapid mixing and dilution of the plume in the receiving water body. This phase occurs while the plume has its motion, given by the discharge velocity or by the difference in density in relation to the ambient water. The phase ends when the discharged effluent encounters a horizontal surface (sea bottom or surface) or stabilizes at a neutral buoyancy level. At the end of this first phase, the dynamic collapse phase begins, where the effluent spreads to the depth at which it stabilized. This difference tends to decrease over time and, at some point, its contribution to the spreading of the effluent will be less than the ambient turbulence.

The third and final phase begins: the far field (or passive dispersion). The effluent, except for the vertical velocity associated with each constituent, has no movement of its own and follows only local hydrodynamics. Mineral particles, such as gravel and heavy materials, may detach from the plume depending on the deposition rate and sinking velocity. Figure 18 presents a schematic representation of this dispersive process.

The numerical formulation of the near-field model (Plume3D) is based on the formulations of Koh & Chang (1973). For passive scattering, a Lagrangian method described in Reed & Hetland (2002) is used.

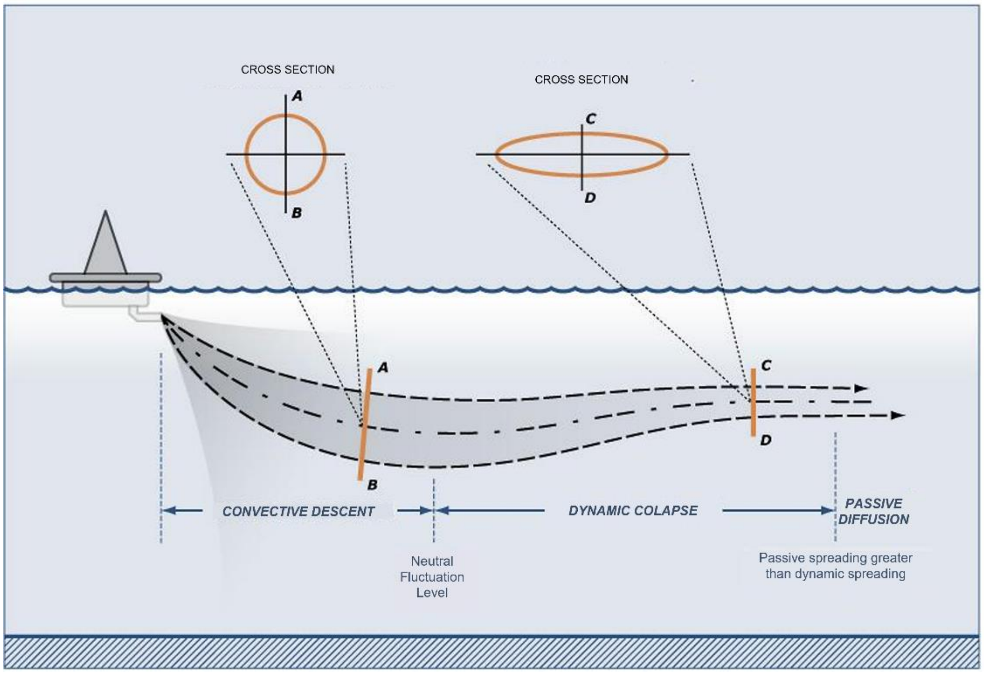


Figure 18: Schematic representation of the three phases described by the effluent. Source: Modified from Brandsma & Smith (1999).

### 4.2.2 Calculation of Environmental Risk

Environmental risk assessment is calculated by comparing exposure and environmental sensitivity, based on the PEC/PNEC ratio. PEC (Predicted Environmental Concentration) values are obtained through effluent dispersion modeling, resulting in a three-dimensional spatial output that varies over time. In contrast, PNEC (Predicted No-Effect Concentration) values are derived from ecotoxicological data. As described in item 2.3 (Definition of Ecotoxicity Threshold), **the PNEC threshold considered in this study is 0.01% (dilution factor of 10,000 times).**

Figure 19 illustrates the relationship between the PEC/PNEC ratio and the associated risk. When PEC/PNEC = 1, it indicates that the PEC value is equal to the PNEC, corresponding to a risk level of 5% — that is, only 5% of the community, usually the most sensitive species, may be affected. When PEC/PNEC > 1, it indicates that the PEC values exceed the PNEC, and there is an associated risk. On the other hand, when PEC/PNEC < 1, the risk is considered acceptable (RYE *et al.*, 2004).

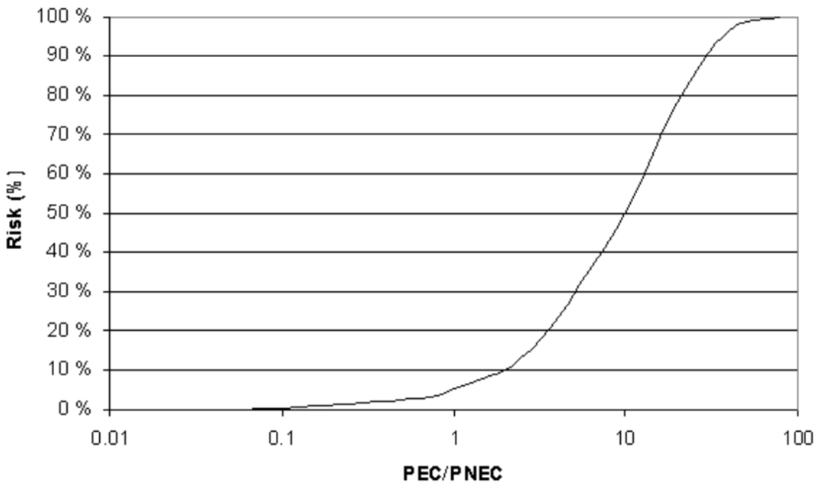


Figure 19: PEC/PNEC ratio and associated risk. Source: SINTEF (2024).

The significant risk maps (>5%) presented in this study are essential to understanding the spatial distribution of potential adverse environmental effects. In the water column, where significant risk tends to be temporary, information on the duration of these risk occurrences is also relevant to assess the potential impact of stressors. Therefore, CLS Brasil developed a methodology to obtain this result, since the DREAM model does not provide it.

This methodology involves iterating over the simulated time, counting the number of times each cell presents a significant risk (>5%). This value is then multiplied by the simulation output frequency, resulting in the total time each cell was at significant risk. The risk result used in this post-processing is the integrated risk across the water column. It is important to note that this approach is conservative, as it counts each occurrence of significant risk in each cell, rather than considering only consecutive occurrences.

### 4.2.3 Simulation Parameters

Simulations in deterministic mode were performed to evaluate the dispersion of effluent on the surface. Deterministic modeling consists of studying the behavior of the contaminant in a given environmental scenario, presenting snapshots of this behavior at times defined by the user.

To run the simulations, it is necessary to specify the simulation duration, the time step, the output step and the number of particles. Table 20 presents all these parameters. For the port simulations, a 15-day discharge and a monitoring time of another 15 days after the discharge were considered, totaling 30 days of simulation. For the shipping routes, a 1-hour discard and approximately 5 days of monitoring were considered, totaling 5 days of simulation. The discharge times were previously presented in Table 19.

Table 20: Information about simulation duration, number of particles, time step, and output of results.

| Parameter | | Value | Unit |
|---|---|---|---|
| Duration of simulations | Port of Tubarão | 30 | days |
| | Navigation routes | 5 | |
| Number of particles | Port of Tubarão | 20,000 | - |
| | Navigation routes | 5,000 | |
| Time step | Port of Tubarão | 5 | min |
| | Navigation routes | 1 to 2 | min |
| Results output | Port of Tubarão | 30 | min |
| | Navigation routes | 2 to 4 | min |

In modeling studies, the relationship between the resolution of the designed grid and the scale of the phenomenon being studied is vital to obtaining good results. It should be noted that a large grid that covers the entire dispersion region may not have sufficient resolution to accurately map the region closest to the discharge, with higher concentrations. In such cases, an artificial numerical dilution may occur, since the concentration results must be seen as average values in the volume defined by the dimensions of the grid cells.

Since the main objective of this study is to analyze the dispersion of wash water, two regular grids with different resolutions were chosen, one with a higher resolution for the Port of Tubarão and two with a lower resolution for each navigation route. The use of different grid configurations for the port area and navigation routes allowed for maintaining a high resolution in the coastal region, in addition to covering the entire area of the routes.

The grid used in the port has a zonal and meridional resolution of 10 m and a vertical resolution of 5 m. While the grids of the navigation routes have a zonal and meridional resolution of 25 m and a vertical resolution of 10 m. Table 21 presents the main information on the grids used in the simulations.

Table 21: Information about the grid configurations used in this study.

| Location | Limits | Extension | Horizontal Resolution | Vertical Resolution | N° Elements |
|---|---|---|---|---|---|
| Port of Tubarão | 20°21' - 20°16' S<br>40°18' - 40°12' W | 10 km<br>(E-W and N-S) | 10 m | 5 m | 1,000 x 1,000 |
| Coastal Route | 20°31'S - 20°18'S<br>40°10' - 39°56'W | 25 km<br>(E-W and N-S) | 25 m | 10 m | 1,000 x 1,000 |
| Offshore Route | 20°38'S - 20°25'S<br>39°48' - 39°33'W | 25 km<br>(E-W and N-S) | 25 m | 10 m | 1,000 x 1,000 |

## 4.3. Environmental Forces

The environmental forces used in this study will be presented below: winds, currents, and sea salinity and temperature profiles. The selection of deterministic scenarios is also described in this item.

### 4.3.1 Winds

The wind data used as a force in the model come from ERA5, the latest generation of the ECMWF (European Centre for Medium-Range Weather Forecasts) Reanalysis and the first produced as an operational service, with an hourly temporal and spatial resolution of 31 km at 137 atmospheric levels, from the surface to 0.01 hPa (Hennermann, 2017).

ERA5 combines large quantities of historical observations into global estimates using advanced modeling and data assimilation systems. ERA5 was produced using 4DVar data assimilation in CY41R2 of ECMWF's Integrated Forecast System (IFS). Observations used in ERA-5 data assimilation include satellite data and *in situ* data. Among the satellite data are data from different sensors from a range of satellites that include AQUA, ERS-2, ENVISAT, JASON-1, and JASON-2, among many others. *In situ* observations come from the WMO Information System (WIS) and include data from land stations, drift buoys, data from vessels, radiosondes, and radars, among others.

Below are monthly wind analyses for the ERA5 grid points closest to the discharge points considered in each scenario.

#### 4.3.1.1 Port of Tubarão

Figure 20 shows the wind roses for the point closest to the port discharge site, in addition to the occurrence tables of direction and intensity (Table 22 and Table 23), for the year 2012. N and NNE winds are predominant with intensities between 4 and 8 m/s.

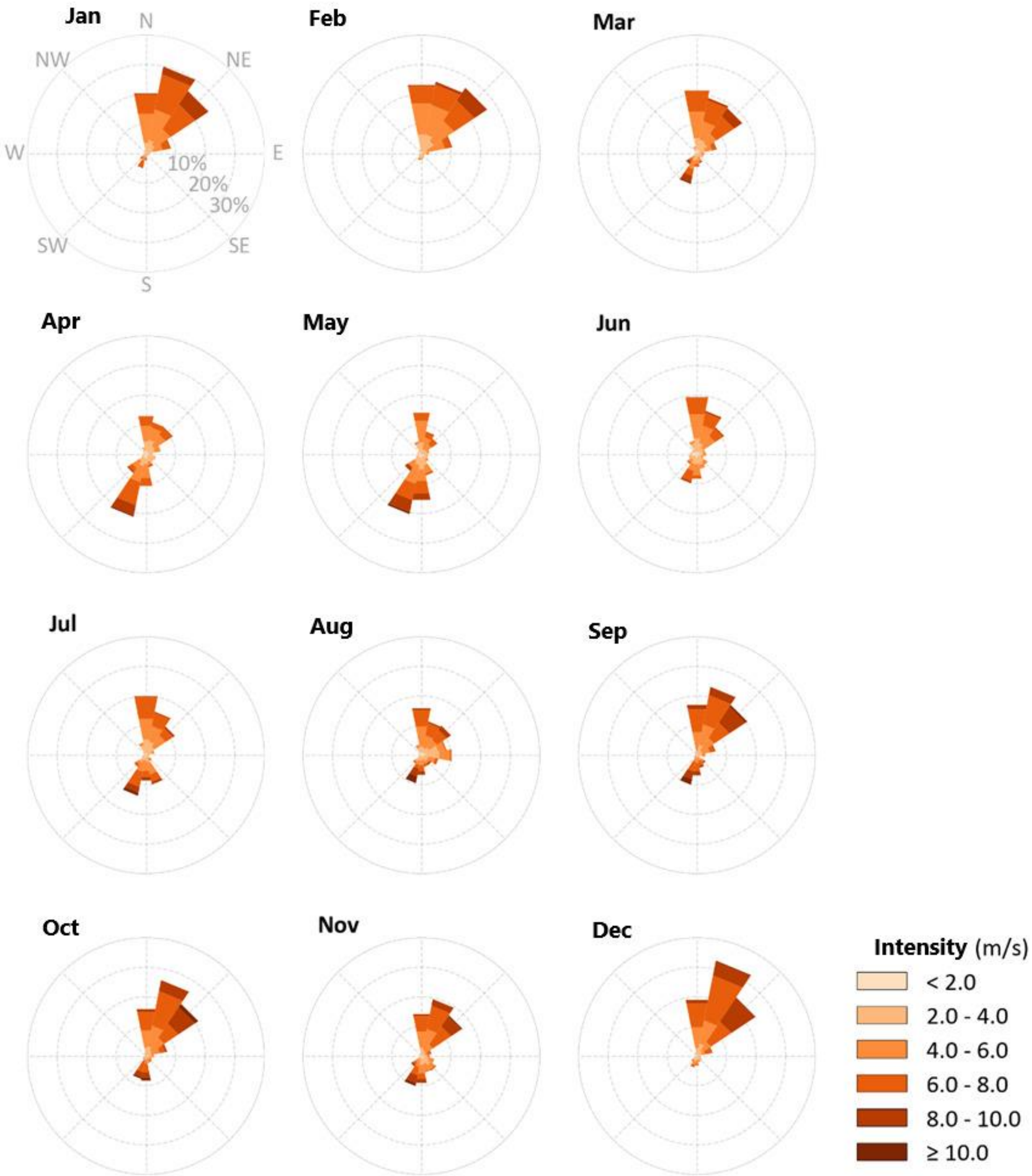


Figure 20: Wind roses, for the year 2012, from the analyzed point to the Port of Tubarão.

Table 22: Monthly occurrence (%) of wind direction, for the year 2012, from the analyzed point to the Port of Tubarão.

| Direction | Months | | | | | | | | | | | |
|---|---|---|---|---|---|---|---|---|---|---|---|---|
| | J | F | M | A | M | J | J | A | S | O | N | D |
| N | 20.7 | 23.58 | 21.68 | 13.15 | 14.34 | 19.68 | 20.3 | 16.08 | 17.31 | 16.17 | 14.4 | 19.35 |
| NNE | 29.97 | 24.75 | 19.18 | 11.11 | 7.93 | 15 | 15.01 | 11.65 | 23.56 | 26.16 | 19.63 | 32.89 |
| NE | 25.45 | 26.72 | 18.46 | 10.93 | 6.54 | 11.11 | 11.74 | 12.05 | 20.46 | 21.24 | 16.62 | 23.84 |
| ENE | 8.6 | 10.64 | 6.9 | 5.14 | 2.73 | 2.92 | 3 | 8.69 | 6.44 | 7.35 | 3.47 | 5.42 |
| E | 1.25 | 2.55 | 2.46 | 2.27 | 2.24 | 3.15 | 0.94 | 10.35 | 2.73 | 2.73 | 2.87 | 1.08 |
| ESE | 0.81 | 0.83 | 2.33 | 3.43 | 2.33 | 2.36 | 0.94 | 5.87 | 0.88 | 2.02 | 4.44 | 1.52 |
| SE | 0.67 | 1.27 | 1.79 | 2.96 | 2.96 | 4.4 | 2.28 | 4.03 | 3.61 | 2.42 | 6.02 | 2.06 |
| SSE | 0.4 | 1.76 | 3.36 | 4.49 | 7.3 | 5.09 | 10.08 | 4.08 | 4.4 | 2.46 | 5.69 | 2.2 |
| S | 2.28 | 2.16 | 4.48 | 10.88 | 15.68 | 8.38 | 8.69 | 6.77 | 6.85 | 8.47 | 9.21 | 3.23 |
| SSW | 5.06 | 2.35 | 10.48 | 21.53 | 20.61 | 9.95 | 13.98 | 9.63 | 10.19 | 7.89 | 10.32 | 3.94 |
| SW | 2.42 | 1.03 | 4.39 | 7.64 | 6.77 | 4.07 | 4.84 | 3.45 | 0.97 | 1.16 | 4.21 | 2.24 |
| WSW | 0.4 | 0.54 | 0.45 | 1.48 | 1.97 | 2.78 | 1.43 | 1.03 | 0.28 | 0.31 | 0.56 | 0.36 |
| W | 0.45 | 0.1 | 0.63 | 0.65 | 1.21 | 2.41 | 0.63 | 0.81 | 0.32 | 0.09 | 0.46 | 0.09 |
| WNW | 0.22 | 0.15 | 0.45 | 0.69 | 1.57 | 1.99 | 0.49 | 0.54 | 0.28 | 0.18 | 0.46 | 0.13 |
| NW | 0.22 | 0.1 | 0.54 | 1.16 | 1.25 | 1.94 | 1.21 | 1.3 | 0.46 | 0.31 | 0.65 | 0.4 |
| NNW | 1.08 | 1.47 | 2.42 | 2.5 | 4.57 | 4.77 | 4.44 | 3.67 | 1.25 | 1.03 | 0.97 | 1.25 |

Table 23: Monthly occurrence (%) of wind intensity, for the year 2012, from the analyzed point to the Port of Tubarão.

| Months | Intensity (m/s) | | | | | |
|---|---|---|---|---|---|---|
| | < 2.0 | 2.0 - 4.0 | 4.0 - 6.0 | 6.0 - 8.0 | 8.0 - 10.0 | ≥ 10.0 |
| Jan | 3.36 | 17.38 | 34.99 | 35.48 | 8.6 | 0.18 |
| Feb | 6.27 | 25.2 | 38.28 | 23.43 | 6.76 | 0.05 |
| Mar | 8.6 | 24.15 | 31 | 27.55 | 8.11 | 0.58 |
| Apr | 13.56 | 29.26 | 31.44 | 20.56 | 4.77 | 0.42 |
| May | 12.32 | 28.9 | 31.99 | 18.32 | 7.66 | 0.81 |
| Jun | 15.83 | 30.37 | 33.15 | 18.89 | 1.76 | - |
| Jul | 7.57 | 27.33 | 31.85 | 26.66 | 5.38 | 1.21 |
| Aug | 11.74 | 27.46 | 30.2 | 20.74 | 7.3 | 2.55 |
| Sep | 4.77 | 13.8 | 27.5 | 34.95 | 15.97 | 3.01 |
| Oct | 4.39 | 15.5 | 27.42 | 34.09 | 15.5 | 3.09 |
| Nov | 8.38 | 18.61 | 30.79 | 28.94 | 11.3 | 1.99 |
| Dec | 5.65 | 17.92 | 24.15 | 36.02 | 15.73 | 0.54 |

### 4.3.1.2 Coastal Shipping Route

Figure 21 shows the wind roses for the point closest to the discharge site on the coastal shipping route, in addition to the occurrence tables of direction and intensity (Table 24 and Table 25), for the years 2012 to 2014. NNE and NE winds are predominant with intensities between 4 and 8 m/s.

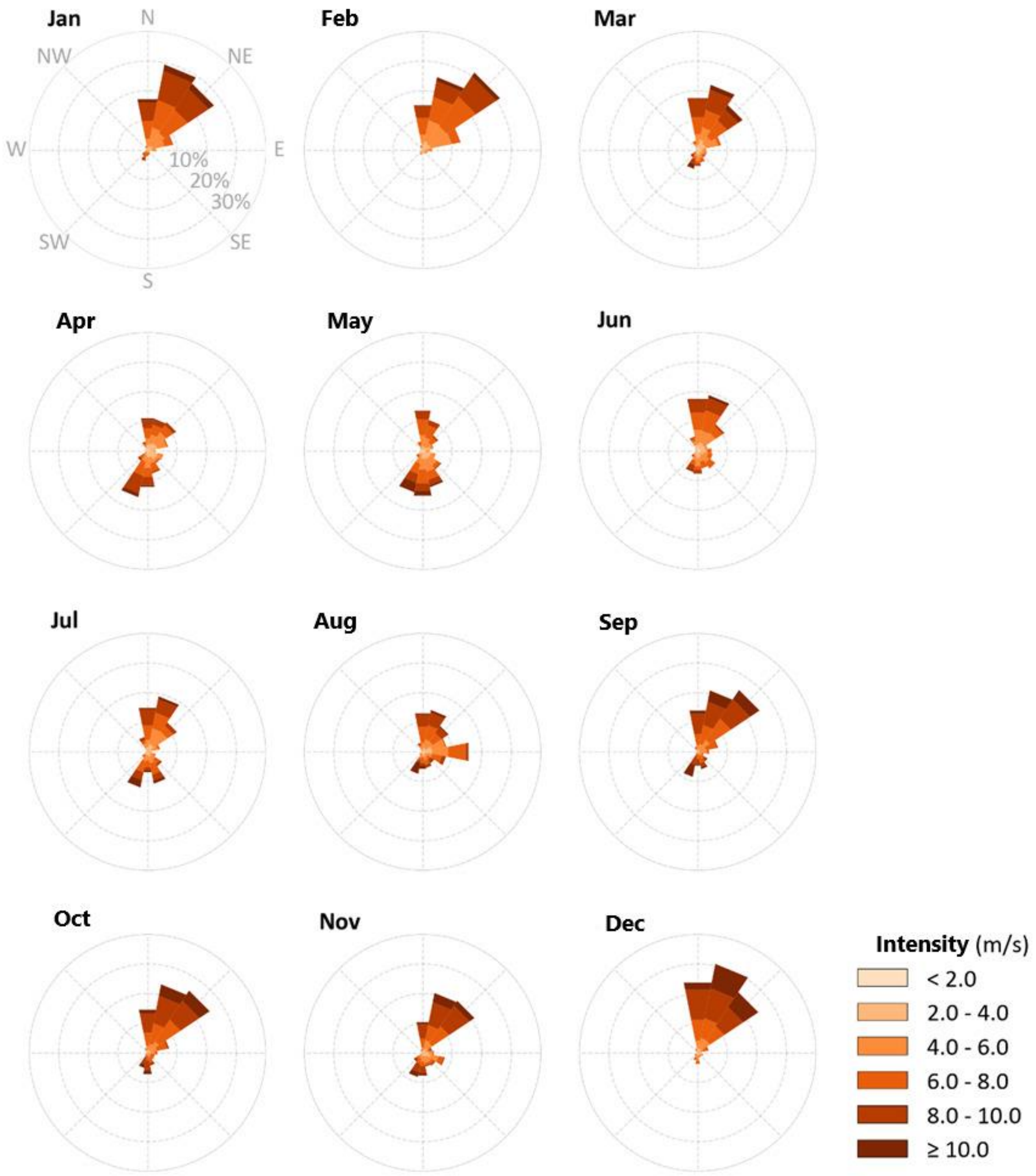


Figure 21: Wind roses, for the years 2012 to 2014, from the analyzed point to the coastal navigation route.

Table 24: Monthly occurrence (%) of wind direction, for the years 2012 to 2014, from the analyzed point to the coastal navigation route.

| Direction | Months | | | | | | | | | | | |
|---|---|---|---|---|---|---|---|---|---|---|---|---|
| | J | F | M | A | M | J | J | A | S | O | N | D |
| N | 17.47 | 15.39 | 17.92 | 11.2 | 13.89 | 17.87 | 15.14 | 13.26 | 14.21 | 14.83 | 10.56 | 24.1 |
| NNE | 29.44 | 25.1 | 22.45 | 11.11 | 10.66 | 19.21 | 19.13 | 14.43 | 21.16 | 23.57 | 20.6 | 30.6 |
| NE | 27.06 | 31.47 | 18.28 | 11.67 | 6.41 | 10.88 | 12.01 | 10.57 | 25.14 | 25.27 | 21.11 | 24.64 |
| ENE | 8.92 | 13.14 | 8.11 | 7.13 | 3.81 | 3.47 | 4.35 | 8.29 | 7.04 | 7.48 | 3.29 | 3.76 |
| E | 2.91 | 3.28 | 2.78 | 2.73 | 2.37 | 4.72 | 1.25 | 15.77 | 3.89 | 3.36 | 3.89 | 1.03 |
| ESE | 0.9 | 1.86 | 3.23 | 5.51 | 4.53 | 5.19 | 2.91 | 8.11 | 2.08 | 2.55 | 7.73 | 2.06 |
| SE | 0.94 | 1.72 | 3.14 | 5.05 | 7.62 | 7.22 | 5.91 | 4.66 | 4.03 | 2.69 | 5.28 | 1.61 |
| SSE | 1.66 | 1.23 | 4.35 | 7.78 | 12.54 | 6.11 | 10.98 | 5.56 | 5.97 | 4.44 | 4.81 | 1.61 |
| S | 2.02 | 0.83 | 5.47 | 12.36 | 15.41 | 7.87 | 7.03 | 5.87 | 4.72 | 7.35 | 7.78 | 3.9 |
| SSW | 3.81 | 1.72 | 6.5 | 15.93 | 14.25 | 7.27 | 12.28 | 7.57 | 8.61 | 5.24 | 8.33 | 2.6 |
| SW | 2.2 | 1.13 | 2.91 | 3.98 | 2.6 | 2.55 | 2.2 | 1.34 | 0.46 | 0.81 | 3.61 | 1.16 |
| WSW | 0.58 | 0.69 | 0.49 | 0.69 | 0.94 | 0.74 | 0.4 | 0.45 | 0.19 | 0.13 | 0.46 | 0.31 |
| W | 0.22 | 0.44 | 0.45 | 0.46 | 0.49 | 0.69 | 0.49 | 0.36 | 0.23 | 0.13 | 0.32 | 0.27 |
| WNW | 0.18 | 0.15 | 0.4 | 0.51 | 0.4 | 0.28 | 0.36 | 0.18 | 0.32 | 0.18 | 0.56 | 0.22 |
| NW | 0.22 | 0.25 | 0.36 | 0.65 | 0.81 | 0.97 | 0.4 | 0.45 | 0.14 | 0.27 | 0.42 | 0.58 |
| NNW | 1.48 | 1.62 | 3.18 | 3.24 | 3.27 | 4.95 | 5.15 | 3.14 | 1.81 | 1.7 | 1.25 | 1.52 |

Table 25: Monthly occurrence (%) of wind intensity, for the years 2012 to 2014, from the analyzed point to the coastal navigation route.

| Months | Intensity (m/s) | | | | | |
|---|---|---|---|---|---|---|
| | < 2.0 | 2.0 - 4.0 | 4.0 - 6.0 | 6.0 - 8.0 | 8.0 - 10.0 | ≥ 10.0 |
| Jan | 1.66 | 8.6 | 24.15 | 33.11 | 27.02 | 5.47 |
| Feb | 3.04 | 15.25 | 30.83 | 29.56 | 18.09 | 3.24 |
| Mar | 5.33 | 18.28 | 23.61 | 25.63 | 21.55 | 5.6 |
| Apr | 7.69 | 22.08 | 26.53 | 23.89 | 16.39 | 3.43 |
| May | 8.2 | 16.49 | 28.94 | 26.79 | 13.58 | 6 |
| Jun | 8.52 | 19.31 | 28.94 | 27.59 | 13.8 | 1.85 |
| Jul | 2.91 | 16.22 | 27.73 | 27.64 | 19.67 | 5.82 |
| Aug | 4.48 | 13.89 | 26.43 | 30.42 | 17.16 | 7.62 |
| Sep | 1.9 | 4.86 | 16.62 | 30.83 | 31.34 | 14.44 |
| Oct | 1.21 | 6.27 | 16.13 | 32.84 | 31.23 | 12.32 |
| Nov | 3.84 | 11.76 | 21.25 | 24.72 | 29.44 | 8.98 |
| Dec | 3.36 | 9.27 | 16.4 | 24.69 | 29.39 | 16.89 |

#### 4.3.1.3 *Offshore* Navigation Route

Figure 22 shows the wind roses for the point closest to the discharge site on the offshore navigation route, in addition to the occurrence tables of direction and intensity (Table 26 and Table 27), for the years 2012 to 2014. NNE winds are predominant with intensities between 4 and 8 m/s.


Figure 22: Wind roses, for the years 2012 to 2014, from the analyzed point to the offshore navigation route.

Table 26: Monthly occurrence (%) of wind direction, for the years 2012 to 2014, from the analyzed point to the offshore navigation route.

| Direction | Months | | | | | | | | | | | |
|---|---|---|---|---|---|---|---|---|---|---|---|---|
| | J | F | M | A | M | J | J | A | S | O | N | D |
| N | 12.95 | 10.39 | 15.64 | 8.61 | 9.99 | 14.58 | 14.38 | 9.99 | 9.68 | 12.01 | 9.26 | 22.4 |
| NNE | 31.81 | 26.76 | 24.91 | 12.22 | 12.95 | 21.71 | 18.1 | 18.73 | 27.5 | 29.57 | 21.34 | 38.35 |
| NE | 27.96 | 31.23 | 17.16 | 9.72 | 7.12 | 11.67 | 12.99 | 8.2 | 19.49 | 19.53 | 21.06 | 20.03 |
| ENE | 8.65 | 16.37 | 9.59 | 9.35 | 3.9 | 5.69 | 6.94 | 7.21 | 10 | 10.8 | 4.63 | 4.48 |
| E | 6 | 5.64 | 4.88 | 4.4 | 3.54 | 6.53 | 1.93 | 19.31 | 5.14 | 3.81 | 5.23 | 1.39 |
| ESE | 1.03 | 2.65 | 4.39 | 7.41 | 8.83 | 6.57 | 5.38 | 10.17 | 2.82 | 3.54 | 8.47 | 2.33 |
| SE | 1.52 | 0.93 | 4.84 | 5.93 | 11.92 | 8.52 | 9.01 | 6.05 | 4.54 | 2.64 | 5.37 | 1.34 |
| SSE | 0.99 | 0.34 | 3.94 | 10.65 | 12.19 | 8.38 | 7.97 | 5.15 | 6.62 | 5.38 | 5.09 | 1.93 |
| S | 2.11 | 0.59 | 2.6 | 12.18 | 12.05 | 5.05 | 9.63 | 4.53 | 3.7 | 6.63 | 5.69 | 2.55 |
| SSW | 2.51 | 0.98 | 4.57 | 9.63 | 8.87 | 3.7 | 7.17 | 5.02 | 6.85 | 3.41 | 6.62 | 1.7 |
| SW | 2.24 | 0.88 | 2.33 | 2.87 | 1.93 | 1.57 | 1.3 | 0.9 | 0.65 | 0.27 | 2.45 | 0.45 |
| WSW | 0.49 | 0.78 | 0.58 | 0.79 | 0.58 | 0.6 | 0.27 | 0.22 | 0.23 | 0.18 | 0.93 | 0.36 |
| W | 0.27 | 0.59 | 0.49 | 0.65 | 0.63 | 0.23 | 0.36 | 0.36 | 0.14 | 0.13 | 0.74 | 0.31 |
| WNW | 0.22 | 0.29 | 0.45 | 0.74 | 0.4 | 0.46 | 0.18 | 0.18 | 0.32 | 0.36 | 0.46 | 0.04 |
| NW | 0.04 | 0.1 | 0.9 | 0.42 | 0.76 | 0.93 | 0.22 | 0.4 | 0.32 | 0.49 | 0.32 | 0.49 |
| NNW | 1.21 | 1.47 | 2.73 | 4.44 | 4.35 | 3.8 | 4.17 | 3.58 | 1.99 | 1.25 | 2.31 | 1.84 |

Table 27: Monthly occurrence (%) of wind intensity, for the years 2012 to 2014, from the analyzed point to the offshore navigation route.

| Months | Intensity (m/s) | | | | | |
|---|---|---|---|---|---|---|
| | < 2.0 | 2.0 - 4.0 | 4.0 - 6.0 | 6.0 - 8.0 | 8.0 - 10.0 | ≥ 10.0 |
| Jan | 1.08 | 7.93 | 25.04 | 36.56 | 24.82 | 4.57 |
| Feb | 3.14 | 13.48 | 32.3 | 33.58 | 15.64 | 1.86 |
| Mar | 4.75 | 20.56 | 24.42 | 25.45 | 20.61 | 4.21 |
| Apr | 5.93 | 22.27 | 32.73 | 22.87 | 13.8 | 2.41 |
| May | 4.79 | 17.56 | 32.71 | 27.37 | 13.58 | 3.99 |
| Jun | 5.42 | 20.65 | 29.4 | 28.8 | 14.81 | 0.93 |
| Jul | 3.27 | 11.2 | 32.21 | 29.61 | 18.86 | 4.84 |
| Aug | 2.02 | 11.65 | 24.96 | 33.33 | 21.68 | 6.36 |
| Sep | 1.02 | 3.7 | 16.2 | 34.63 | 30.37 | 14.07 |
| Oct | 0.54 | 4.57 | 14.29 | 34.5 | 34.23 | 11.87 |
| Nov | 3.24 | 10.14 | 21.3 | 27.92 | 29.35 | 8.06 |
| Dec | 2.02 | 8.78 | 17.16 | 24.28 | 28.63 | 19.13 |

### 4.3.2 Currents

For the currents, hydrodynamic modeling results were used, as described in item 3 (Hydrodynamic Modeling):

→ Results of hydrodynamic modeling obtained by the DELFT3D model, for the area of the Port of Tubarão and Vitória Bay (ANNEX I); and

→ Hydrodynamic modeling results obtained by the ROMS model for navigation routes (CLS Brasil, 2022a; CLS Brasil 2022b).

#### 4.3.2.1 Port of Tubarão

Figure 23 shows the monthly surface current roses for the point closest to the port discharge, in addition to the occurrence tables of direction and intensity (Table 28 and Table 29), for the year 2012. Currents are predominant to the W and WNW and weaker currents, with intensities lower than 0.01 m/s.

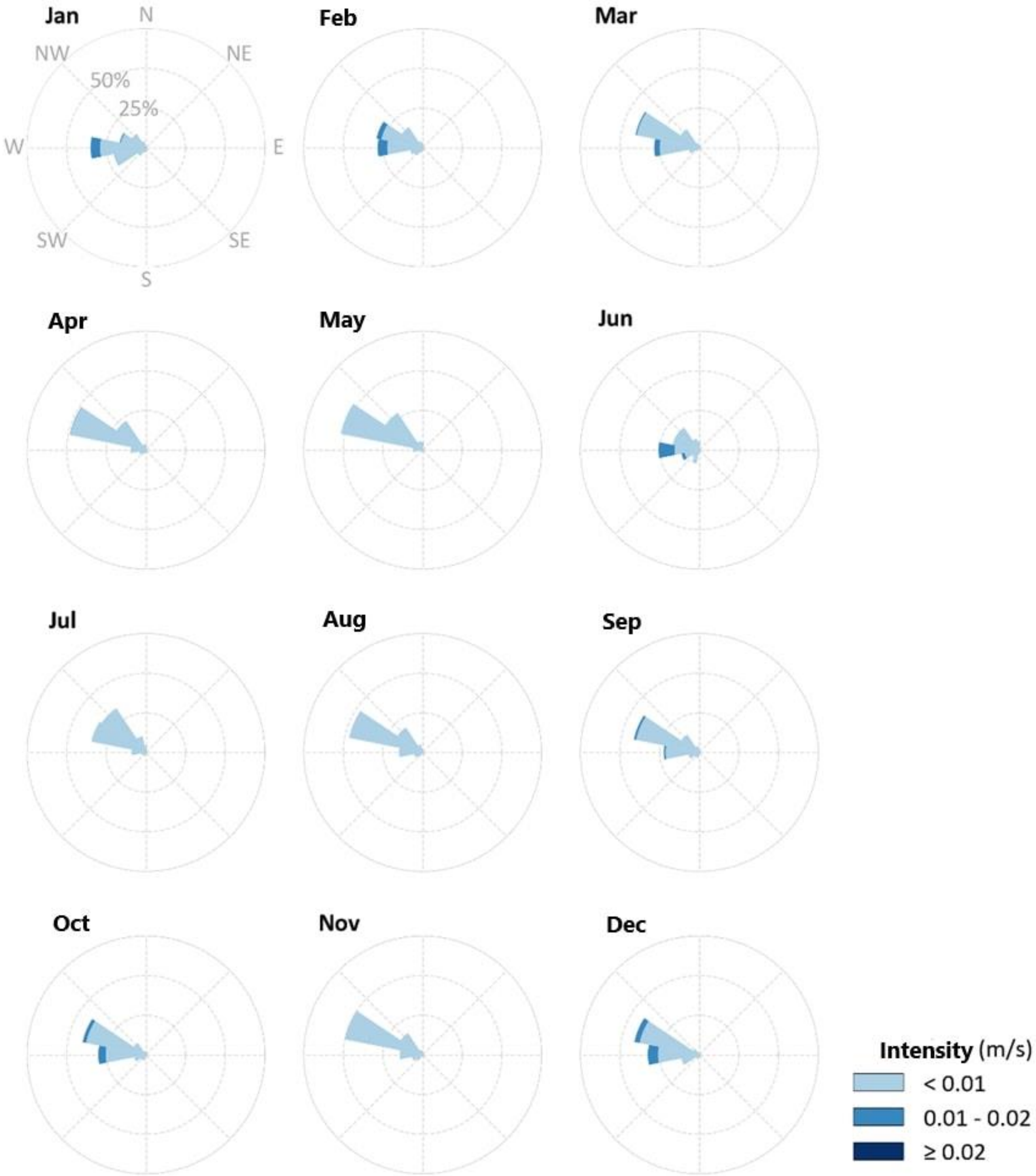


Figure 23: Monthly surface currents for the year 2012, from the analyzed point to the Port of Tubarão.

Table 28: Monthly occurrence (%) of surface current direction, for the year 2012, from the analyzed point to the Port of Tubarão.

| Direction | Months | | | | | | | | | | | |
|---|---|---|---|---|---|---|---|---|---|---|---|---|
| | J | F | M | A | M | J | J | A | S | O | N | D |
| N | 0.96 | 3.14 | 1.57 | 3.57 | 5.07 | 5.31 | 4.33 | 2.56 | 3 | 2.22 | 2.67 | 1.03 |
| NNE | - | - | - | - | - | - | - | - | - | - | - | - |
| NE | - | - | - | - | - | - | - | - | - | - | - | - |
| ENE | - | - | - | - | - | - | - | - | - | - | - | - |
| E | - | - | - | - | - | - | - | - | - | - | - | - |
| ESE | - | - | - | - | - | - | - | - | - | - | - | - |
| SE | - | - | - | - | - | - | - | - | - | - | - | - |
| SSE | - | - | - | - | - | - | - | - | - | - | - | - |
| S | 2.64 | 1.83 | 1.31 | 1.79 | 1.09 | 2.04 | 0.36 | 1.14 | 1.09 | 0.67 | 0.8 | 1.65 |
| SSW | 3.12 | 3.4 | 1.05 | 2.08 | 0.36 | 8.57 | 2.53 | 1.14 | 3.54 | 3.56 | 1.34 | 2.68 |
| SW | 6.25 | 6.02 | 2.89 | 3.57 | 0.36 | 5.31 | 1.81 | 3.69 | 3.54 | 3.78 | 4.28 | 2.47 |
| WSW | 20.43 | 7.85 | 6.56 | 4.46 | 0.36 | 11.43 | 2.89 | 5.4 | 6.81 | 7.56 | 6.68 | 11.55 |
| W | 34.86 | 28.27 | 28.35 | 9.52 | 6.16 | 25.71 | 9.03 | 14.77 | 22.34 | 30 | 14.44 | 32.37 |
| WNW | 16.83 | 29.58 | 40.94 | 48.81 | 52.54 | 17.14 | 35.02 | 47.16 | 41.96 | 40.67 | 50 | 41.65 |
| NW | 10.58 | 15.71 | 14.17 | 22.32 | 28.26 | 17.14 | 33.57 | 19.03 | 13.62 | 9.11 | 16.58 | 4.54 |
| NNW | 4.33 | 4.19 | 3.15 | 3.87 | 5.8 | 7.35 | 10.47 | 5.11 | 4.09 | 2.44 | 3.21 | 2.06 |

Table 29: Monthly occurrence (%) of surface current intensity, for the year 2012, from the analyzed point to the Port of Tubarão.

| Months | Intensity (m/s) | | |
|---|---|---|---|
| | < 0.01 | 0.01 - 0.02 | ≥ 0.02 |
| Jan | 93.03 | 6.97 | - |
| Feb | 90.84 | 9.16 | - |
| Mar | 95.8 | 4.2 | - |
| Apr | 99.7 | 0.3 | - |
| May | 100 | - | - |
| Jun | 87.76 | 12.24 | - |
| Jul | 100 | - | - |
| Aug | 100 | - | - |
| Sep | 97.55 | 2.45 | - |
| Oct | 93.11 | 6.89 | - |
| Nov | 100 | - | - |
| Dec | 90.31 | 9.69 | - |

### 4.3.2.2 Coastal Shipping Route

Figure 24 shows the monthly surface current roses for the point closest to the discharge site on the coastal navigation route, in addition to the direction and intensity occurrence tables (Table 30 and Table 31), for the years 2012 to 2014. SSW currents and currents are predominant with intensities between 0.6 and 0.8 m/s.

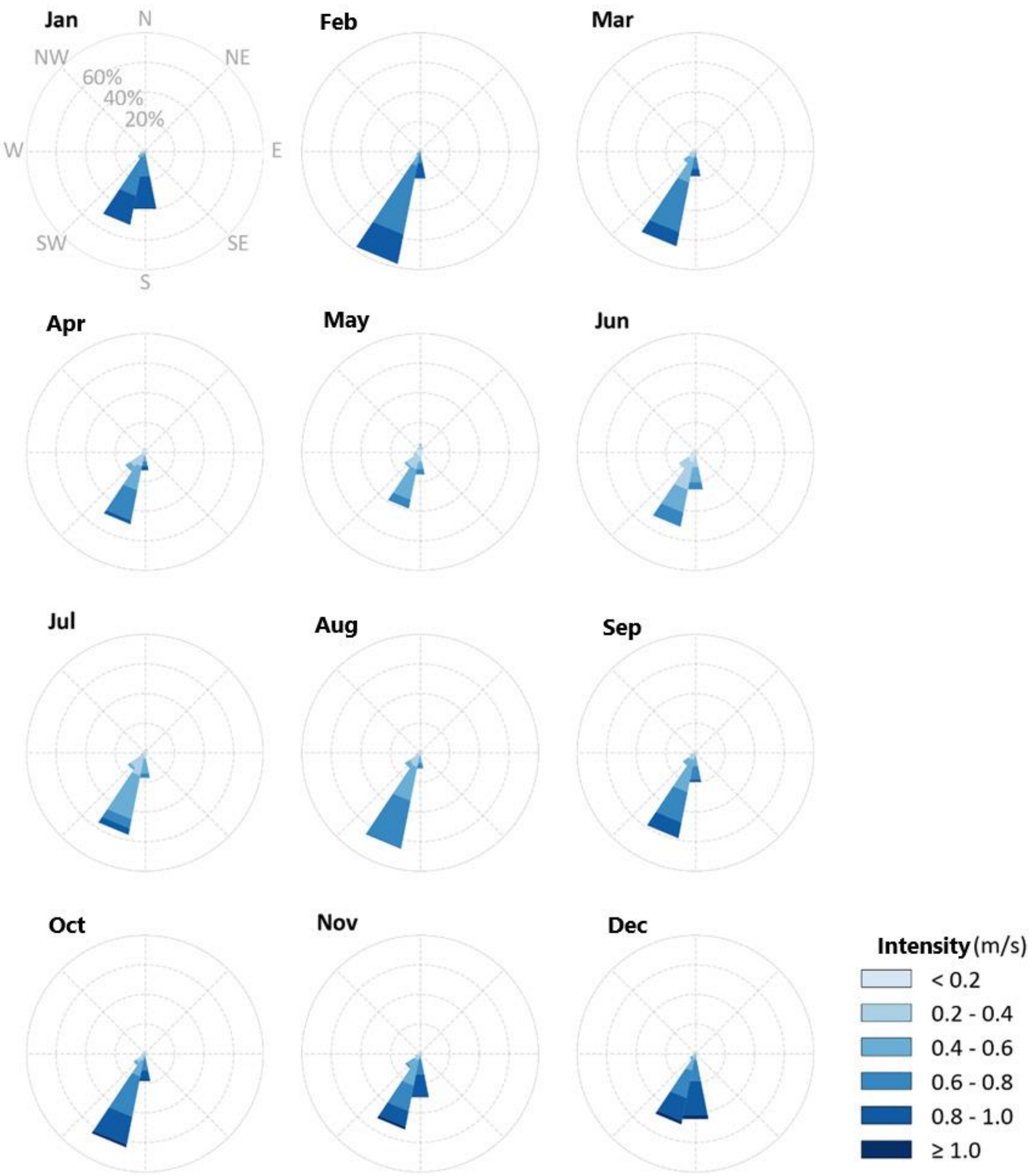


Figure 24: Rose of monthly surface currents, for the years 2012 to 2014, from the analyzed point to the coastal navigation route.

Table 30: Monthly occurrence (%) of surface current direction, for the years 2012 to 2014, from the analyzed point to the coastal navigation route.

| Direction | Months | | | | | | | | | | | |
|---|---|---|---|---|---|---|---|---|---|---|---|---|
| | J | F | M | A | M | J | J | A | S | O | N | D |
| N | - | - | - | 2.96 | 5.47 | 0.09 | 1.43 | 2.06 | 1.02 | 0.63 | - | - |
| NNE | - | - | 0.09 | 2.59 | 3.76 | 0.09 | 3.05 | 1.16 | 0.46 | 0.09 | - | - |
| NE | - | - | - | 1.11 | 1.7 | 0.09 | 0.54 | 0.54 | 0.28 | - | - | - |
| ENE | - | - | - | 0.74 | 0.72 | - | 0.09 | 0.18 | - | 0.09 | - | - |
| E | - | - | - | 0.83 | 0.72 | 0.09 | - | - | - | - | - | - |
| ESE | - | - | 0.09 | 0.65 | 0.63 | 0.09 | 0.09 | - | - | - | - | - |
| SE | - | - | - | 1.67 | 1.08 | 0.28 | 0.09 | 0.09 | - | - | - | - |
| SSE | - | - | 0.09 | 1.57 | 1.52 | 1.02 | 0.45 | 0.36 | 0.46 | 0.18 | 0.46 | 0.09 |
| S | 39.61 | 18.82 | 17.2 | 12.59 | 15.5 | 25.74 | 17.2 | 10.75 | 20.19 | 18.82 | 30.09 | 45.07 |
| SSW | 50.81 | 77.75 | 65.59 | 49.81 | 39.07 | 51.57 | 56.54 | 66.13 | 58.89 | 64.61 | 52.31 | 48.75 |
| SW | 5.82 | 3.43 | 9.77 | 15.83 | 12.99 | 13.43 | 14.07 | 12.54 | 10.28 | 9.32 | 12.13 | 4.57 |
| WSW | 3.41 | - | 4.21 | 2.22 | 4.84 | 3.8 | 2.96 | 3.23 | 3.98 | 2.69 | 3.43 | 0.99 |
| W | 0.36 | - | 2.51 | 1.48 | 3.58 | 2.04 | 1.16 | 0.9 | 0.93 | 0.81 | 1.3 | 0.54 |
| WNW | - | - | 0.36 | 1.48 | 2.51 | 0.93 | 0.81 | 0.45 | 0.93 | 0.27 | 0.28 | - |
| NW | - | - | 0.09 | 2.22 | 2.78 | 0.37 | 0.63 | 0.27 | 1.2 | 0.99 | - | - |
| NNW | - | - | - | 2.22 | 3.14 | 0.37 | 0.9 | 1.34 | 1.39 | 1.52 | - | - |

Table 31: Monthly occurrence (%) of surface current intensity, for the years 2012 to 2014, from the analyzed point to the coastal navigation route.

| Months | Intensity (m/s) | | | | | |
|---|---|---|---|---|---|---|
| | < 0.2 | 0.2 - 0.4 | 0.4 - 0.6 | 0.6 - 0.8 | 0.8 - 1.0 | ≥ 1.0 |
| Jan | 0.63 | 6.45 | 7.8 | 43.1 | 41.22 | 0.81 |
| Feb | - | 2.25 | 11.57 | 55.29 | 30.88 | - |
| Mar | 4.03 | 13.26 | 25.45 | 42.56 | 14.7 | - |
| Apr | 21.94 | 23.98 | 23.8 | 24.81 | 5.46 | - |
| May | 27.33 | 32.35 | 30.38 | 9.86 | 0.09 | - |
| Jun | 21.39 | 37.31 | 26.48 | 14.81 | - | - |
| Jul | 10.75 | 32.71 | 42.74 | 9.41 | 4.39 | - |
| Aug | 10.66 | 20.61 | 32.08 | 36.11 | 0.54 | - |
| Sep | 10.37 | 13.33 | 33.15 | 30.37 | 12.31 | 0.46 |
| Oct | 2.06 | 16.49 | 16.58 | 36.47 | 25.63 | 2.78 |
| Nov | 5.93 | 9.91 | 26.3 | 29.44 | 25.93 | 2.5 |
| Dec | 0.63 | 6.54 | 15.05 | 33.6 | 39.34 | 4.84 |

### 4.3.2.3 Offshore Navigation Route

Figure 25 shows the monthly surface current roses for the point closest to the discharge site on the offshore navigation route, in addition to the direction and intensity occurrence tables (Table 32 and Table 33), for the years 2012 to 2014. Currents are predominant between S and SW and currents with intensities between 0.1 and 0.3 m/s.

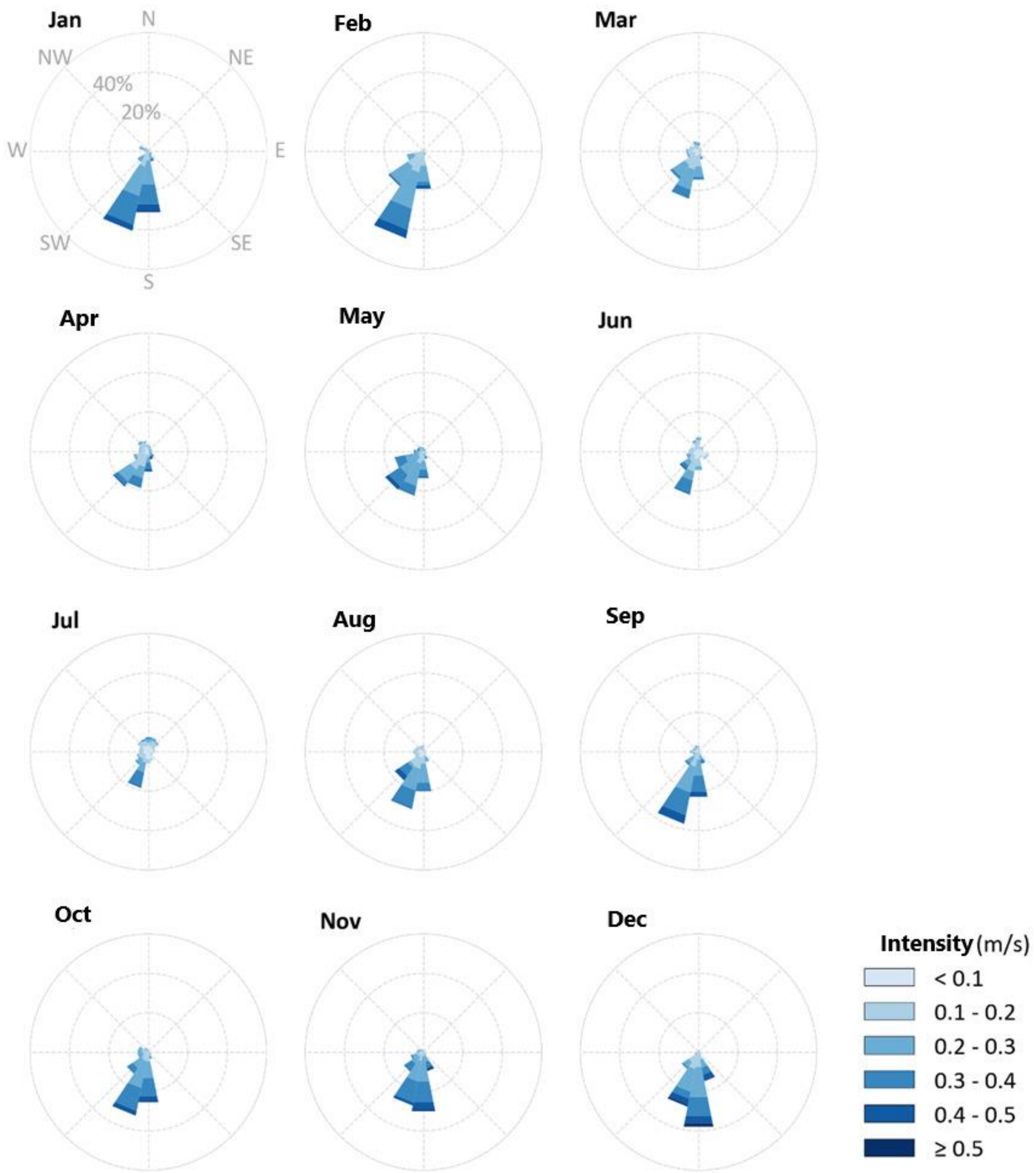


Figure 25: Monthly surface current rose, for the years 2012 to 2014, from the analyzed point to the offshore navigation route.

Table 32: Monthly occurrence (%) of surface current direction, for the years 2012 to 2014, from the analyzed point to the offshore navigation route.

| Direction | Months | | | | | | | | | | | |
|---|---|---|---|---|---|---|---|---|---|---|---|---|
| | J | F | M | A | M | J | J | A | S | O | N | D |
| N | 0.27 | 0.29 | 4.21 | 3.24 | 1.88 | 7.22 | 7.53 | 3.41 | 2.87 | 0.45 | 0.56 | 1.08 |
| NNE | 0.09 | 0.1 | 1.79 | 2.78 | 0.81 | 2.22 | 7.53 | 1.16 | 1.48 | 0.36 | 0.37 | 0.45 |
| NE | 0.18 | 0.1 | 1.16 | 1.48 | 1.43 | 3.15 | 6.54 | 0.18 | 0.74 | 0.45 | 0.09 | 0.18 |
| ENE | 0.27 | 0.1 | 1.79 | 1.94 | 1.08 | 2.59 | 3.58 | 0.27 | 0.46 | 0.09 | 0.37 | 0.45 |
| E | 0.36 | 0.2 | 1.61 | 0.46 | 0.45 | 2.41 | 3.23 | 0.09 | 0.74 | 0.18 | 0.19 | 0.54 |
| ESE | 0.54 | 0.1 | 0.9 | 1.94 | 0.18 | 5.56 | 2.33 | 0.27 | 1.2 | 0.27 | 0.56 | 0.99 |
| SE | 2.15 | 0.29 | 1.25 | 3.61 | 1.52 | 5.19 | 2.78 | 0.81 | 0.74 | 1.7 | 1.48 | 1.08 |
| SSE | 5.56 | 2.16 | 4.39 | 4.26 | 3.94 | 3.33 | 4.84 | 5.38 | 6.3 | 3.49 | 9.81 | 15.05 |
| S | 31.63 | 19.51 | 14.78 | 10.37 | 13.71 | 9.63 | 5.91 | 20.34 | 23.24 | 25.81 | 30.56 | 38.53 |
| SSW | 41.31 | 45.2 | 24.73 | 18.98 | 22.94 | 22.41 | 18.73 | 29.66 | 37.31 | 32.89 | 27.69 | 28.23 |
| SW | 6.63 | 21.47 | 17.38 | 21.57 | 23.39 | 11.57 | 8.06 | 17.56 | 8.52 | 13.17 | 11.94 | 10.3 |
| WSW | 1.08 | 8.73 | 6.18 | 7.78 | 14.96 | 6.3 | 6 | 4.57 | 2.87 | 5.38 | 6.57 | 1.88 |
| W | 2.33 | 0.88 | 6.27 | 4.72 | 4.93 | 5.19 | 4.66 | 5.47 | 4.17 | 5.65 | 3.43 | 0.36 |
| WNW | 4.84 | 0.49 | 4.93 | 4.81 | 3.23 | 4.35 | 4.93 | 4.3 | 3.06 | 5.2 | 3.15 | 0.09 |
| NW | 2.15 | 0.29 | 3.41 | 6.48 | 3.14 | 2.87 | 6.54 | 3.41 | 2.87 | 2.69 | 1.85 | 0.18 |
| NNW | 0.63 | 0.1 | 5.2 | 5.56 | 2.42 | 6.02 | 6.81 | 3.14 | 3.43 | 2.24 | 1.39 | 0.63 |

Table 33: Monthly occurrence (%) of surface current intensity, for the years 2012 to 2014, from the analyzed point to the offshore navigation route.

| Months | Intensity (m/s) | | | | | |
|---|---|---|---|---|---|---|
| | < 0.1 | 0.1 - 0.2 | 0.2 - 0.3 | 0.3 - 0.4 | 0.4 - 0.5 | ≥ 0.5 |
| Jan | 2.24 | 23.57 | 39.25 | 27.69 | 6.63 | 0.63 |
| Feb | 5.2 | 31.57 | 42.84 | 13.73 | 6.67 | - |
| Mar | 21.77 | 40.05 | 29.93 | 8.15 | 0.09 | - |
| Apr | 18.7 | 38.43 | 24.63 | 14.44 | 3.52 | 0.28 |
| May | 6 | 22.58 | 43.73 | 23.3 | 4.03 | 0.36 |
| Jun | 36.57 | 38.24 | 14.17 | 9.72 | 1.3 | - |
| Jul | 42.65 | 33.15 | 13.89 | 9.77 | 0.54 | - |
| Aug | 20.88 | 30.2 | 27.06 | 18.28 | 3.58 | - |
| Sep | 12.04 | 24.54 | 31.67 | 24.26 | 7.5 | - |
| Oct | 5.2 | 23.66 | 38.98 | 26.52 | 5.02 | 0.63 |
| Nov | 5.74 | 17.78 | 37.5 | 30.46 | 7.22 | 1.3 |
| Dec | 4.39 | 26.61 | 37.81 | 17.83 | 10.3 | 3.05 |

### 4.3.3 Scenario Selection

The selection of scenarios was aimed at representing the most relevant conditions according to the area of analysis. Therefore, the criteria chosen for the Port of Tubarão were different compared to the navigation routes. In the case of the port, it was appropriate to evaluate not only the current intensities, but also the tidal variations. Extreme scenarios were chosen, allowing a comparison of the behavior of the effluent under contrasting conditions.

In short, the following scenarios were defined:

→ Port of Tubarão:

- Spring tide (syzygy) and more intense currents: equivalent to faster dispersion in the environment;
- Neap tide (quadrature) and weaker currents: equivalent to slower dispersion in the environment.

→ Navigation routes:

- More intense currents: equivalent to faster dispersion in the environment;
- Weaker currents: equivalent to slower dispersion in the environment.

The assessment of current intensity was carried out based on time series obtained through hydrodynamic modeling (detailed in item 3).

In the Port of Tubarão, moving averages with 15-day windows were applied to the coastal simulation data, and analyzed together with the time series of the sea level at the discharge point. The objective was to identify periods of more intense currents that coincided with the syzygy (largest tidal range) and quadrature (smallest tidal range). The selected periods begin on 06/04/2012 for the syzygy scenario and on 11/18/2012 for the quadrature scenario. The time series of current and sea level for these periods are presented in Figure 26 and Figure 27.

It can be observed that, even in the most intense scenario, the magnitude of the currents in the Port of Tubarão does not exceed 0.04 m/s, with a sea level amplitude of almost 2 m. In the quadrature scenario, the currents remain below 0.03 m/s, with a tidal amplitude of approximately 1 m.

For the shipping routes, 5-day windows of the current intensity of the offshore simulation at the initial discard point were analyzed. The analyses included an assessment of the frequency of currents above the 95th percentile (intense scenario) and below the 5th percentile (weak scenario). A complementary analysis was also performed at the intermediate points of the coastal and offshore shipping areas.

The current series of the selected periods presented in Figure 28 are for the coastal route and in Figure 29 for offshore route. For the coastal route, the analyzed periods correspond to February 20 to 25, 2013 (intense) and April 24 to 29, 2012 (weak). For the offshore route, the periods are from December 28, 2012 to January 2, 2013 (intense) and July 16 to 21, 2013 (weak).

In the intense scenarios, there is a predominance of the BC flow to the south, while in the weak scenarios, there is a reversal of direction in the simulation period due to the presence of meanders and vortices. Regarding intensity, stronger currents are observed on the continental shelf, associated with the coastal route, with an average of 0.75 m/s and a maximum of 0.81 m/s for the simulated period. In the offshore route, the average current is 0.47 m/s in the 5 days of simulation. In the weak scenario, the coastal average is approximately 0.14 m/s and offshore, 0.13 m/s.

Table 34: Initial date of simulations for each scenario.

| Scenario: | Simulation start date |
|---|---|
| Port of Tubarão | |
| Syzygy scenario | June 04, 2012 |
| Quadrature scenario | November 18, 2012 |
| Coastal Route | |
| Intense currents scenario | February 20, 2013 |
| Weak currents scenario | April 24, 2012 |
| Offshore Route | |
| Intense currents scenario | December 28, 2012 |
| Weak currents scenario | July 16, 2013 |

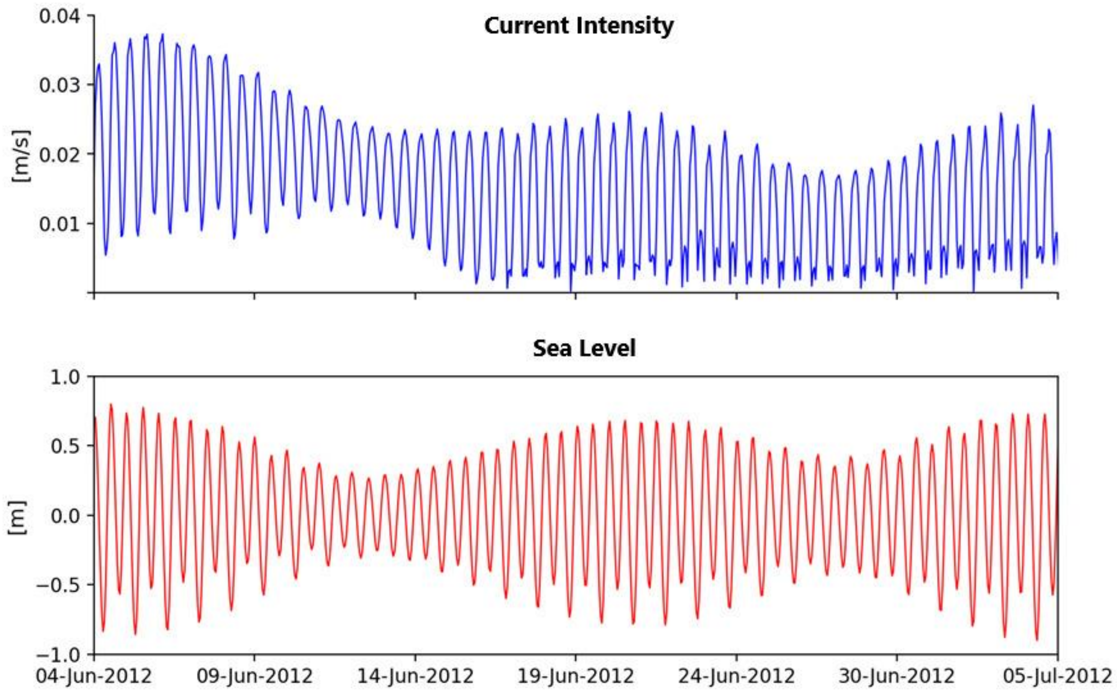


Figure 26: Time series of current intensity (upper panel) and sea level (lower panel) for the syzygy scenario and more intense currents in Port of Tubarão.

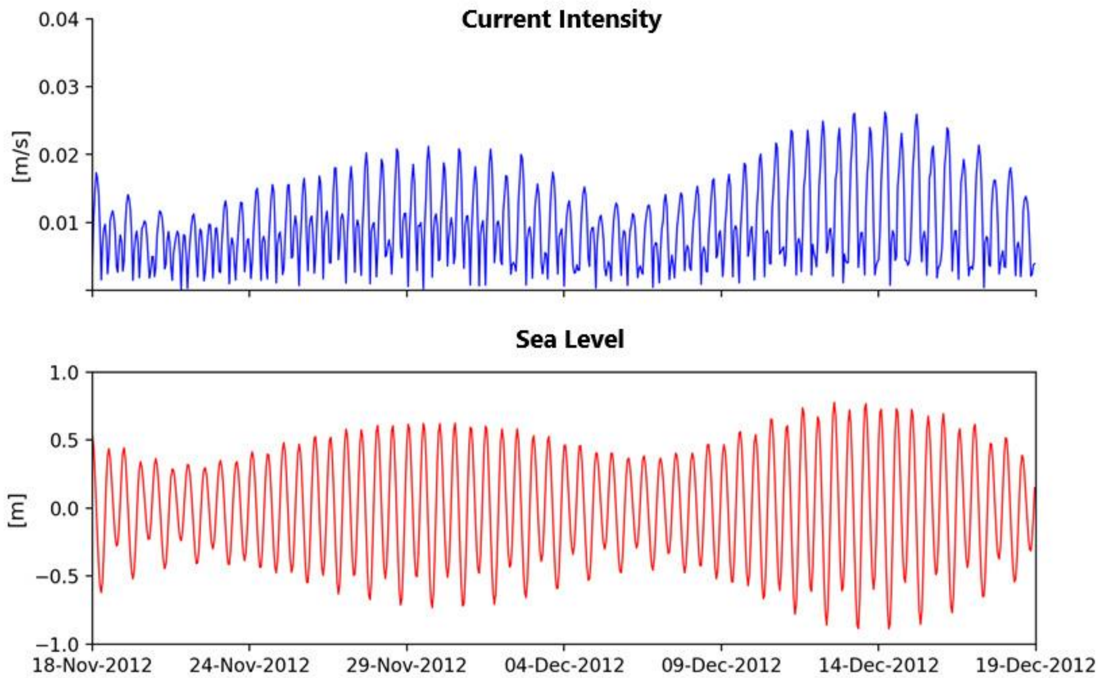


Figure 27: Time series of current intensity (upper panel) and sea level (lower panel) for the quadrature and weaker currents scenario node Port of Tubarão.

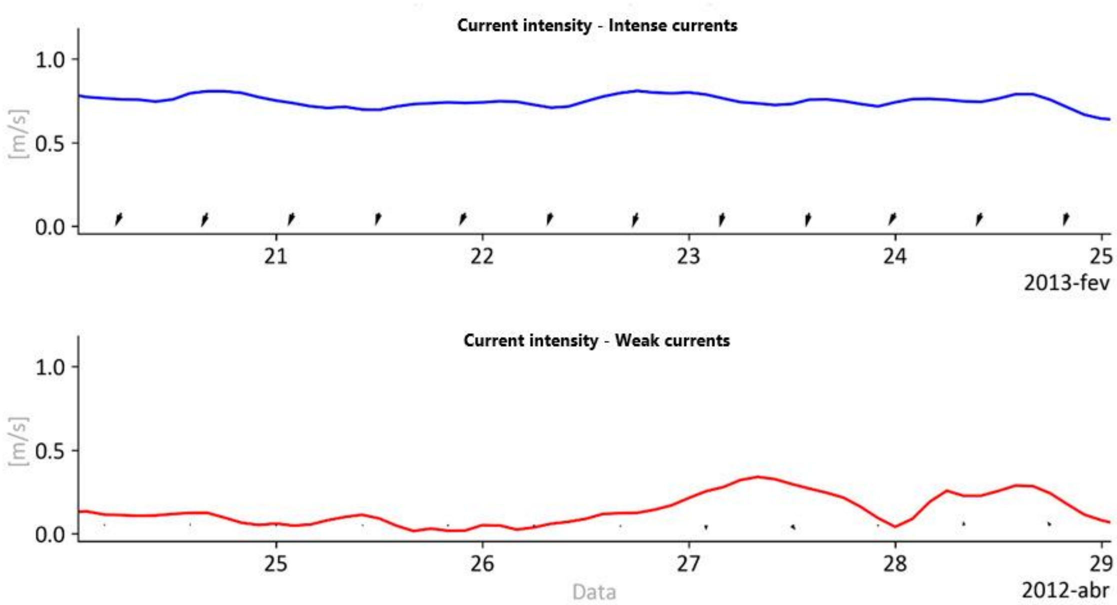


Figure 28: Time series of current intensity and direction for the strong current scenario (upper panel) and for the weak current scenario (lower panel) in the coastal shipping route.

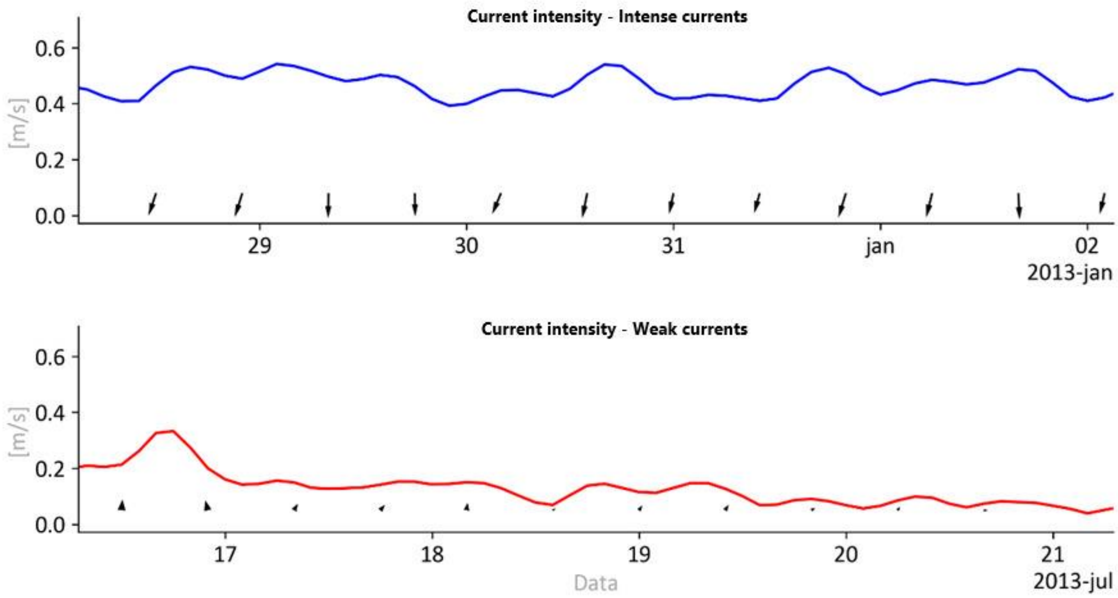


Figure 29: Time series of current intensity and direction for the strong current scenario (upper panel) and for the weak current scenario (lower panel) in the offshore shipping route.

### 4.3.4 Salinity and Sea Temperature

To define the salinity and temperature profiles to be incorporated into the dispersion modeling, the results of the hydrodynamic models were used.

The profiles presented in Figure 30 and Figure 31 represent the average of the data from the grid point closest to the discharge, for each region in the navigation route, contained within the selected modeling period (item 4.3.3 - Scenario Selection, Table 34). For the scenarios of the Port of Tubarão, information was inserted only on the surface, due to the depth of the discharge point (Table 35).

Table 35: Average surface temperature and salinity values used in the simulations for the Port of Tubarão.

| Location | Scenario | Temperature (°C) | Salinity |
|---|---|---|---|
| Port of Tubarão | Syzygy scenario | 24.04 | 35.48 |
| | Quadrature scenario | 24.90 | 36.55 |

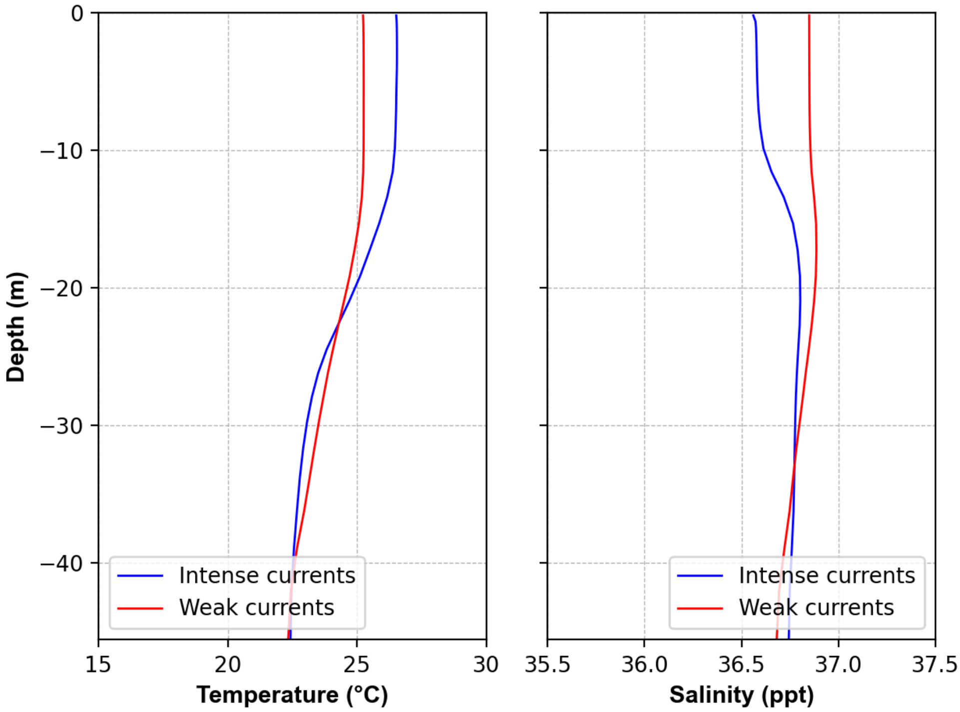


Figure 30: Sea salinity and temperature profiles for the coastal shipping route scenario.

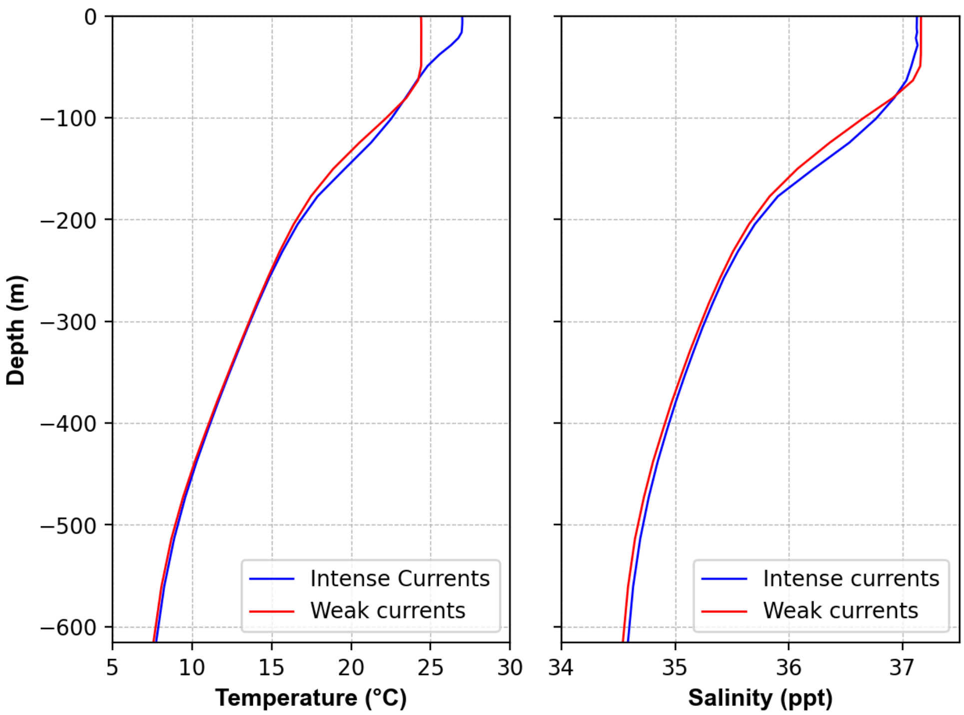


Figure 31: Sea salinity and temperature profiles for the offshore shipping route scenario.

As described in item 4.1 (Characteristics of the Discharges), the effluent density was calculated based on the surface temperature and salinity values obtained for each scenario (Table 36).

Table 36: Surface density values calculated for each scenario and used in the simulations as the density of the Scrubbers wash water.

| Location | Scenario | Surface density (kg/m³) |
|---|---|---|
| Port of Tubarão | Syzygy scenario | 1,023.99 |
| | Quadrature scenario | 1,024.54 |
| Coastal Route | Intense currents scenario | 1,024.05 |
| | Weak currents scenario | 1,024.67 |
| Offshore Route | Intense currents scenario | 1,024.33 |
| | Weak currents scenario | 1,025.16 |

## 4.4. Results

This section presents the main results of the Scrubbers wash water dispersion simulations for the different modeled scenarios. Table 37 provides a summary of all the results to be presented. In total, six deterministic simulations were performed, with two for the Port of Tubarão and four for the navigation routes.

Table 37: Summary of deterministic scenarios simulated in this study.

| Location | Scenario |
|---|---|
| Port of Tubarão | Syzygy scenario |
| | Quadrature scenario |
| Coastal Route | Intense currents scenario |
| | Weak currents scenario |
| Offshore Route | Intense currents scenario |
| | Weak currents scenario |

The monitoring threshold, PNEC, was 0.01% (10,000-fold dilution), as described in item 4.2.2 (Calculation of Environmental Risk). From the definition of PNEC, it is possible to calculate the associated environmental risk. When the concentration observed in the environment is equal to the value of this threshold, it is considered that there is a significant risk equal to 5% (i.e. 5% of the community, generally the most sensitive species, may be affected by the discharge).

The results will be presented in the following ways:

- **Integration of maximum concentration in the water column and in time**: to determine the area occupied by the effluent, the maximum concentration that the plume obtained for each grid point was extracted, analyzing all vertical layers and simulation times. In other words, for each time step of the simulation, the maximum concentration value was recorded at each grid point in each vertical layer and, at the end of the entire period, the maximum was extracted in time and in the water column. This processing results in a horizontal field containing the highest concentration value for each grid cell considering all vertical layers and simulation times;

- **Snapshots of maximum concentration in the water column:** the previous analysis obtains the area occupied by the effluent in a conservative way, but does not portray the behavior of the plume at a given moment in the simulation. To this end, examples of effluent concentration are presented for certain moments after the start of the simulation;
- **Risk integration in the column and in time**: to determine the area occupied by the effluent above the monitoring threshold, the maximum risk (detailed in item 4.2.2 - Calculation of Environmental Risk) above 5% associated with the plume concentration for each grid point was extracted, analyzing all vertical layers and simulation times. This processing results in a horizontal field containing the highest risk value for each grid cell considering all vertical layers and simulation times;
- **Duration of risk in the column above 5%**: the previous analysis obtains the area occupied by the risk associated with the effluent. However, this analysis does not indicate the duration of the significant risk. Additionally, the significant risk (>5%) is ephemeral, lasting on a scale of days. Considering this, fields with the duration of the significant risk for each grid cell are also presented. The details of this post-processing developed by CLS Brasil are presented in item 4.2.2 (Calculation of Environmental Risk).

### 4.4.1 Port of Tubarão

The results obtained for the Port of Tubarão are presented below. Firstly, in terms of effluent concentration for the syzygy scenarios (items 4.4.1.1 e 4.4.1.2). Next, the risk results are presented, aiming at a comparison between both deterministic syzygy and quadrature tide scenarios (item 4.4.1.3). Finally, a comparative table with the results obtained is presented (item 4.4.1.4).

The **total concentration** in the water column was higher in the quadrature scenario, reaching a maximum value of 60.8% throughout the entire modeling domain, while in the syzygy scenario, the maximum value was 43.7%. Concentrations above 10% were restricted to the vicinity of the discharge, less than 100 m away. While concentrations above 1% were recorded up to 450 m away.

The **significant risk associated with a concentration of 0.01%** reached a maximum distance of approximately 4 km in the quadrature scenario and 3 km in the syzygy scenario. Despite these greater distances, the risk in the water column was ephemeral, lasting on a scale of days. The maximum period in which the risk exceeded 5% at the same grid point was around 17 days in both scenarios. After 20 days of simulation, concentrations above the monitored threshold were no longer observed. Considering exposures greater than 1 day (i.e., locations exposed to a significant risk for more than one day), the maximum distance was reduced to approximately 2 km.

In general, the comparison between the scenarios shows that the quadrature scenario presented a greater extent and duration of significant risk. Although these differences are not substantial, the distribution suggests that the more intense currents in the syzygy scenario favored a greater dilution of the effluent in the marine environment, resulting in a smaller reach and shorter time for the 0.01% concentration threshold associated with significant risk.

#### 4.4.1.1 Syzygy Tide Scenario

Figure 32 shows the area occupied by concentrations above 0.01% (PNEC) throughout the entire simulation period. Meanwhile, Figure 33 to Figure 36 show snapshots throughout the simulation, ranging from 6 hours to 432 hours after discharge. In all these figures, the concentration displayed represents the maximum obtained in the water column.

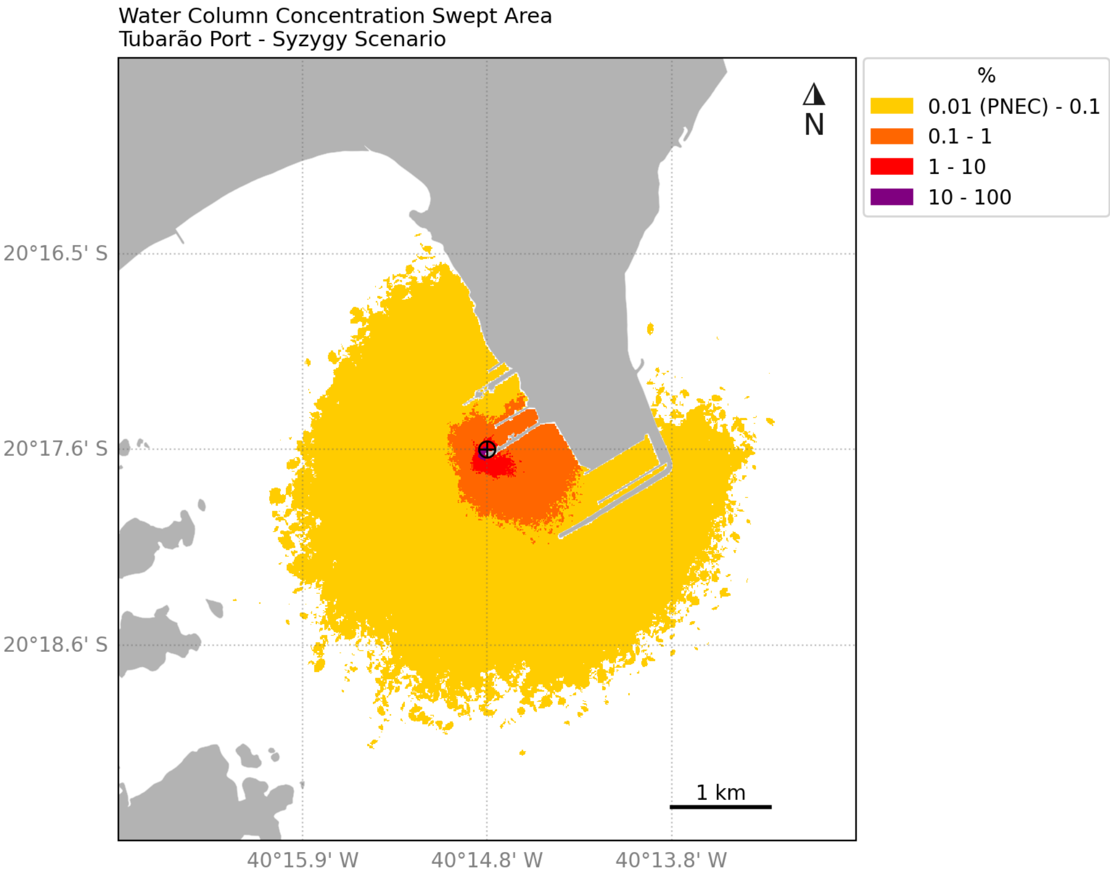


Figure 32: Swept area of maximum concentration in the water column, in Port of Tubarão, for the syzygy scenario.

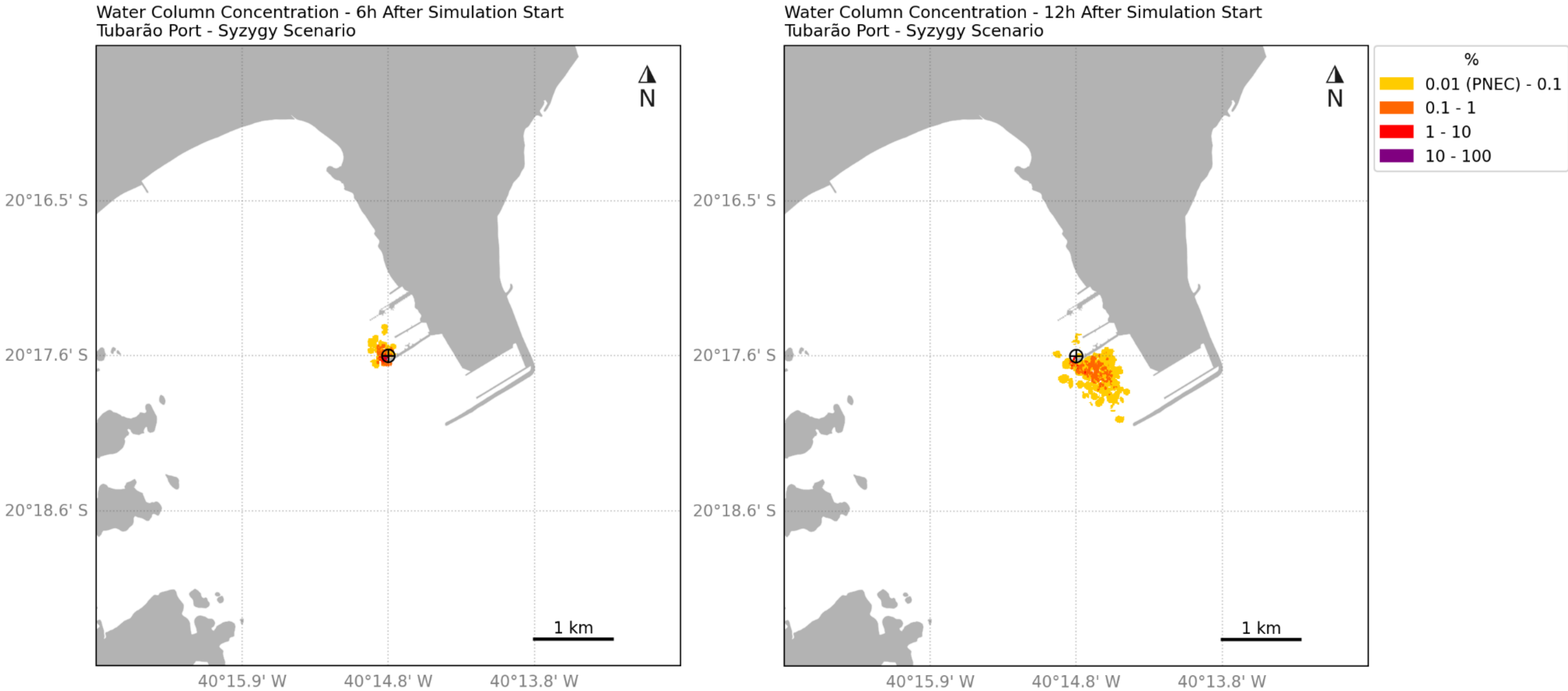


Figure 33: Maximum concentration in the water column after 6 h and 12 h from the start of the simulation (start of discharge), at the Port of Tubarão, for the syzygy scenario.

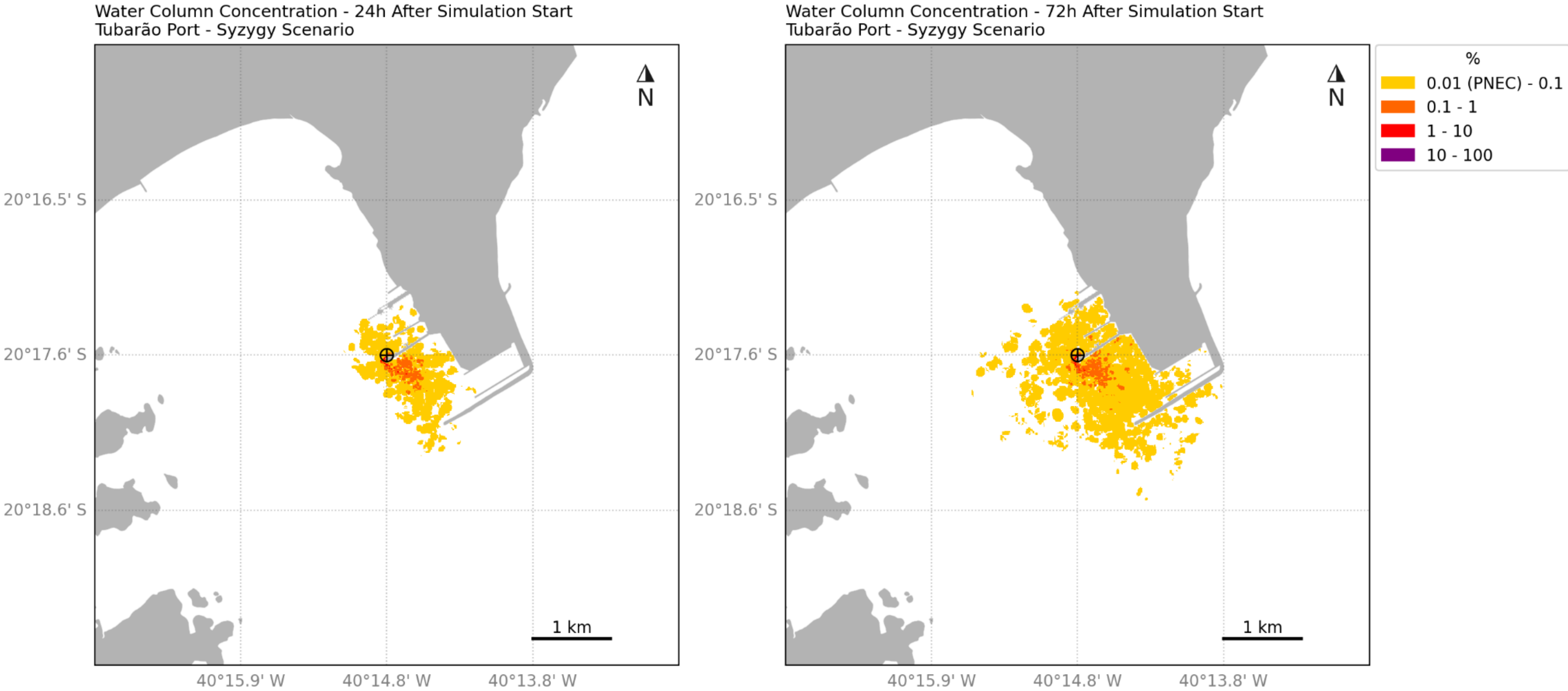


Figure 34: Maximum concentration in the water column after 24 h (1 day) and 72 h (3 days) from the start of the simulation (start of disposal), at the Port of Tubarão, for the syzygy scenario.

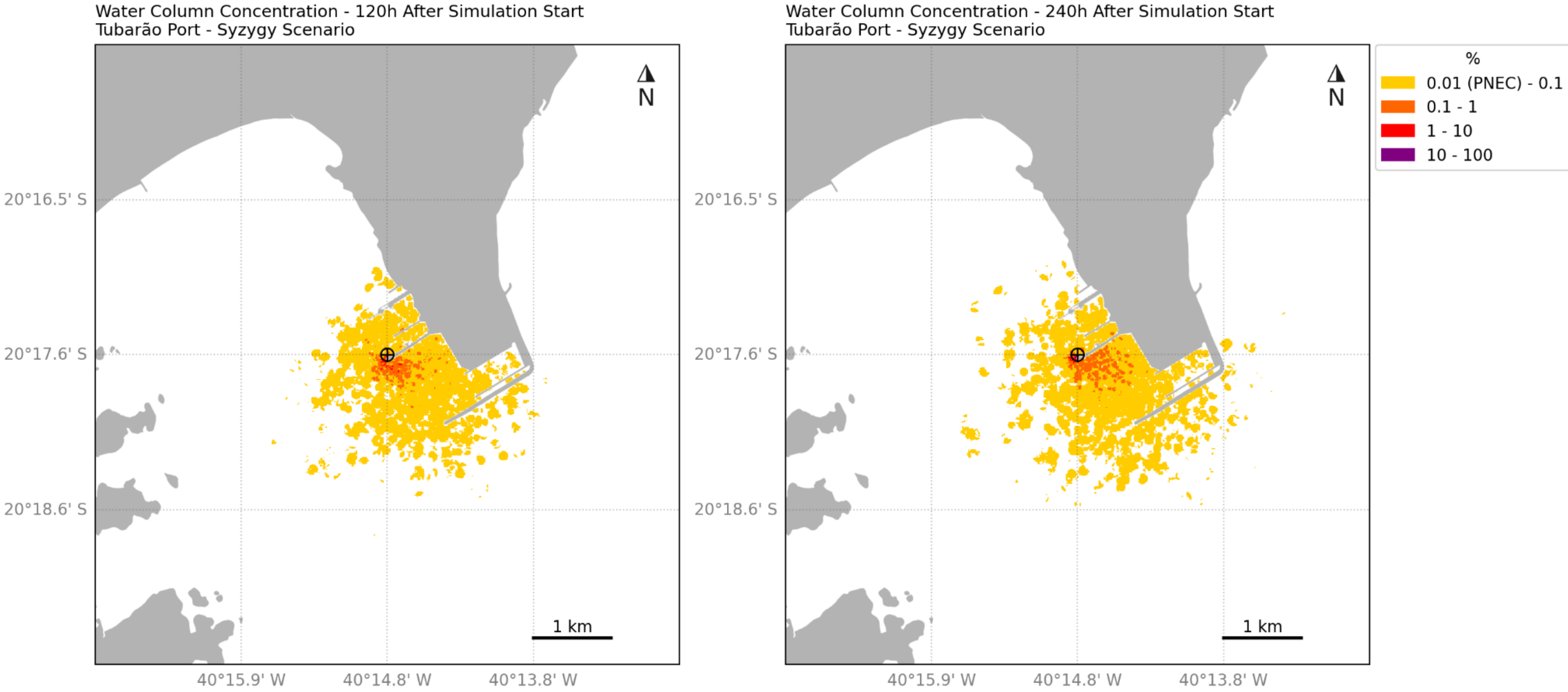


Figure 35: Maximum concentration in the water column after 120 h (5 days) and 240 h (10 days) from the start of the simulation (start of discharge), at the Port of Tubarão, for the syzygy scenario.

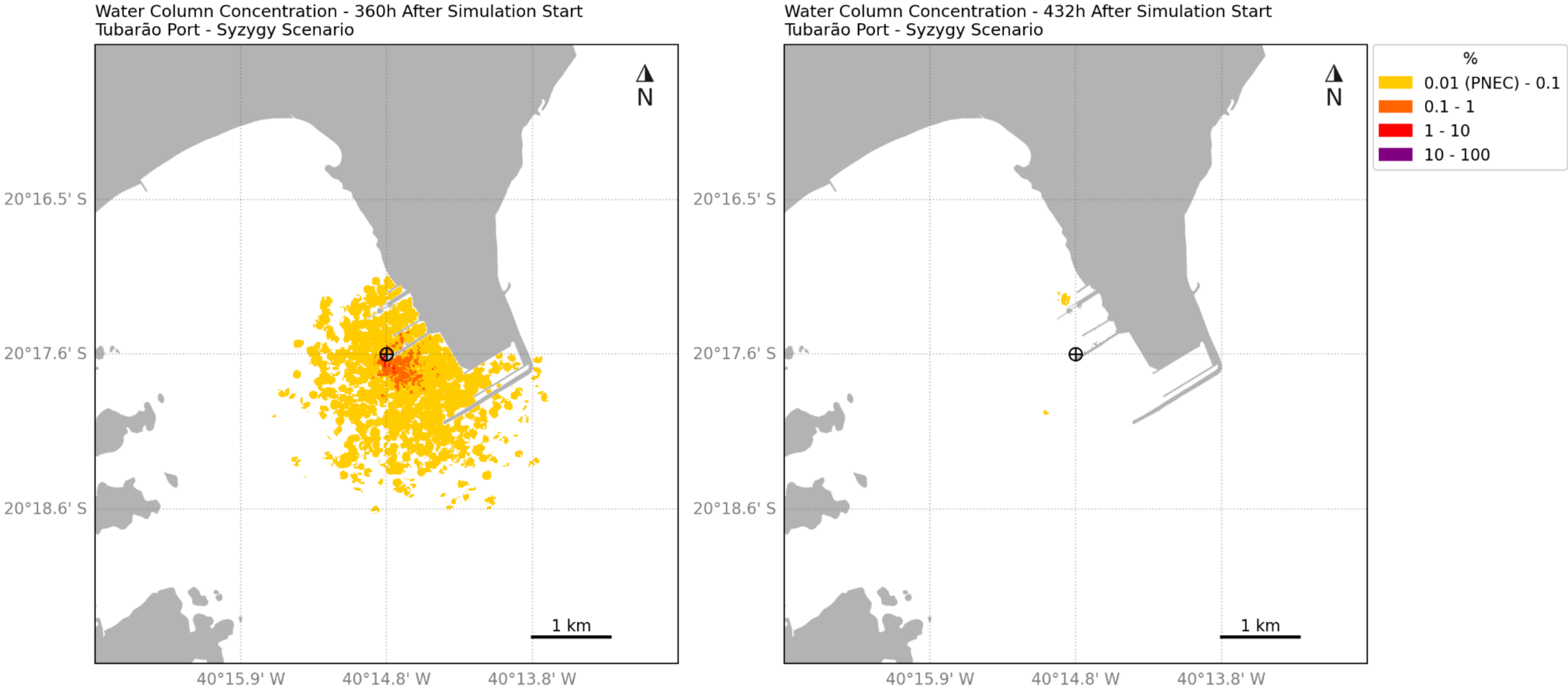


Figure 36: Maximum concentration in the water column after 360 h (15 days) and 432 h (18 days) from the start of the simulation (start of discharge), at the Port of Tubarão, for the syzygy scenario.

#### 4.4.1.2 Quadrature Scenario

Figure 37 shows the area occupied by concentrations above 0.01% (PNEC) throughout the entire simulation period. Meanwhile, Figure 38 to Figure 41 show snapshots throughout the simulation, ranging from 6 hours to 432 hours after discharge. In all these figures, the concentration displayed represents the maximum obtained in the water column.

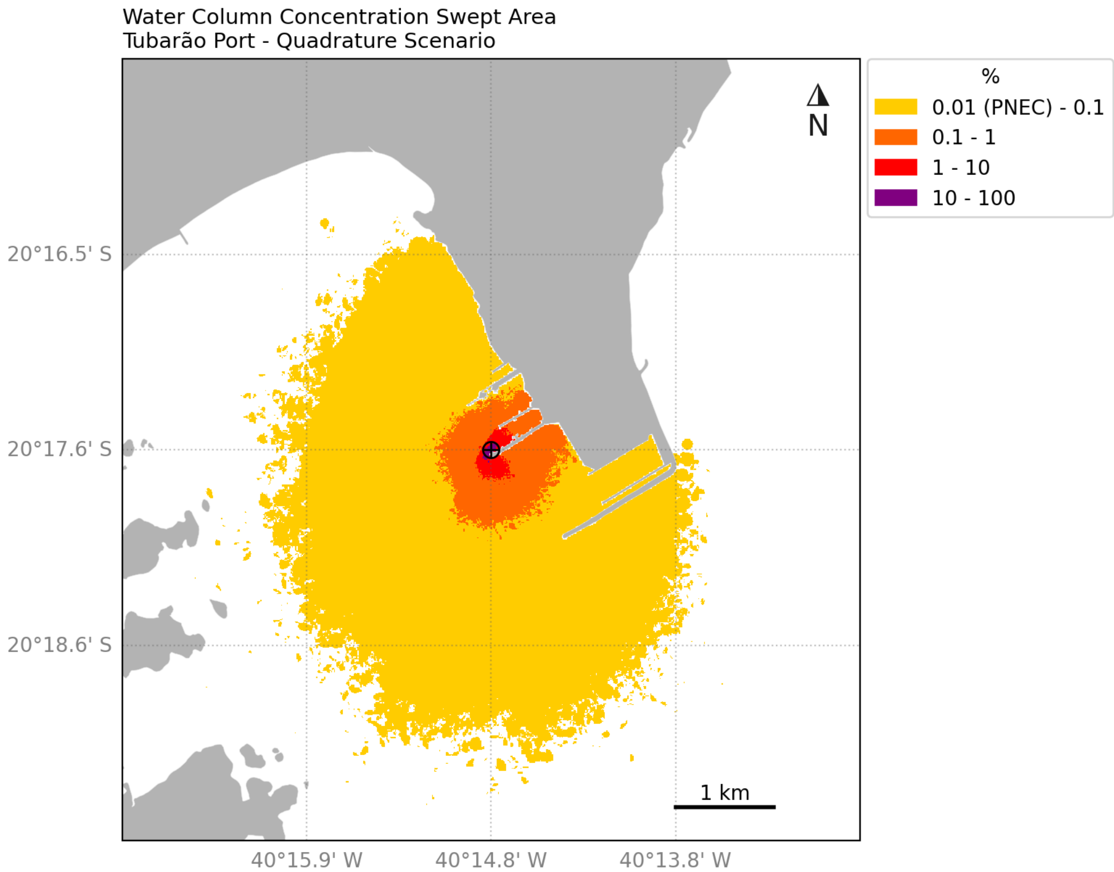


Figure 37: Swept area of maximum concentration in the water column, in the Port of Tubarão, for the quadrature scenario.

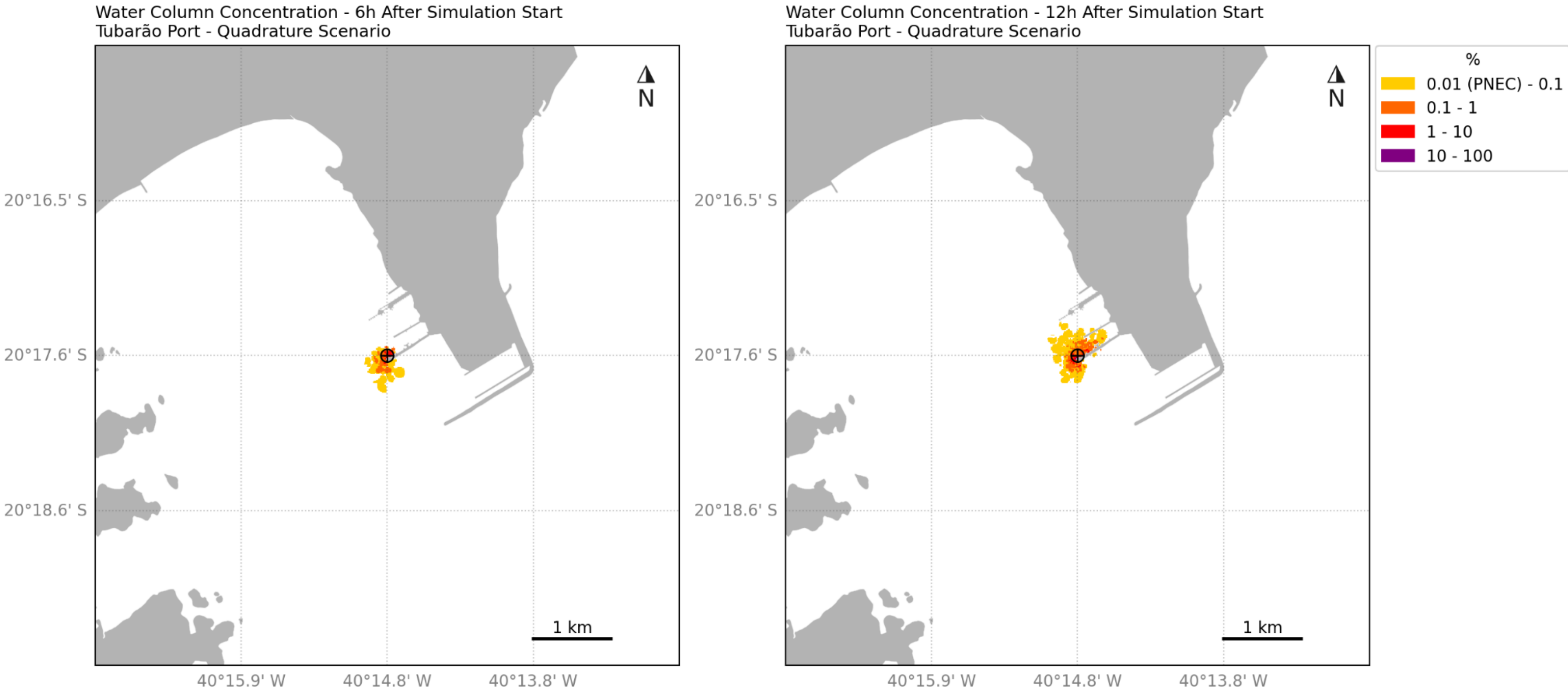


Figure 38: Maximum concentration in the water column after 6 h and 12 h from the start of the simulation (start of discharge), at the Port of Tubarão, for the quadrature scenario.

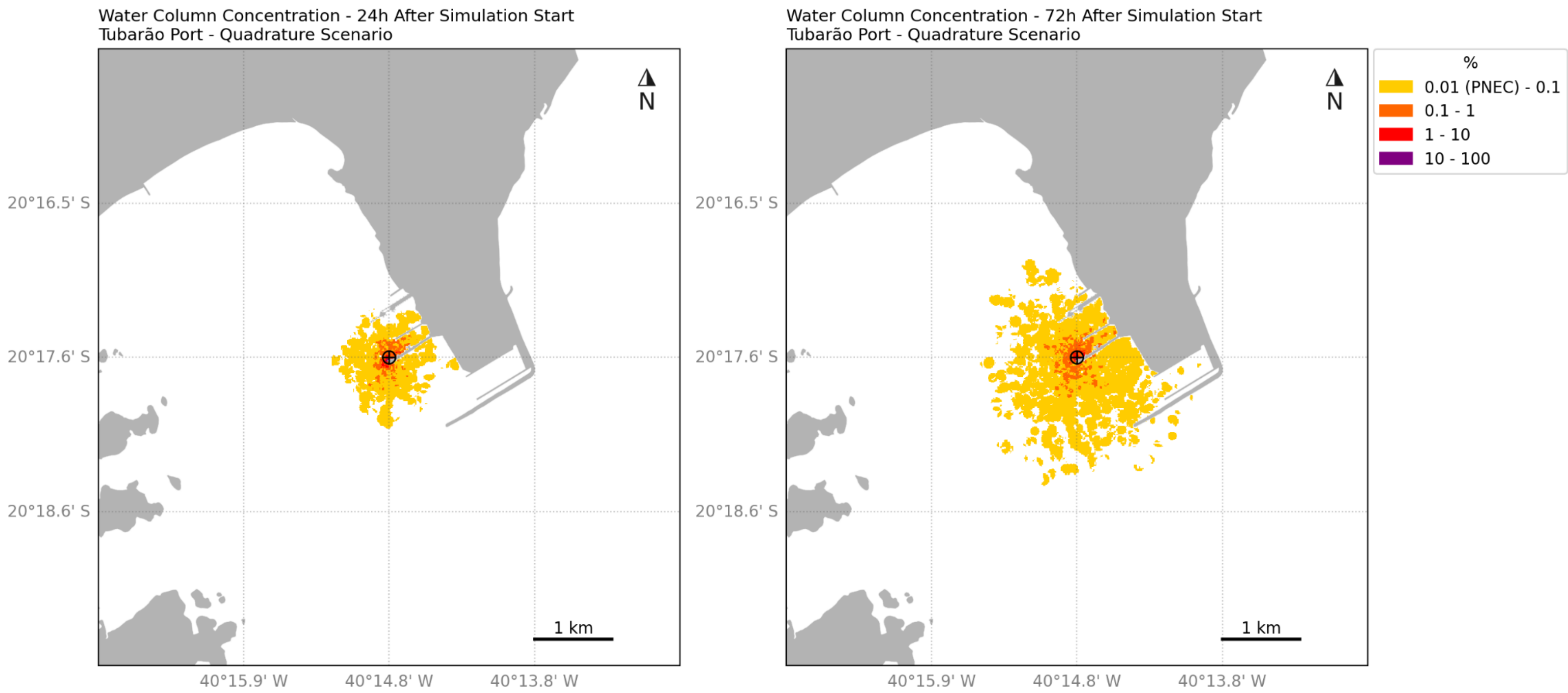


Figure 39: Maximum concentration in the water column after 24 h (1 day) and 72 h (3 days) from the start of the simulation (start of discharge), at the Port of Tubarão, for the quadrature scenario.

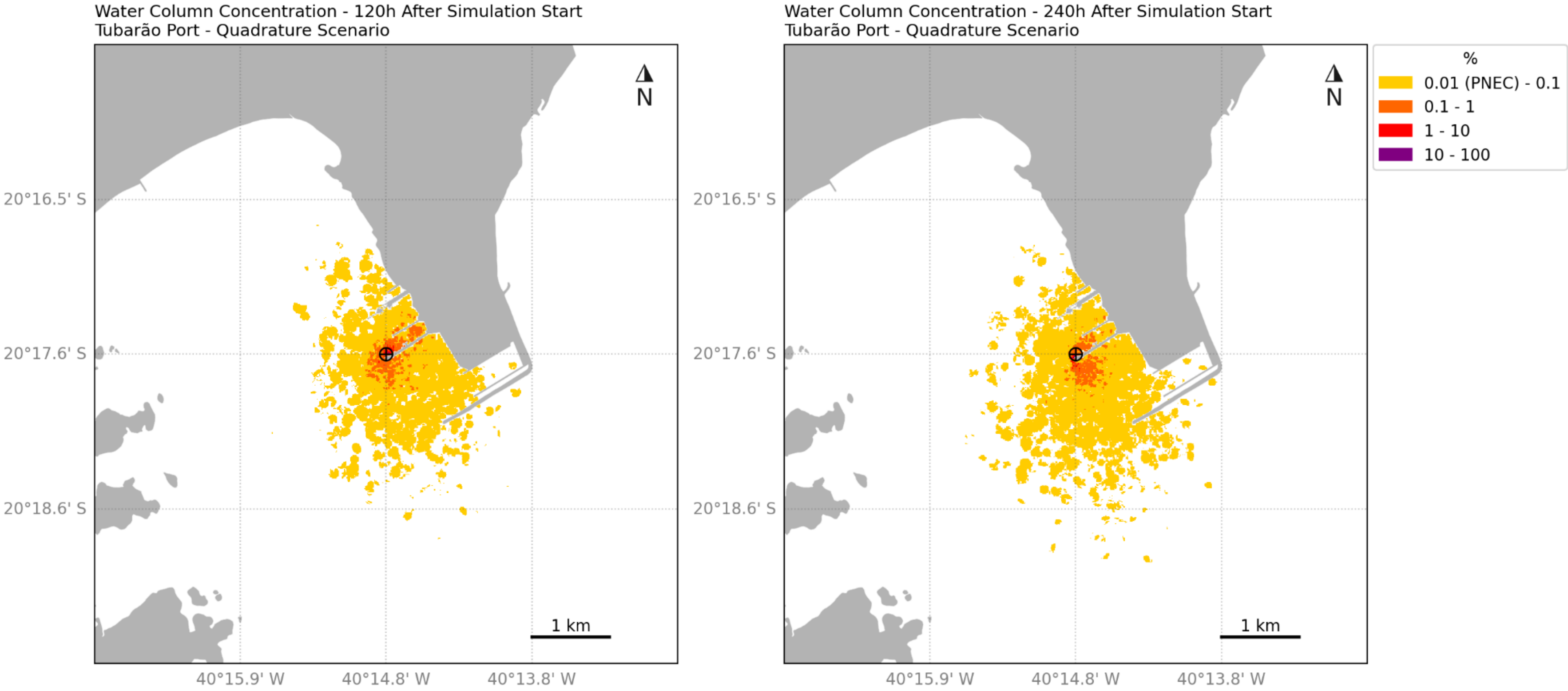


Figure 40: Maximum concentration in the water column after 120 h (5 days) and 240 h (10 days) from the start of the simulation (start of discharge), at the Port of Tubarão, for the quadrature scenario.

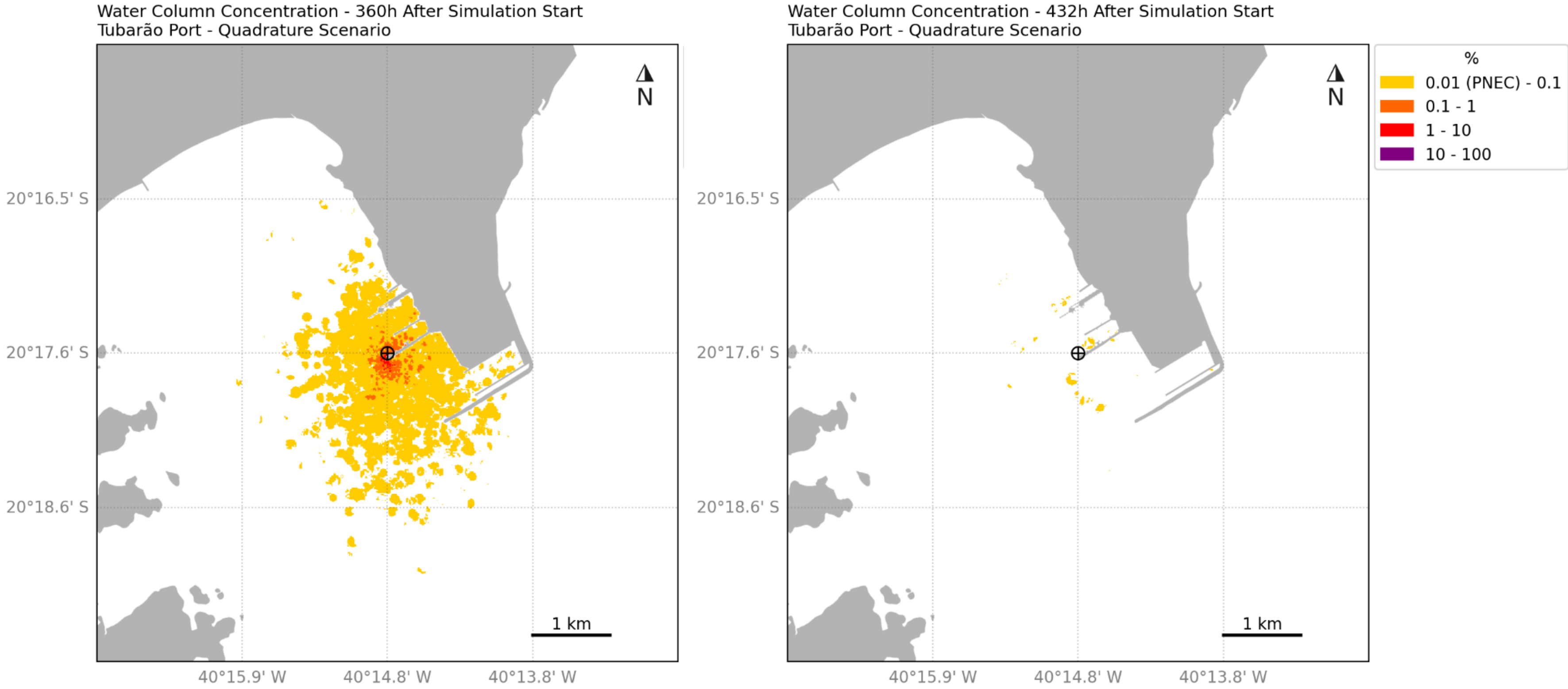


Figure 41: Maximum concentration in the water column after 360 h (15 days) and 432 h (18 days) from the start of the simulation (start of discharge), at the Port of Tubarão, for the quadrature scenario.

#### 4.4.1.3 Significant Risk

Figure 42 presents the cumulative significant risk (above 5%) in the water column throughout the simulation. To compare the simulated syzygy and quadrature tide scenarios, the results are presented in isolines. Figure 43 presents the time during which the environment is subject to significant risk.

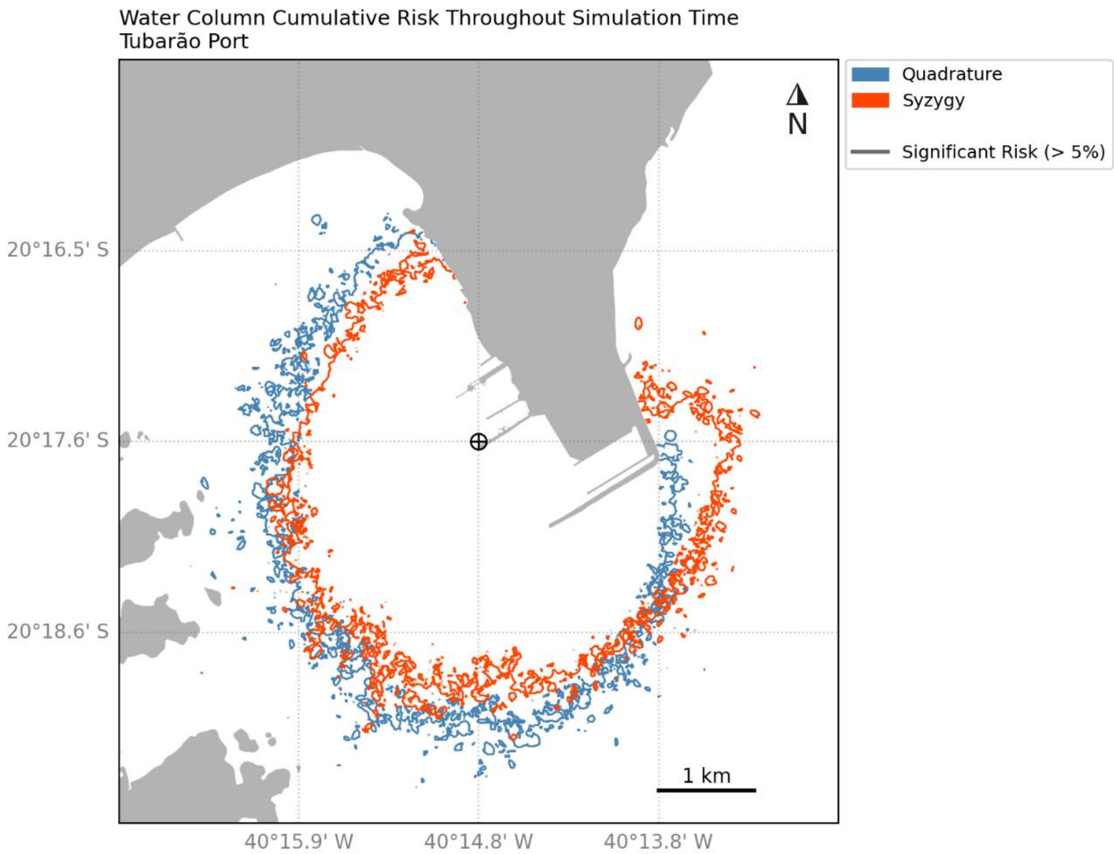


Figure 42: Significant risk (> 5%) associated with concentrations above the PNEC (0.01%), in the Port of Tubarão, for the syzygy and quadrature tide scenarios.

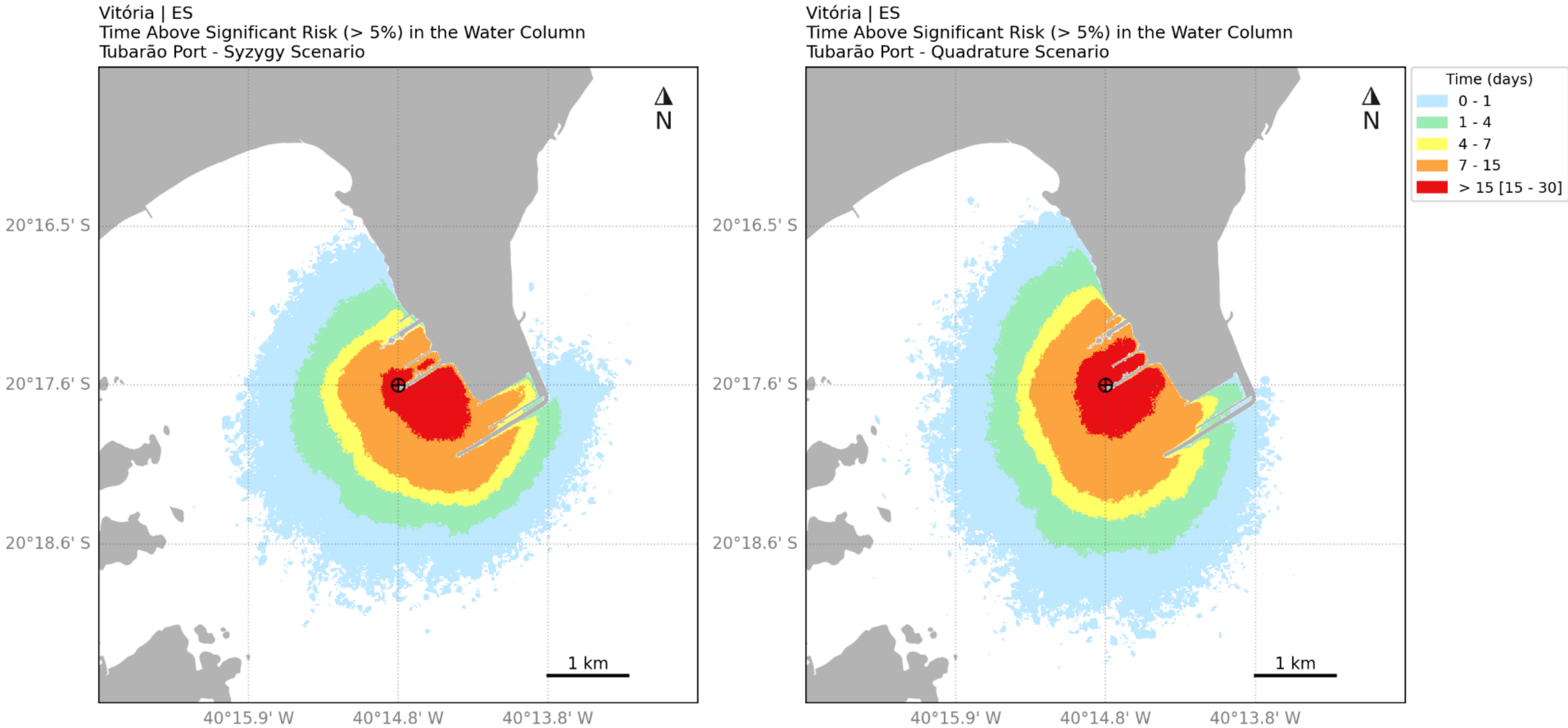


Figure 43: Time during which the environment is subject to significant risk (> 5%), in the Port of Tubarão, for the syzygy and quadrature scenarios.

#### 4.4.1.4 Comparative Tables

Table 38 and Table 39 present the main results obtained for the Port of Tubarão for both simulated scenarios: syzygy and quadrature.

Table 38: Maximum distances obtained for certain concentrations, from 0.01% to 10%, for the syzygy and quadrature tide scenarios.

| Port of Tubarão | Percentage (%) | Distance | |
|---|---|---|---|
| | | Syzygy scenario | Quadrature scenario |
| Concentration: | 0.01 (PNEC) | 3.3 km | 3.8 km |
| | 0.1 | 1.2 km | 940 m |
| | 1 | 450 m | 380 m |
| | 10 | 120 m | 130 m |

Table 39: Main distances and maximum durations obtained for significant risk.

| Significant Risk > 5% | Syzygy scenario | Quadrature Scenario |
|---|---|---|
| Maximum distance from significant risk (equivalent to concentrations above 0.01%) | 3.3 km | 3.8 km |
| Maximum distance from the risk lasting more than 1 day | 2.2 km | 2.2 km |
| Maximum duration of risk at the same grid point | 16.7 days | 17.0 days |

### 4.4.2 Navigation Routes

For the coastal and offshore navigation routes, conditions with stronger and weaker currents were simulated, as described in section 4.3.3 (Scenario Selection), to represent extreme deterministic scenarios. Unlike the approach used for the Port of Tubarão, in which a fixed source was considered, the route scenarios consider a mobile source. The displacement of the vessel along the route in a period of 1 hour towards the port, at a speed of 13.5 knots, covering approximately 13.5 nautical miles (~25 km), is simulated.

The discharge was modeled to occur over a 1-h period, with an additional 5-day monitoring period. For both routes, a 25-m resolution grid was used, the minimum resolution required to cover the entire 25-km extension.

The results indicated that concentrations above the 0.01% threshold (PNEC) were only observed for very short periods (less than 10 minutes) during the simulations. The PNEC threshold adopted in this study is linked to chronic toxicity, which refers to long-term effects such as changes in metabolism, growth, reproduction, mutations, and mortality in organisms, typically resulting from exposures lasting several days. Acute toxicity refers to short-term effects that lead to the lethality of organisms within a timeframe of less than 96 hours.

It is worth mentioning that, in particle modeling, the concentration values obtained represent averages in the volume of the grid cells, defined by the horizontal and vertical resolution of 25 m x 25 m x 10 m, totaling 6,250 m³ (Table 21). Since the values are average concentrations in this volume, it is possible that higher concentrations occur at distances smaller than the grid resolution (25 m) in the real scenario. However, even if higher values appear, they are expected to be rapidly diluted after the vessel passes. It is also observed that the effect of turbulence induced by the propeller and the ship's movement was not considered in these simulations. Thus, it is concluded that the chronic toxic effects and environmental risks associated with these discharge configurations, in the shipping routes, are practically nonexistent.

However, comparatively, it is observed that the effluents discharged along the shipping routes are the same as those at the Port of Tubarão, with similar configurations in terms of depth, discharge diameter and orientation angle. The main differences lie in the current conditions and the fact that the discharge source is mobile rather than fixed. The mobility of the vessel appears to be the main factor that results in a more effective dilution of the effluent along the route, which explains the absence of significant risks observed along the route. At the Port of Tubarão, the scenarios indicated significant risks at distances of up to 4 km from the discharge point. Therefore, it is possible to state that if the discharge occurs from a stationary vessel or even moving at a reduced speed along these routes, it is possible that the chronic risks in these scenarios would be substantially different and may no longer be non-existent.

# 5. Conclusion

This study was carried out as a third stage of Vale's contribution efforts to assess the risks and impacts of discharge water from Exhaust Gas Cleaning Systems (EGSE generated by open-loop EGCS), the second for which CLS Brasil was responsible:

- 1st stage – assessment of the quality and characterization of the inlet water and the EGSE generated by open-loop EGCS (SGS, 2022);
- 2nd stage – assessment of the potential impacts of discharging scrubber wash water at sea for the Port of Tubarão/ES and its navigation route, Asia-Brazil, using computational numerical modeling (Vale & CLS Brasil, 2024); and
- 3rd stage – assessment of environmental risks resulting from the discharge of scrubbers wash water in the marine environment, focusing on the Port of Tubarão/ES and the coastal region (current study).

In Vale & CLS Brasil (2024), no significant changes in water and sediment quality were predicted, taking as reference the quality standards established by CONAMA Resolutions No. 357/05 and No. 454/12, respectively. Regarding acidification, the simulations carried out with the AquaEnv model also indicated practically insignificant changes.

In turn, the present study represents an advance in studies already carried out. The potential impacts of the discharge of Scrubbers wash water are predicted based on an environmental risk assessment that takes into account the potential toxicity of the effluent, not limited to selected substances. In this way, it is possible to carry out a comprehensive assessment of the effluent as a whole and not just the concentrations of the substances present in the effluent. With this, the analysis of the toxic effects of unknown substances began to be considered, in addition to the synergistic effects between all the components of the effluent, in accordance with the MEPC.1/Circ.899 guidelines.

The main conclusions of this study are:

A **Target Lipid Model (TLM)** was performed to assess the toxic potential of EGSE, for the evaluation of ecotoxicological effects (risk concentration that protects 95% of species from 7 different taxonomic groups) in low engine power scenarios associated with the berthing situation in ports, medium and high powers, in coastal and offshore shipping routes, regarding 11 PAHs.

- No evidence of acute toxic effects was found in any of the engine power scenarios analyzed;
- In a low engine power situation, no potential chronic effect of the effluents was detected either.
- However, along the shipping route, four effluents showed evidence of chronic toxicity, suggesting a potential toxic effect of 50% on organisms in the vicinity of the discharge.

The ecotoxicity of EGSE generated by open-loop EGCS was based on a **literature review and compilation of secondary data** from test results evaluated for lethality as well as different sublethal endpoints, in test organisms representing different trophic levels, in short-term (microtox), acute and chronic tests. The consolidation of results respected the premise considered more conservative, selecting the worst results among those analyzed.

- Among all the results compiled from the literature, the most critical EGSE concentration value that causes adverse effects in at least 10% of the tested population was 1%.

The ecotoxicity results are expressed in effluent concentrations, while the definition of a **PNEC (Predicted No-Effect Concentration)** requires a conversion. The reference PNEC for this study was calculated following the guidelines of the ECHA (European Chemicals Agency). Since the conditions of laboratory test methods differ from natural conditions, it is considered more likely that ecosystems are more sensitive to EGSE than the test organisms. The PNEC was estimated by dividing the lowest toxic concentration value (1%) by the indicated assessment factor (100) for long-term toxicity results on at least three different trophic levels.

- The reference PNEC adopted in this work was 0.01% (dilution factor of 10,000 times).
- The same value was used for the shipping route situations and for the situation of a ship berthed in port.
- It should be noted that this threshold is conservative, since it is a value derived from the most toxic concentration found and, in the case of the port scenario, due to the non-identification of base references in the literature for a low engine power, for which the TLM indicated, for example, that there was no evidence of acute or chronic toxic effects.

The assessment of environmental risks is based on the **PEC/PNEC ratio**, with PEC (Predicted Environmental Concentration) being the EGSE concentration in the sea, calculated after its dilution by the processes of transport and turbulent dispersion. In this project, calculated through simulations of the dispersion of effluents into the sea performed with DREAM, considering hypothetical discards inside the sheltered area of the Port of Tubarão, Vitória-ES, and in two positions on the shipping route. In the simulations of EGSE dispersion generated by open-loop EGCS at sea, for the coastal route and offshore route, discharges were considered with the vessel moving at a speed of 13.5 knots towards the port. For the discharge simulations at the Port of Tubarão, discharge in a fixed position for 15 uninterrupted days was considered, assuming that this would be the maximum stay of a ship in the port.

- In the case of **discharges along shipping routes**, both in the coastal region and in the deeper region (offshore), concentrations above 0.01% (or PEC/PNEC=1 and environmental risk 5%) are associated with exposure times on the order of minutes and are likely to undergo dilution shortly after the ship passes. Thus, it is possible to conclude that the chronic toxic effects and consequent environmental risks resulting from these discharges along shipping routes are practically non-existent. It is worth noting that in these simulations the effect of turbulence induced by the vessel's propeller and movement are not considered.
- In the case of **discharges at the Port of Tubarão**, the simulations conducted indicated an environmental risk of 5% (i.e. 5% of the species could be affected) at approximately 4 km from

the discharge point. It is important to highlight that these conclusions derive from the fact that the same PNEC value was used for the navigation route situations and for the situation of a ship berthed in the port (a conservative adoption, although unrealistic for a situation of a ship berthed in a port with minimal operation).

The literature presents various risk assessments regarding EGCS discharge, with mixed conclusions. Although EGSE dilution is expected to occur soon after discharge, exposure concentrations may be relevant in shipping routes. Effects in shipping routes and coastal waters were generally predicted to be low; however, effects in ports remain an area of uncertainty and potential concern due to lower contaminant dispersion and higher background concentrations of contaminants from other sources.

Even considering the low toxicity of the effluent compared to the dilution capacity of the medium, there is concern about the bioaccumulation of contaminants, especially in the port region, if this effluent is discharged in the region. On coastal and offshore routes, this concern is considerably reduced. However, on these routes, the synergistic effect of vessel traffic must be considered. In any situation, however, the biodegradation capacity of this effluent must be clearly and thoroughly assessed, even to be able to consider, or not, the effects of bioaccumulation.

**It is recommended that** the decision to allow or not the discharge of Scrubber wash water generated by open-loop EGCS, in a port region, be assessed on a case-by-case basis and preceded by:

- assessment of the ecotoxicity of the effluent respecting the engine power categorization adopted for the TLM assessment must be respected, considering organisms representing at least 3 different levels, since the TLM analysis made it clear that the engine power influences the composition of the effluent generated, therefore, its ecotoxicity; and
- execution of an Environmental Characterization Project (Baseline) to evaluate the region, mainly the hydrocarbonoclastic biota and the benthic biota and all ecosystem interactions, not only with the EGSE to be discarded, but all other substances that may reach that ecosystem from any other sources.

Finally, it is understood that it is necessary to implement Environmental Monitoring Projects for continuous evaluation of the possible effects of EGSE discharges in port environments where the discharge of EGSE generated by open-loop EGCS may be accepted.

# 6. Bibliography

Aebischer, N.J., Coulson, J.C., Colebrookl, J.M., 1990. Parallel long-term trends across four marine trophic levels and weather. Nat. 347, pages 753–755. https://doi.org/ 10.1038/347753a0, 1990 3476295.

Amante, C. and B.W. Eakins. 2009. ETOPO1 1 Arc-Minute Global Relief Model: Procedures, Data Sources and Analysis. NOAA Technical Memorandum NESDIS NGDC-24, 19 pp, Whole-world gridas available on-line at [http://ngdc.noaa.gov/mgg/global/global.html] from the NOAA, NESDIS, National Geophysical Data Center, Boulder, Colorado USA.

Brain, R. A., & Hanson, M. L. 2021. The press sells newspapers, we should not sell ecotoxicology. Environmental Toxicology and Chemistry, 40(5), 1239.

Brandsma, M.; Smith, J. 1999. Offshore Operators Committee Mud and Produced Water Discharge Model - Report and User Guide. In: Relatório EPR.29PR.99. Production Operations Division. Exxon Production Research Company. Houston, Texas.

CLS Brasil. 2022a. Modelagem Hidrodinâmica. Bloco C-M-661 / Bacia de Campos. Prepared for PETRONAS in February, 2022. Report available at https://licenciamento.ibama.gov.br/.

CLS Brasil. 2022b. Modelagem Hidrodinâmica. Bloco Pau Brasil / Bacia de Santos. Prepared for BP Energy do Brasil in July, 2022. Report available at https://licenciamento.ibama.gov.br/.

CONAMA n° 357 de 2005. Resolução n° 357, de 17 de março de 2005. Publicada no DOU n° 53, de 18/03/2005, seção 1, págs. 58-59.

CONAMA n° 454 de 2012. Resolução n° 454, de 01 de novembro de 2012. Publicada no DOU n° 216, de 08/11/2012, seção 1, pág. 66-69.

DELTARES. 2021. Delft3D-FLOW User Manual: Simulation of multi-dimensional hydrodynamic flows and transport phenomena, including sediments (version 3.15). Retrieved from https://www.deltares.nl/en/software/delft3d-4-suite/.

DHI. 2021. A/S - BWL-DK / Final report / 11826102 / Ecotoxicity testing and risk assessment of wash water from open loop scrubbers/EGSCA/ Final report.

Di Toro, D. M., McGrath, J. A., & Hansen, D. J. (2000). Technical basis for narcotic chemicals and PAH criteria in water and tissue. Environmental toxicology and Chemistry, 1951-1970.

ECHA - European Chemicals Agency. 2008. Guidance on information requirements and chemical safety assessment. Chapter R.10: Characterisation of dose [concentration]-response for environment.

Egbert, G,D,, Erofeeva, S, Y, 2002: Efficient inverse modeling of barotropic ocean tides, J, Atmos, Oceanic Technol,, 19(2), 183-204.

Eldridge, R., Jourdan B., Hansonb M. 2022. A Critical Review of the Availability, Reliability, and Ecological Relevance of Arctic Species Toxicity Tests for Use in Environmental Risk Assessment. Environmental Toxicology and Chemistry. Volume 41. Number1. págs 46–72

Gadd, J., Hickey, C., Moores, J. 2020. Risks from Discharges from Exhaust Gas Cleaning - Scoping for Environmental Risk Assessment. Report. Page 63

Haidvogel, D.B., H. Arango, W.P. Budgell, B.D. Cornuelle, *et al*. 2008, Ocean forecasting in terrain-following coordinates: Formulation and skill assessment of the Regional Ocean Modeling System, Journal of Computational Physics, 227, 3595-3624.

Hansen, J. P. 2012. Exhaust Gas Scrubber Installed Onboard MV Ficaria Seaways. Environmental Project N° 1429. Page 31.

Hennermann, K. ERA5 Data Documentation. Available at: https://software.ecmwf.int/wiki/display/CKB/ERA5+data+documentation Accessed on 09/20/2017.

Hofmann, A.F., Soetaert, K., Middelburg, J.J., Meysman, F.J.R. 2010b. AquaEnv - An Aquatic Acid-Base Modelling Environment in R. Aquatic Geochemistry, 16, 507-546. DOI 10.1007/s10498-009-9084-1.

Hufnagl, M., Liebezeit, G., Behrends, B. 2005. Effects of Sea Water Scrubbing. Final Report. 145 pages

IMO. 2015. Third IMO GHG Study 2014. Executive Summary and Final Report. Micropress Printers, Suffolk, UK.

Irigoien, X., Hulsman, J., Harris, R.P., 2004. Global biodiversity patterns of marine phytoplankton and zooplankton. Nature 429, Págs 863–867. https://doi.org/10.1038/nature02593, 2004 4296994.

Kamper, A & Madsen, T. 2021. Ecotoxicity testing and risk assessment of wash water from open loop scrubbers. ECGA Report. 73 pages

Koh, R. C. Y.; Chang, Y. 1973. Mathematical Model for Barge Ocean Disposal of Wastes, Relatório EPA-6602-73-029, U.S. Environmental Protection Agency, Corvallis, Oregon.

Koski, M., Stedmon, C., Trapp, S. 2017a. Ecological effects of scrubber water discharge on coastal plankton: Potential synergistic effects of contaminants reduce survival and feeding of the copepod Acartia tonsa. Mar. Environ. 12 pages

Koski, M., Trapp, S., Stedmon, C. 2017b. Ecological effects of scrubber discharge water on marine plankton. Summary report. 13 pages

Koyama, J, Ishimaru, T, Takasaki, K, Takasaki, C, Matsumoto, T, Michio, Y, Yamaji, K. 2018. Report by the expert board for the environmental impact assessment of discharge water from Scrubbers. Report. 71 pages.

Lange, K, Markus, T, Helfst, L. P. 2015. Impacts of Scrubbers on the environmental situation in ports and coastal waters. Report No. (UBA-FB) 002015/E. 88 pages

Larnicol, G., Guinehut S., Rio M.H., Drevillon M., Faugère Y., Hernandez F. 2006. The global observed ocean products of the French Mercator project, 15 years of radar altimetry symposium, Venise.

López, A. L, Marrero, A, Cruz, Y. M, González, M.M. 2023. Environmental assessment model for scrubbers versus alternative mitigation systems for feeder vessels in liner shipping. Research article Environmental Management. 11 pages

Magnusson, K., Magnusson, M., Ostberg, P., Granberg, M., Tiselius, P. 2018. Bioaccumulation of C-14-PCB 101 and C-14-PBDE 99 in the marine planktonic copepod Calanus finmarchicus under different food regimes. Report. 50 pages

McCarty, L. S., Mackay, D., Smith, A. D., Ozburn, G. W., & Dixon, D. G. 1993. Residue-based interpretation of toxicity and bioconcentration QSARs from aquatic bioassays: polar narcotic organics. Ecotoxicology and Environmental Safety, 25(3), 253-270.

McGrath J, Parkerton T, Di Toro D. 2004. Application of the narcosis target lipid model to algal toxicity and deriving predicted-no-effect concentrations. Environ Toxicol Chem 23:2503–2517.

McGrath, J. A., Fanelli, C., Di Toro, D. M., Parkerton, T. F., Redman, A. D., Paumen, M. L., den Haan, K..2018. Re-evaluation of target lipid model-derived HC5 predictions for hydrocarbons. Environmental Toxicology & Chemistry, 37:1579-1593.

McGrath, J. A., Parkerton, T. F., Hellweger, F., & Di Toro, D. M. 2005. Validation of the narcosis target lipid model for petroleum products: Gasoline as a case study. Environmental Toxicology & Chemistry, 24:2382-2394.

McGrath, J., Getzinger, G., Redman, A. D., Edwards, M., Aparicio, A. M., & Vaiopouloud, E. 2021. Application of the Target Lipid Model to Assess Toxicity of Heterocyclic Aromatic Compounds to Aquatic Organisms. Environmental Toxicology & Chemistry, 40:3000-3009.

MEPC.259(68). IMO EGCS Guidelines Resolution MEPC.259(68). 2015 Guidelines for Exhaust Gas Cleaning Systems. Adopted on 15 May 2015.

Meylan, W., Howard, P. 1999. User's guide for EPIWIN. EPI Suite: Estimation Programs Interface for Microsoft Windows, North Syracuse (NY): Syracuse Research Corporation.

OSPAR. 2022. Modelling of discharges to the marine environment from open circuit flue gas Scrubbers on ships in the OSPAR Maritime Area. Quality Status Report 2023.

Picone, M., Distefano, G.G., Marchetto, D., Russo, M., Baccichet, M., Brus o, L., Zangrando, R., Gambaro, A., Ghirardini, A.V. 2022. Impacts of exhaust gas cleaning systems (EGCS) discharge waters on planktonic biological indicators. Mar. Environ. 18 pages

Redman, A. D., Parkerton, T. F., MacGrath, J. A., & Di Toro, D. M. 2012. Petrotox: An aquatic toxicity model for petroleum products. Environmental Toxicology & Chemistry, 31:2498-2506.

Redman, A. D., Parkerton, T. F., Paumen, M. L., McGrath, J. A., den Haan, K., & Di Toro, D. M. 2014. Extension and validation of the target lipid model for deriving predicted no-effect concentrations for soils and sediments. Environmental Toxicology & Chemistry, 33:2679-2687.

Reed, M. & Hetland, B. 2002. DREAM: a Dose-Related Exposure Assessment Model Technical Description of Physical-Chemical Fate Components. SPE International Conference on Health, Safety and Environment in Oil and Gas Exploration and Production, Kuala Lumpur, Malaysia, March 2002.

Schmolke, S, Ewert, K, Kaste, M, Schöngaßner, T, Kirchgeorg, T, Marin-Enriquez, O. 2020. Environmental Protection in Maritime Traffic – Scrubber Wash Water Survey. ERMS Report. 93 pages

SGS. 2022. EGCS Pilot Project- Report. Reference: 0118202104. SGS MARINE FIELD SERVICES & MONITORING. Date: November 29th, 2022.

Teuchies, J., Cox, T. J. S., Van Itterbeeck, K., Meysman, F. J. R., Blust, R. 2020. The impact of scrubber discharge on the water quality in estuaries and ports. Environ. Sci. Eur. 103 pages.

Thor, P. Severe. 2021. Toxic Effects on Pelagic Copepods from Maritime Exhaust Gas Scrubber Effluents. Article. 10 págs https://doi.org/10.1021/acs.est.0c07805

US. Environmental Protection Agency. 2018. Episuite – Estimation Programas Interface SuiteTM for Microsoft Windows, v 4.11. Accessed on March, 2023 and available at <https://www.epa.gov/tsca-screening-tools/epi-suitetm-estimation-program-interface >.

Vale & CLS Brasil. 2024. Modelagem das Descargas da Lavagem de Scrubbers em Ambiente Marinho. Relatório Final / Sumário Executivo (Rev03). Relatório técnico elaborado pela CLS Brasil para a Vale, em 04 de março de 2024.

Viegas. C. A. 2021. Chapter Four - Microbial bioassays in environmental toxicity testing. Volume 115. Pages 115-158 https://doi.org/10.1016/bs.aambs.2021.03.002

Word, J, Wang, C, McGrath, J, Stubblefield, W. 2024. Puget Sound Exhaust Gas Cleaning System (Egcs) Washwater Ecological Risk Assessment. Report.76 págs

Ytreberg, E., Åstrom, S., Fridell, E., 2021a. Valuating environmental impacts from ship emissions– the marine perspective. J. Environ. Manag. 282 págs, 111958 https://doi.org/10.1016/J.JENVMAN.2021.111958.

Ytreberg, E., Hassellov, I.M., Nylund, A.T., Hedblom, M., Al-Handal, A.Y., Wulff, A., 2019. Effects of scrubber washwater discharge on microplankton in the Baltic Sea. Mar. Pollut. Bull. 145, Pages 316–324. https://doi.org/10.1016/J. MARPOLBUL.2019.05.023.

Ytreberg, E., Karlberg, M., Hassellov, I.M., Hedblom, M., Nylund, A.T., Salo, K., Imberg, H., Turner, D., Tripp, L., Yong, J., Wulff, A., 2021b. Effects of seawater scrubbing on a microplanktonic community during a summer-bloom in the Baltic Sea. Environ. Pollut. 291, 118251 https://doi.org/10.1016/J. ENVPOL.2021.118251.

# 7. Annexes

ANNEX I Coastal Hydrodynamic Modeling for the Port of Tubarão / Espírito Santo (ES)

- ANNEX I -

# Coastal Hydrodynamic Modeling for the Port of Tubarão / Espírito Santo (ES)

# Coastal Hydrodynamic Modeling

## Port of Tubarão / Espírito Santo (ES)

**TECHNICAL REPORT [REV.00]**

NOVEMBER 12, 2024

**Prepared by:**

CLS Brasil

CLS Brasil
Rio Branco Av., 311/1205 - Center
20.040-009 - Rio de Janeiro - RJ
Tel./Fax + 55 21 2532.5666
clsbrasil.com

# Summary

# 1. Introduction

The present study was carried out with the objective of simulating the hydrodynamic conditions of the region of the Port of Tubarão and its surroundings. To this end, comprehensive modeling of the Vitória and Espírito Santo Bay (Figure 1) was conducted.

This study used the Delft3D model, an advanced tool for simulating multidimensional hydrodynamic flows and transport phenomena. Delft3D was chosen for its ability to accurately represent the complex interactions between tidal currents, winds and river flows that are the main environmental forces of the study region, in addition to being a widely validated and internationally recognized model.

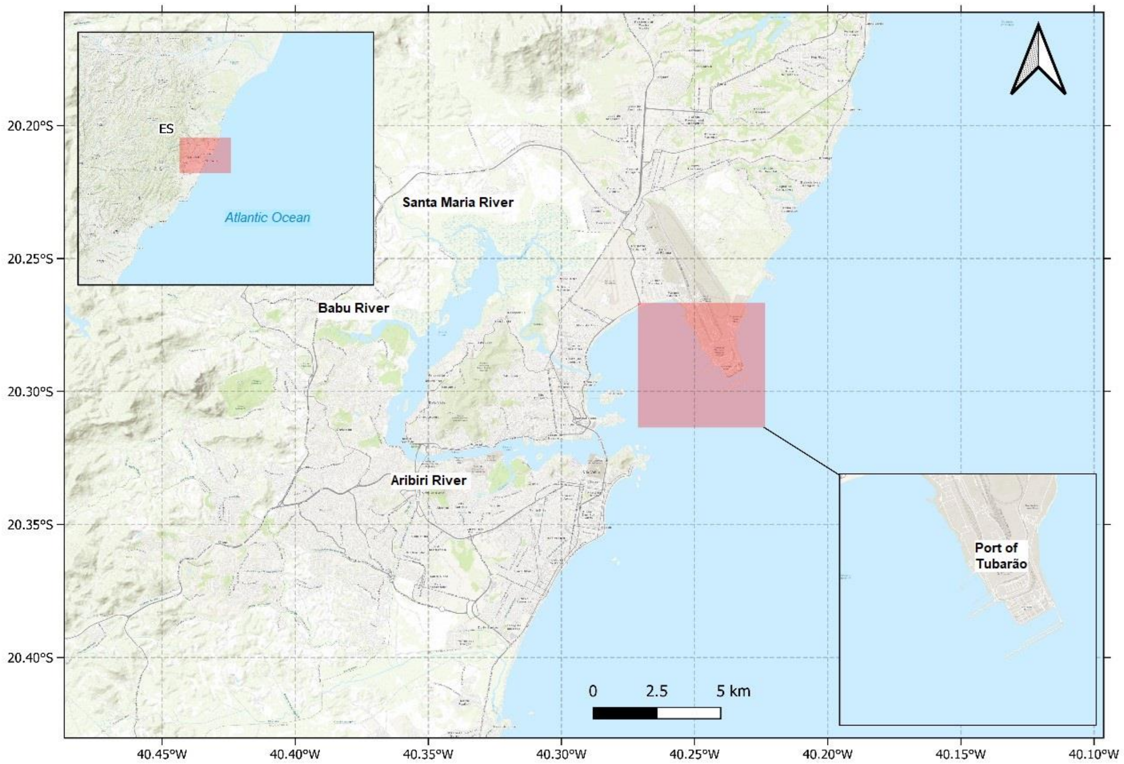


Figure 1: Study Area (*Datum* WGS84).

# 2. Coastal Hydrodynamic Modeling

Coastal regions are extremely heterogeneous, with the presence of estuaries, bays, tidal effects and complex interactions between coastal currents and the open sea. These spatial variations can be as small as meters or kilometers, while deep ocean modeling can consider scales of tens to hundreds of kilometers.

Coastal processes are characterized by rapid and frequent changes, such as semi-diurnal and diurnal tides, short-duration waves and intense local meteorological variations.

The main forces that influence coastal dynamics include bathymetry, wind, tide and freshwater flows, such as rivers and estuaries. These elements not only introduce rapid variations in circulation patterns and particle transport, but also have a direct impact on water quality, coastal erosion and human activities.

The need for coastal hydrodynamic modeling is crucial to accurately capture complex phenomena and their interactions at scales relevant to coastal management, urban planning and environmental protection decisions. Numerical models developed specifically for coastal environments incorporate detailed parameters, refined spatial and temporal resolutions, and algorithms that consider multiple forces in an integrated manner, allowing for more realistic simulations that are applicable to the specific conditions of each coastal region.

## 2.1. Methodology

### 2.1.1 Numerical model

The tool used for the study was Delft3D (Deltares, 2021), a widely used numerical model for hydrodynamic simulations. Developed by Deltares, this model uses the fundamental equations that govern the movement of fluids in aquatic environments. These include the simplified Navier-Stokes equations for shallow waters, as well as transport equations and biochemical and ecological models to simulate physical and chemical processes. Internationally recognized for its extensive validation, Delft3D is reliable for applications such as coastal planning, water quality management, environmental impact studies and flood forecasting.

### 2.1.2 Domain

In order to accurately simulate the hydrodynamics in the Port of Tubarão region, a domain (Figure 2) was defined that covered the entire region of Vitória Bay, Espírito Santo Bay and the inner continental shelf, capturing all necessary environmental forces.

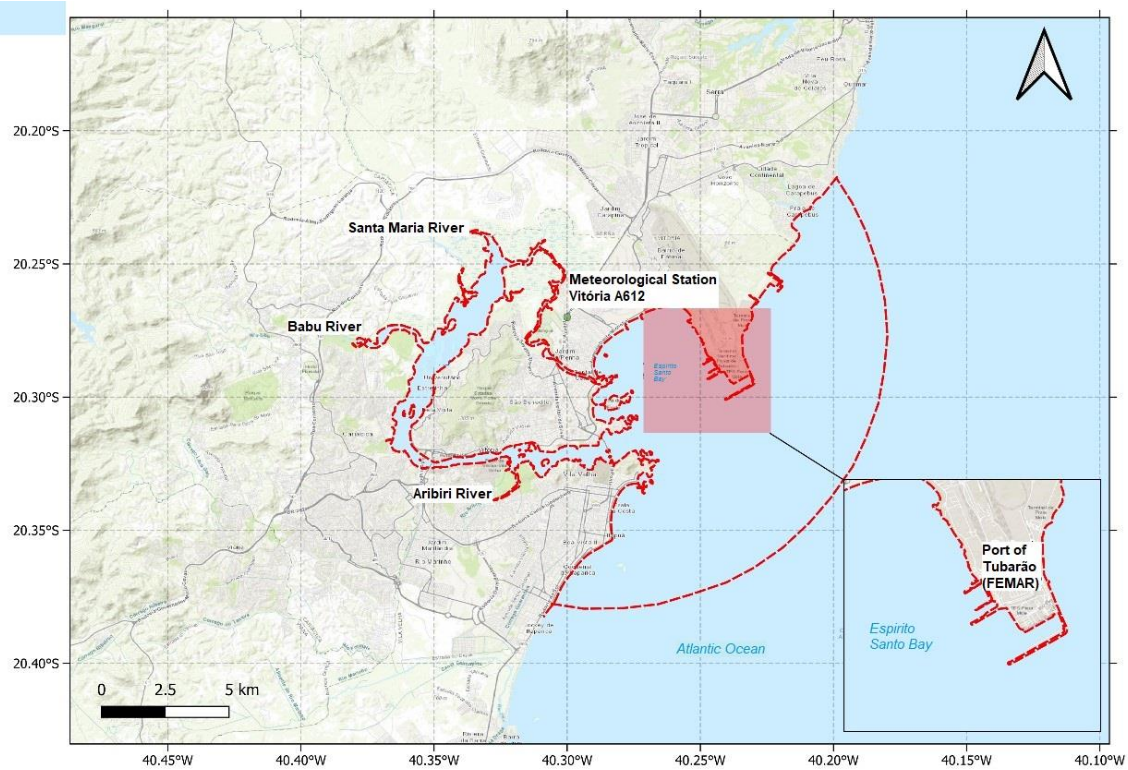


Figure 2: Study domain comprising the fluvial and estuarine parts.

### 2.1.3 Numerical grid

The domain was discretized using a high-resolution curvilinear numerical grid covering the river and estuarine region.

The study area is characterized by shallow waters, where vertical variations in current speeds and directions are often minimal compared to horizontal variations. Under these conditions, two-dimensional (2D) models are suitable for capturing flow characteristics.

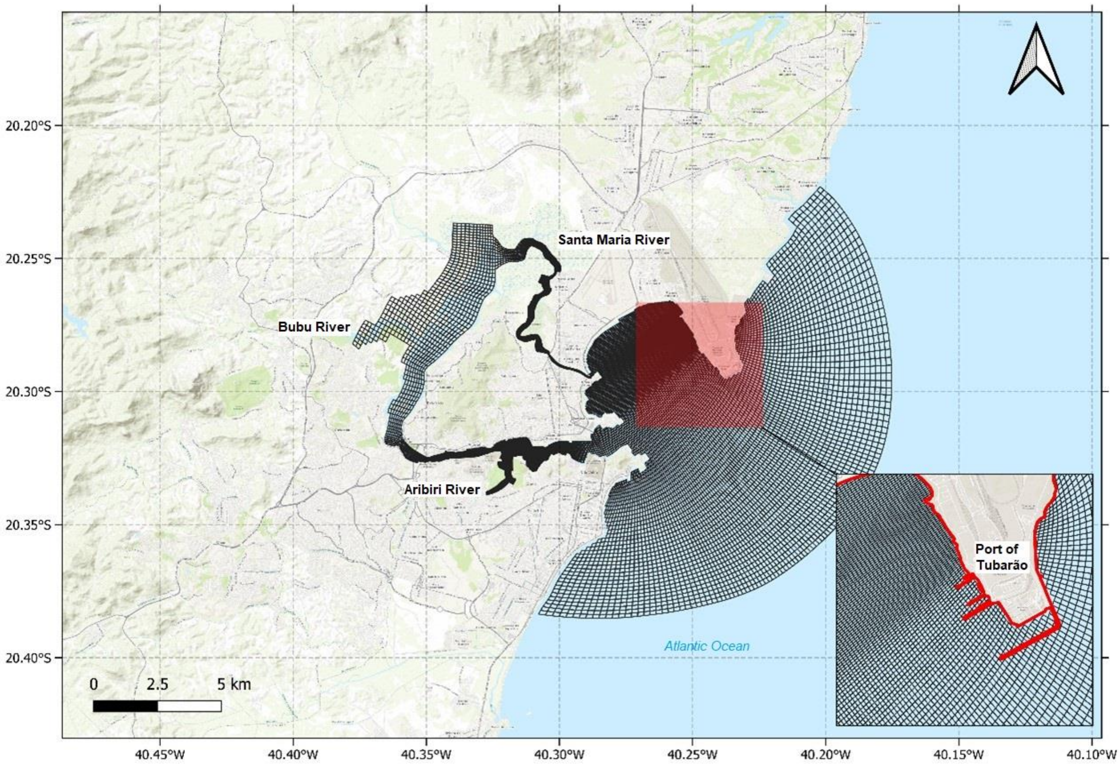


Figure 3: Numerical grid considered in the modeled domain with details for the Port of Tubarão region.

### 2.1.4 Bathymetry

The bathymetry was obtained by scanning the nautical chart – Vicinity of the Ports of Vitória and Tubarão - No. 1410 (Figure 4 and Figure 5).

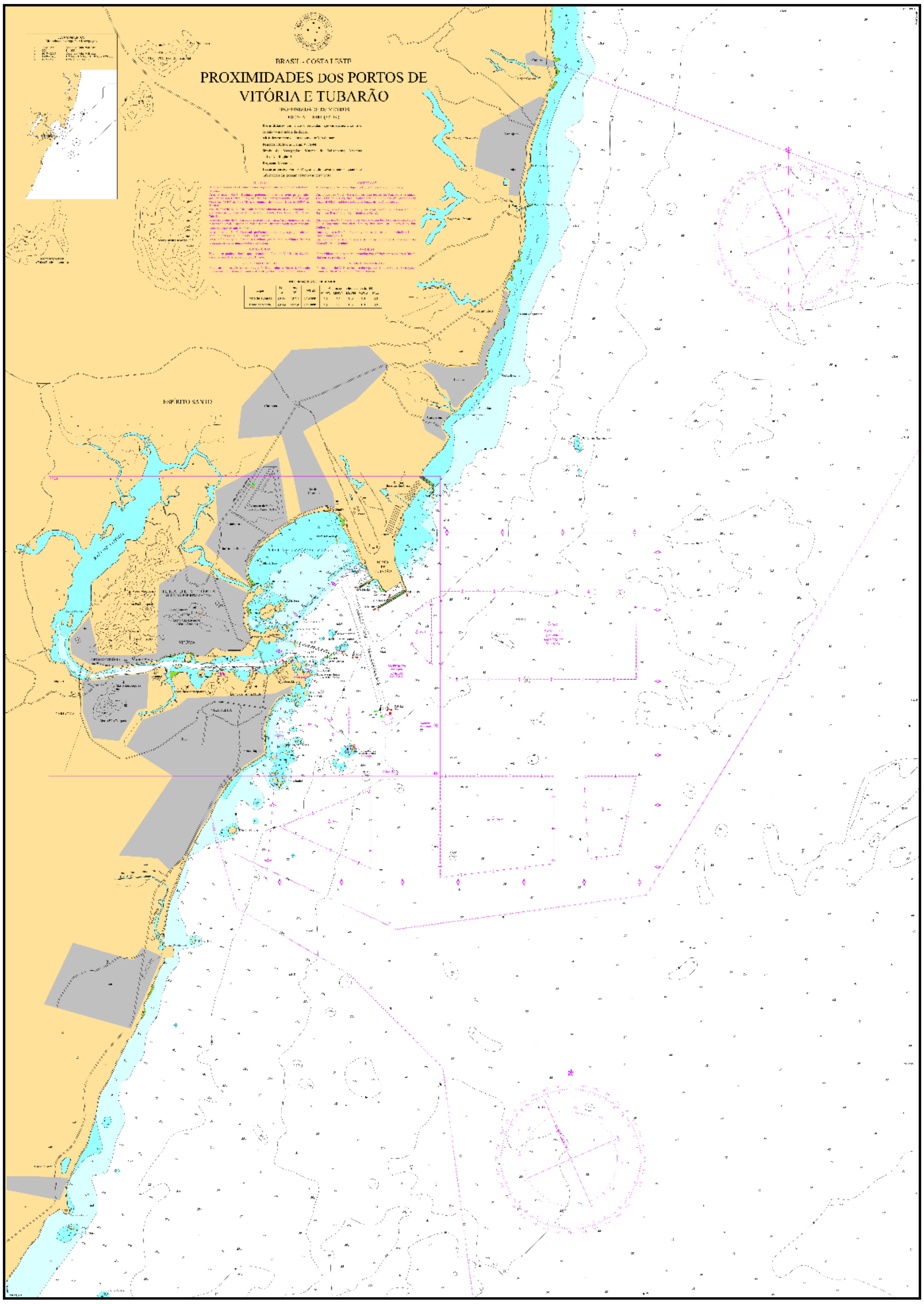


Figure 4: Nautical chart Vicinity of the Ports of Vitória and Tubarão (No. 1410). Official and original text in Portuguese extracted from CHM (2022).

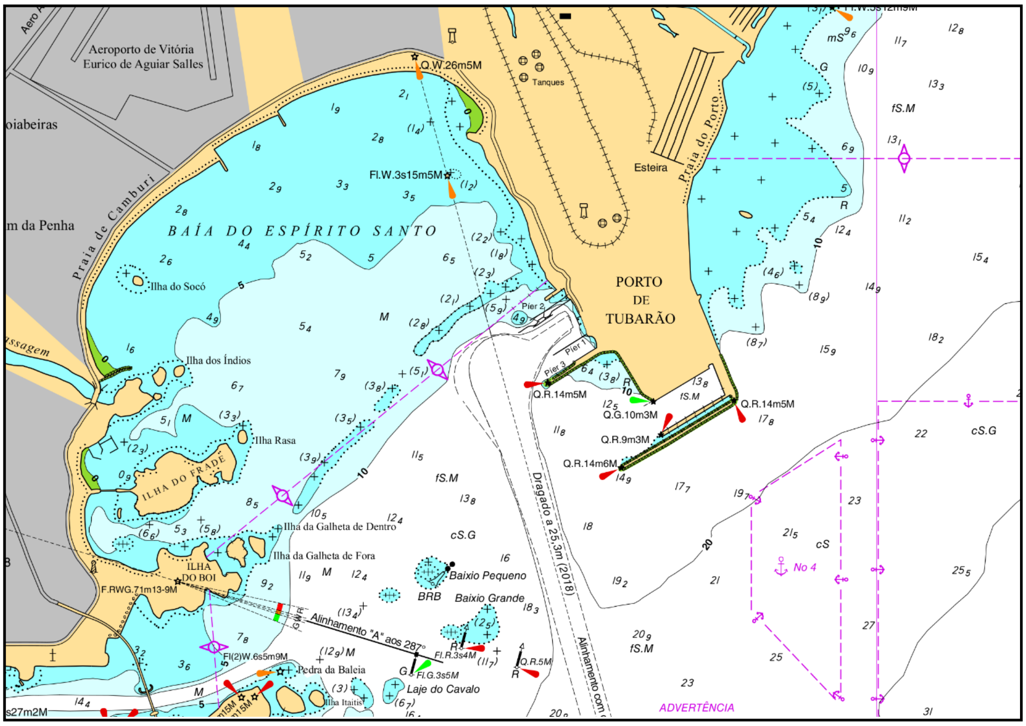


Figure 5: Nautical chart Vicinity of the Ports of Vitória and Tubarão – detail in the Port of Tubarão region (No. 1410). Official and original text in Portuguese extracted from CHM (2022).

The elevations provided by the nautical chart are based on the average low tides of spring. The mean sea level is located 0.8 m above this same reference level. To obtain all elevations in relation to the mean sea level (MSL), 0.8 m was added to each bathymetry value contained in the nautical chart.

A satellite sensitivity analysis was conducted to verify and, if necessary, update recently dredged regions.

After digitizing the bathymetric elevations, the model's bathymetry was generated through triangular interpolation to the numerical grid (Figure 6).

Due to the presence of extensive areas of mangroves in the study area, a "flood and dry" mechanism was implemented. These areas were mapped according to elevation data from Google Earth Pro. This mechanism is particularly relevant for tidal environments, such as mangroves, which are subject to periodic cycles of flooding and emptying.

Delft3D uses specific criteria to determine when a grid cell is considered flooded or dry. These criteria include:

- **Water Level Height:** If the water level in a cell exceeds a critical value, the cell is considered flooded. Example: During high tide, water floods areas of negative bathymetry, flooding mangroves and other intertidal zones.
- **Water Layer Thickness:** The cell is only considered dry if the water layer thickness falls below a predefined minimum value.

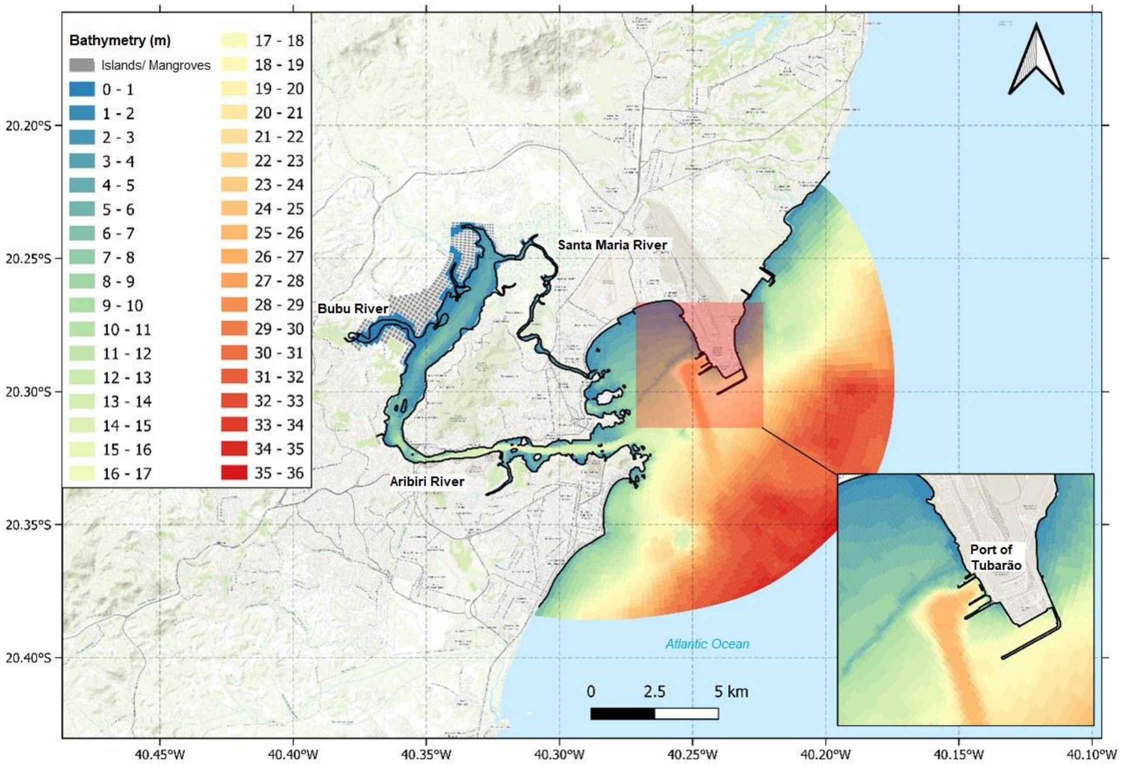


Figure 6: Bathymetry considered in the modeled domain with details for the Port of Tubarão region.

### 2.1.5 Modeling Period

A 30-day simulation period would be able to capture the essential variability of the tidal cycles, covering several spring-neap tidal cycles (typically around 14 days each). However, the study region experiences significant seasonal differences in wind and river flow patterns, which may influence current patterns. Therefore, a 1-year simulation period (2012-1-1 to 2012-12-31) was defined, capable of robustly resolving the hydrodynamic patterns and their seasonality in the study region.

### 2.1.6 Boundary conditions

#### 2.1.6.1 Tide

The time series of water level rise due to the astronomical tide adopted in this study was extracted from the nearest grid point of the global tidal model TPXO9.v5 atlas.

The TPXO9.v5-atlas is the latest global solution of 1/30°x1/30° resolution, obtained by combining the global TPXO9 solution with local high-resolution solutions, developed by Gary Egbert and Lana Erofeeva (2002) at Oregon State University. TPXO9 assimilates more TOPEX/Poseidon (T/P) and TOPEX Tandem satellite radar altimetry data. TPXO9 is one of the most accurate global tidal solutions due to the assimilation of tide gauge data.

The records comprise 11 main harmonic components, which are presented in Table 1.

Table 1: Harmonic components obtained from TPX09.v5 atlas data.

| Constant | Half amplitude (m) | Phase (degrees) |
|---|---|---|
| M2 | 0.495 | 177.195 |
| S2 | 0.228 | 197.772 |
| N2 | 0.071 | 187.991 |
| K2 | 0.063 | 190.059 |
| K1 | 0.050 | 211.430 |
| O1 | 0.087 | 140.325 |
| P1 | 0.016 | 200.787 |
| Q1 | 0.024 | 116.672 |
| M4 | 0.022 | 249.747 |
| MS4 | 0.006 | 314.181 |
| MN4 | 0.007 | 254.709 |

The study region does not have a significant meteorological tide, being dominated by the astronomical tide.

Figure 7 presents the hourly forecast of sea level rise due to astronomical tides for the modeling period.

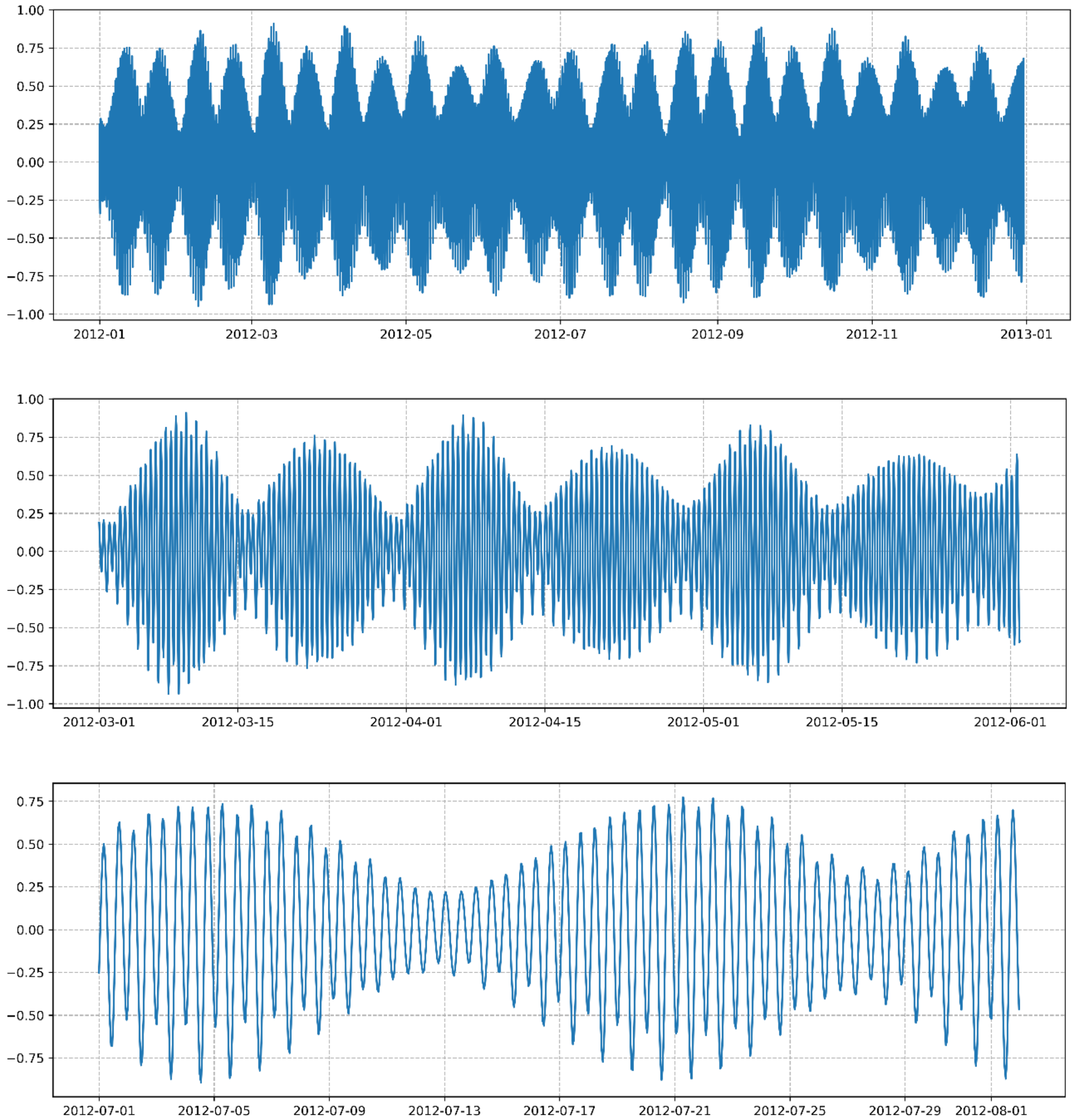


Figure 7: Time series of sea level due to astronomical tides between 01/01/2012 and 12/31/2012 (upper panel), quarterly (central panel) and monthly (lower panel).

### 2.1.6.2 Winds

Hourly wind data were obtained from the conventional station VITÓRIA-ES (A612) of the National Institute of Meteorology – INMET, located near the airport of Vitória (Figure 8).

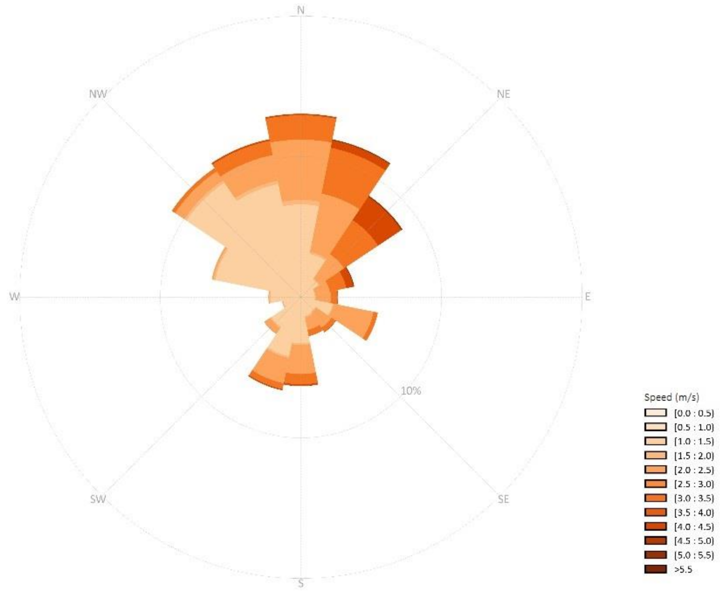


Figure 8: Windrose from VITÓRIA-ES (A612) for the year 2012. Source: INMET.

### 2.1.6.3 River flow

River flow, which represents the volume of fresh water supplied by rivers, data was obtained from Hidroweb, a hydrological data portal maintained by the National Water Agency (ANA). For the main river in the study area, the Santa Maria River, daily historical data recorded over 70 years (Station 5713) were used. From this time series, the monthly climatology of the river flow was calculated, which served as input data for the numerical model (Table 2 and Figure 9).

Table 2: Flow rate ($m^3/h$) climatology of the Santa Maria River flow. Source: ANA.

| Month | Flow rate ($m^3/h$) |
|---|---|
| Jan | 40.56 |
| Feb | 29.77 |
| Mar | 29.92 |
| Apr | 23.85 |
| May | 18.46 |
| Jun | 15.75 |
| Jul | 15.00 |
| Aug | 13.66 |
| Sep | 12.75 |
| Oct | 15.40 |
| Nov | 30.60 |
| Dec | 40.89 |

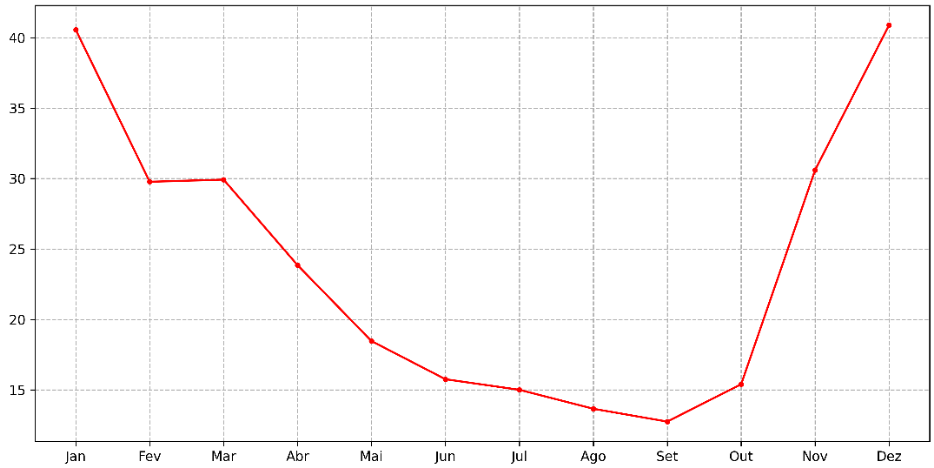


Figure 9: Flow rate ($m^3/h$) climatology of the Santa Maria River flow. Source: ANA.

#### 2.1.6.4 Temperature and Salinity

The temperature and salinity data for the open boundary condition (ocean) were obtained from the hydrodynamic model developed by CLS Brasil, specifically for the southeast region of Brazil. Concerning the river flow, the temperature was assumed to be constant at 24º C, and salinity was considered null (zero).

## 2.2. Results

In the following Figure 10 to Figure 21 instantaneous maps of currents during the summer and winter periods for the following environmental conditions are presented:

- → Spring ebb tide
- → Spring flood tide
- → Neap ebb tide
- → Neap flood tide

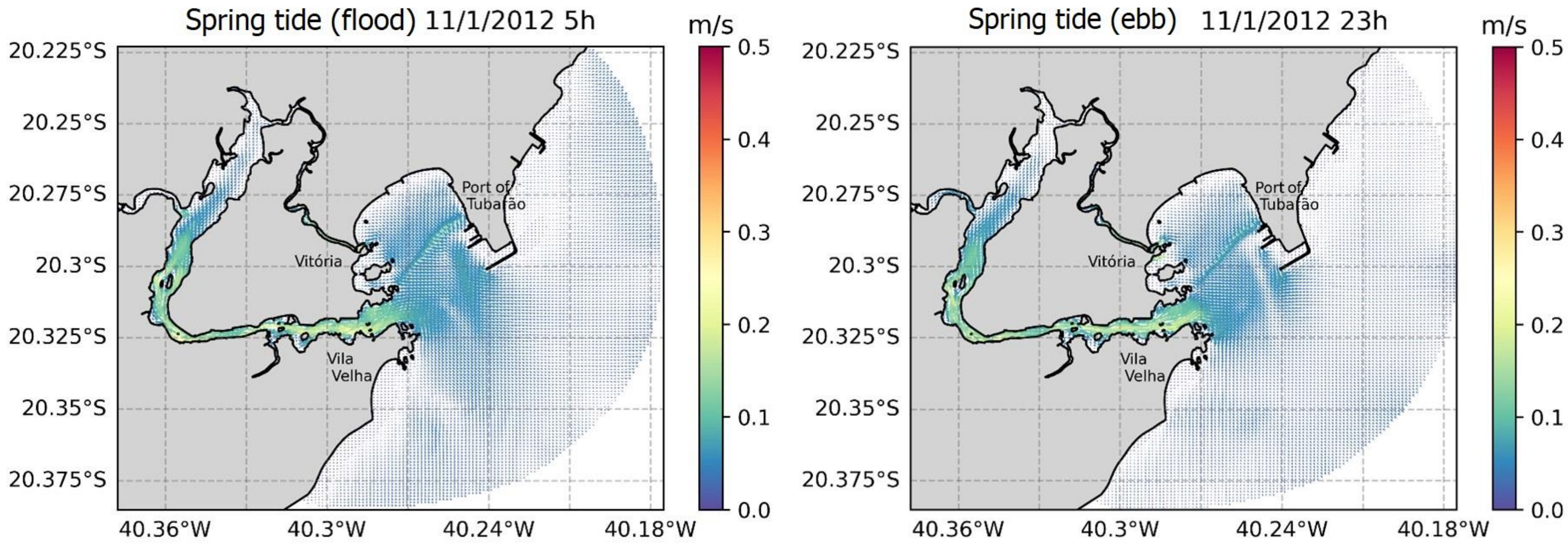


Figure 10: Current map in summer (general domain) at a time of spring tide during flood (left panel) and ebb (right panel) periods.

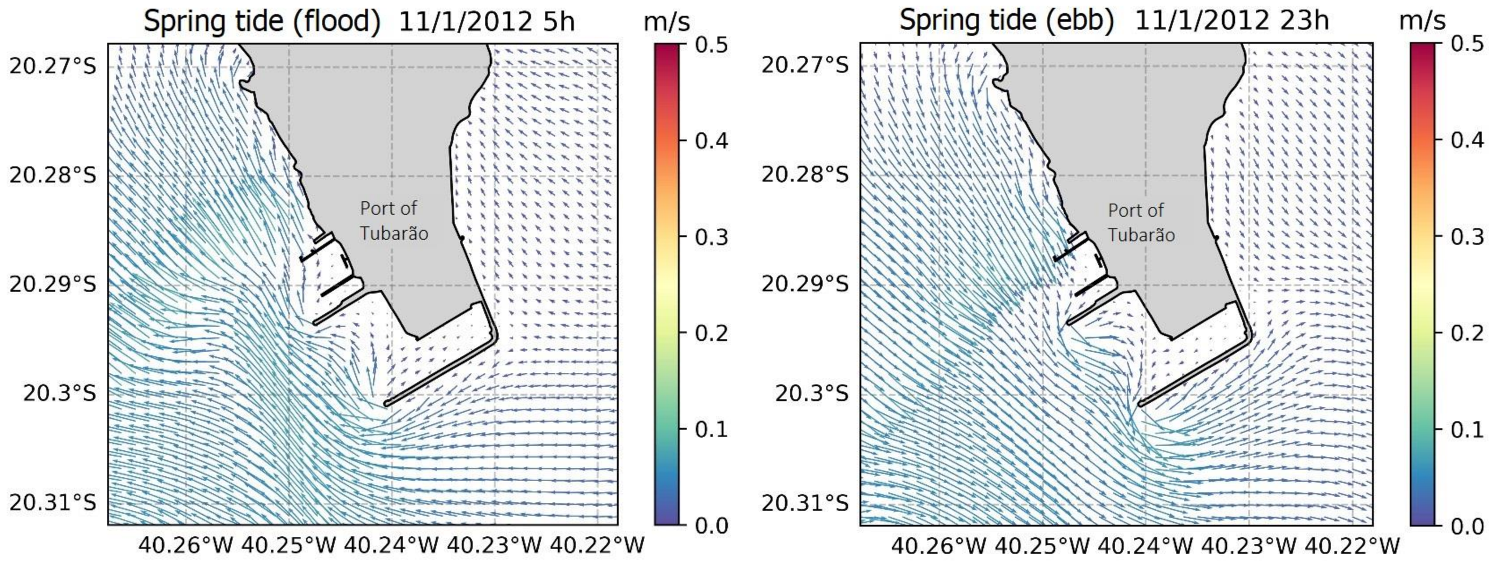


Figure 11: Current map in summer (Port of Tubarão) at a time of spring tide during flood (left panel) and ebb (right panel) periods.

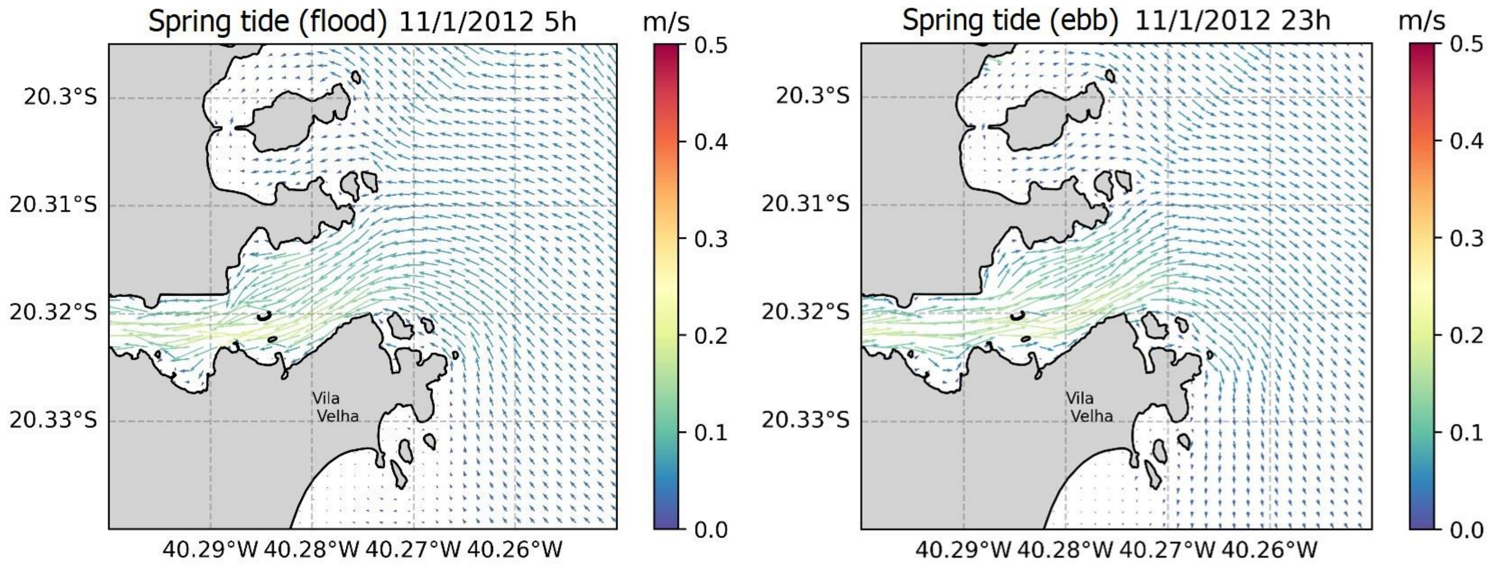


Figure 12: Current map in summer (Vila Velha) at a time of spring tide during flood (left panel) and ebb (right panel) periods.

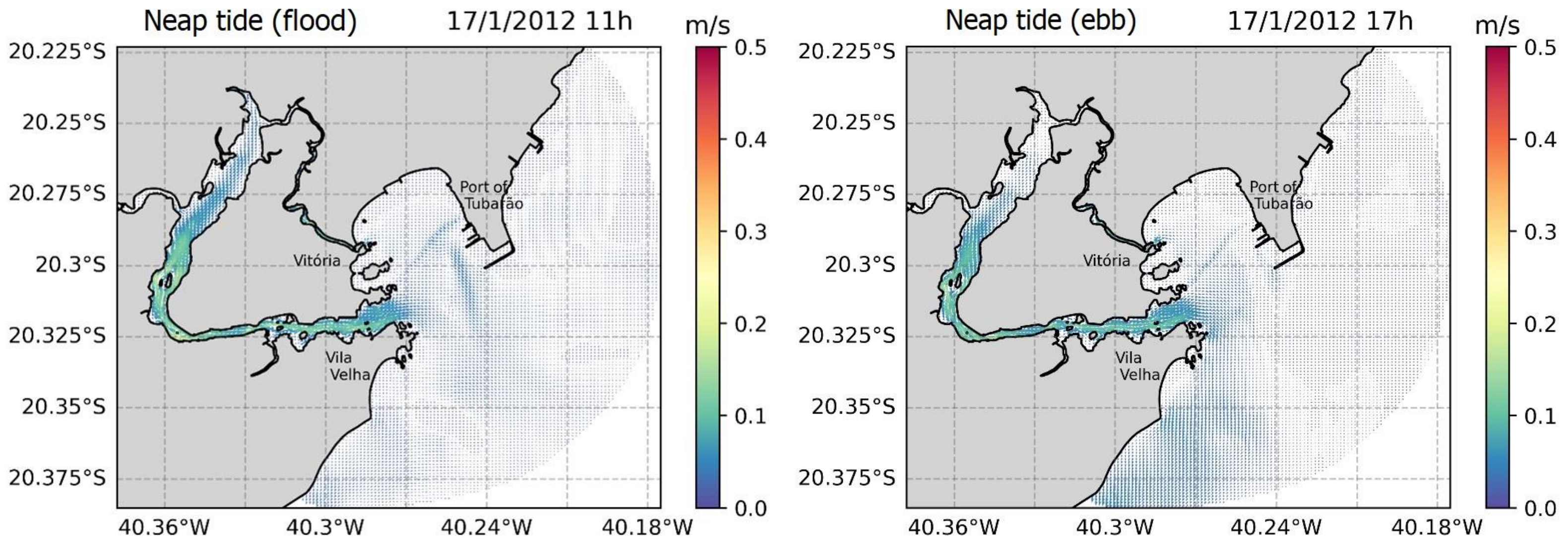


Figure 13: Current map in summer (general domain) at a time of neap tide during flood (left panel) and ebb (right panel) periods.

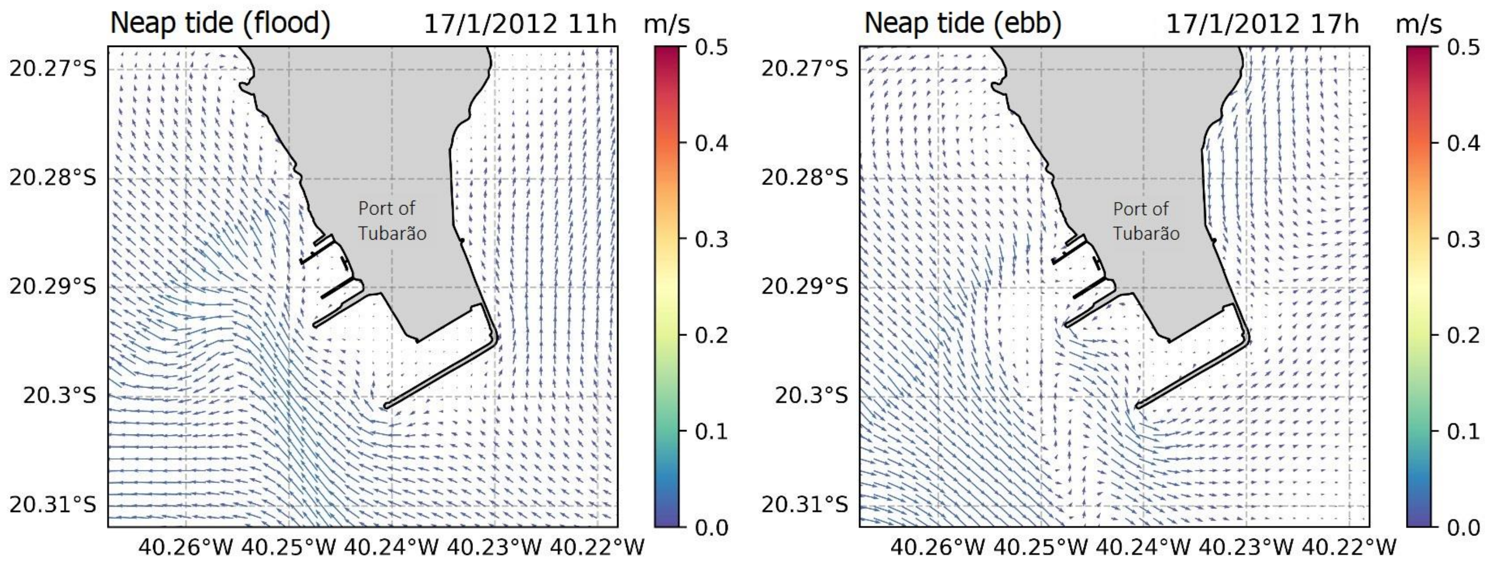


Figure 14: Current map in summer (Port of Tubarão) at a time of neap tide during flood (left panel) and ebb (right panel) periods.

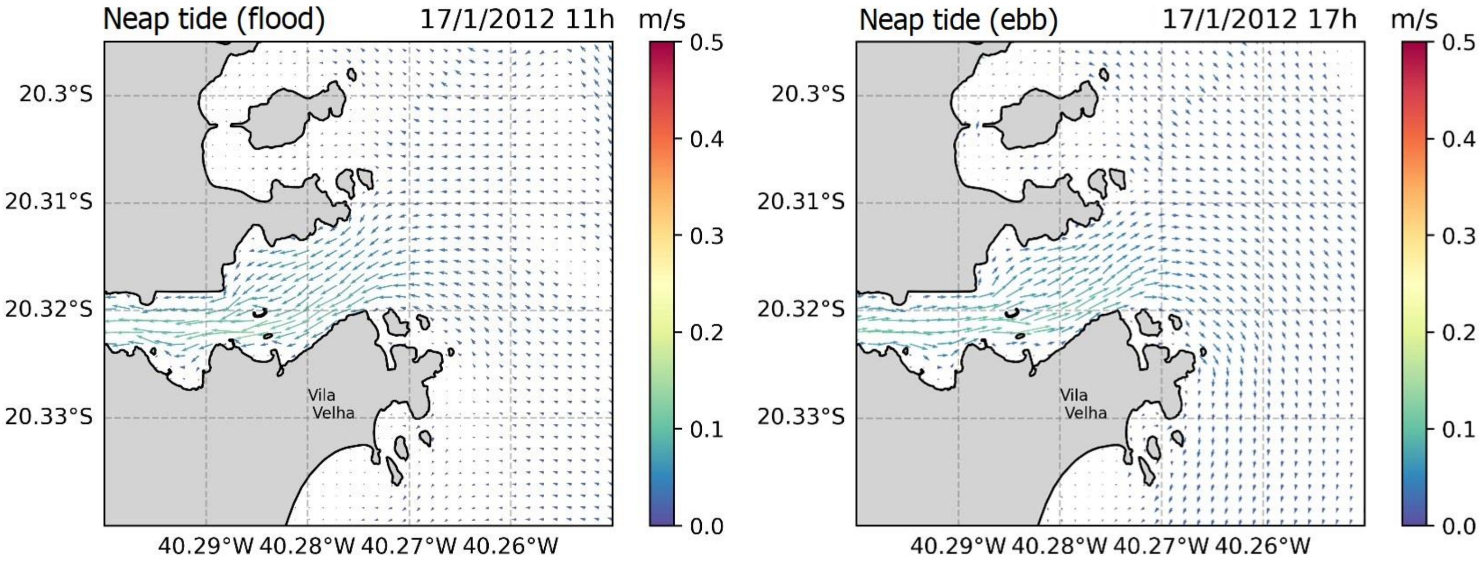


Figure 15: Current map in summer (Vila Velha) at a time of neap tide during flood (left panel) and ebb (right panel) periods.

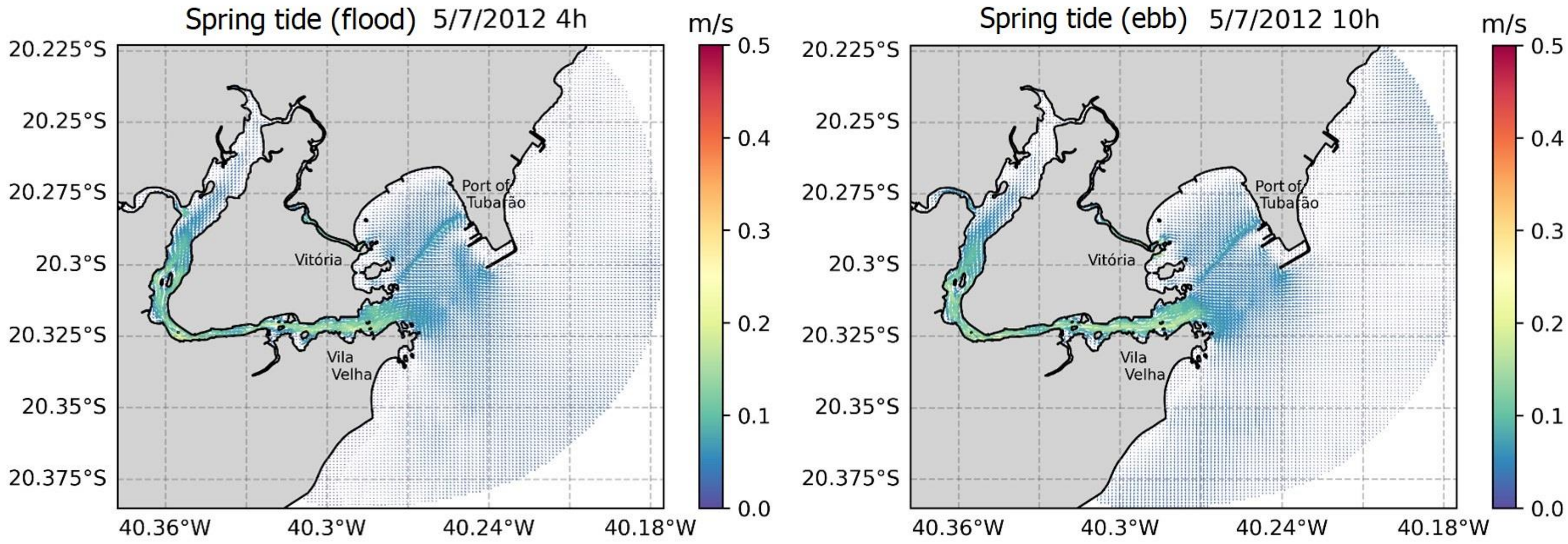


Figure 16: Current map in winter (general domain) at a time of spring tide during flood (left panel) and ebb (right panel) periods.

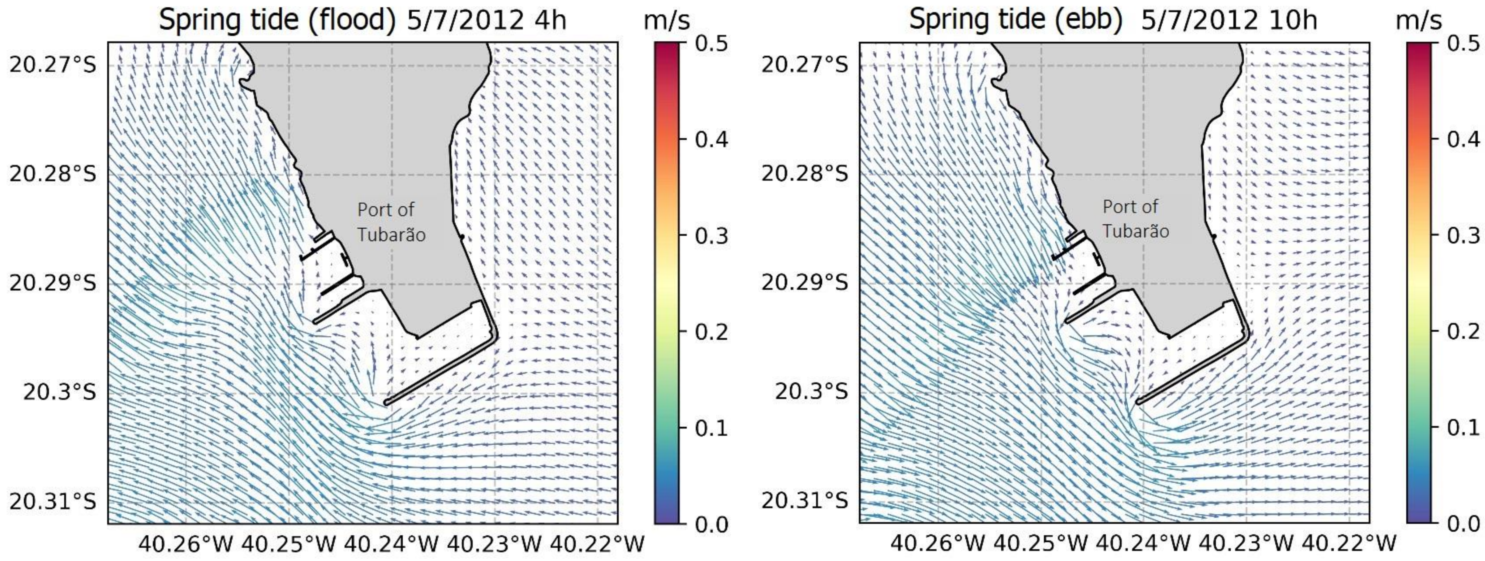


Figure 17: Current map in winter (Port of Tubarão) at a time of spring tide during flood (left panel) and ebb (right panel) periods.

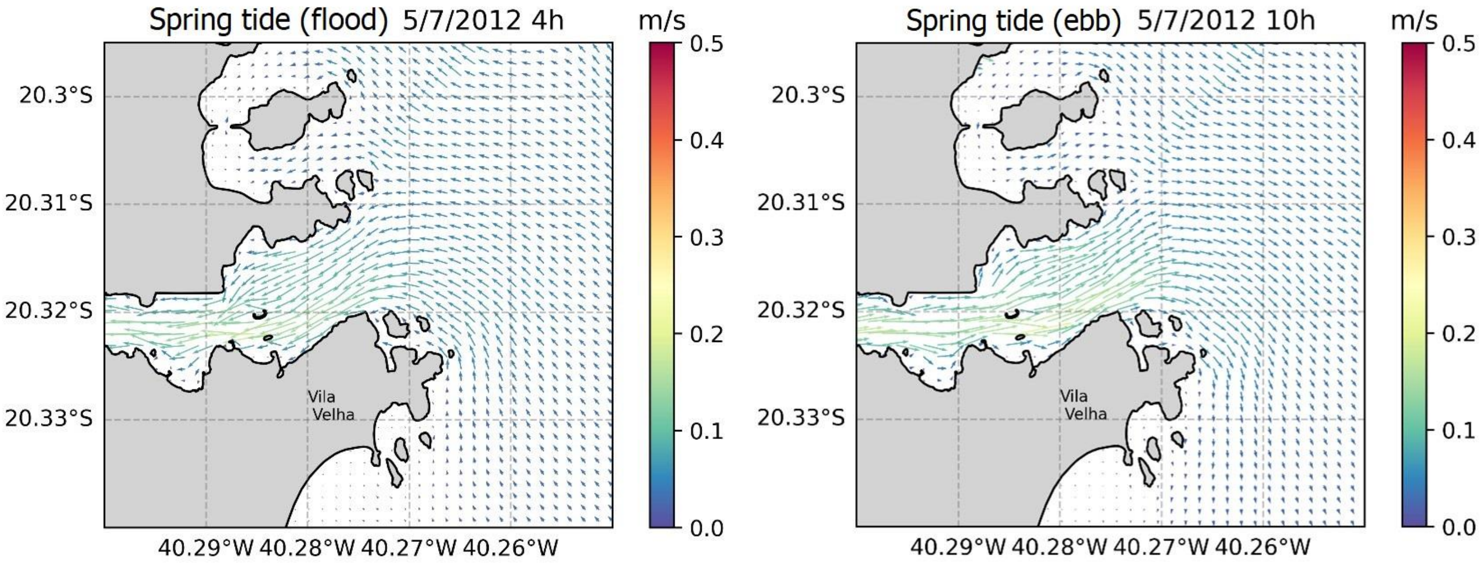


Figure 18: Current map in winter (Vila Velha) at a time of spring tide during flood (left panel) and ebb (right panel) periods.

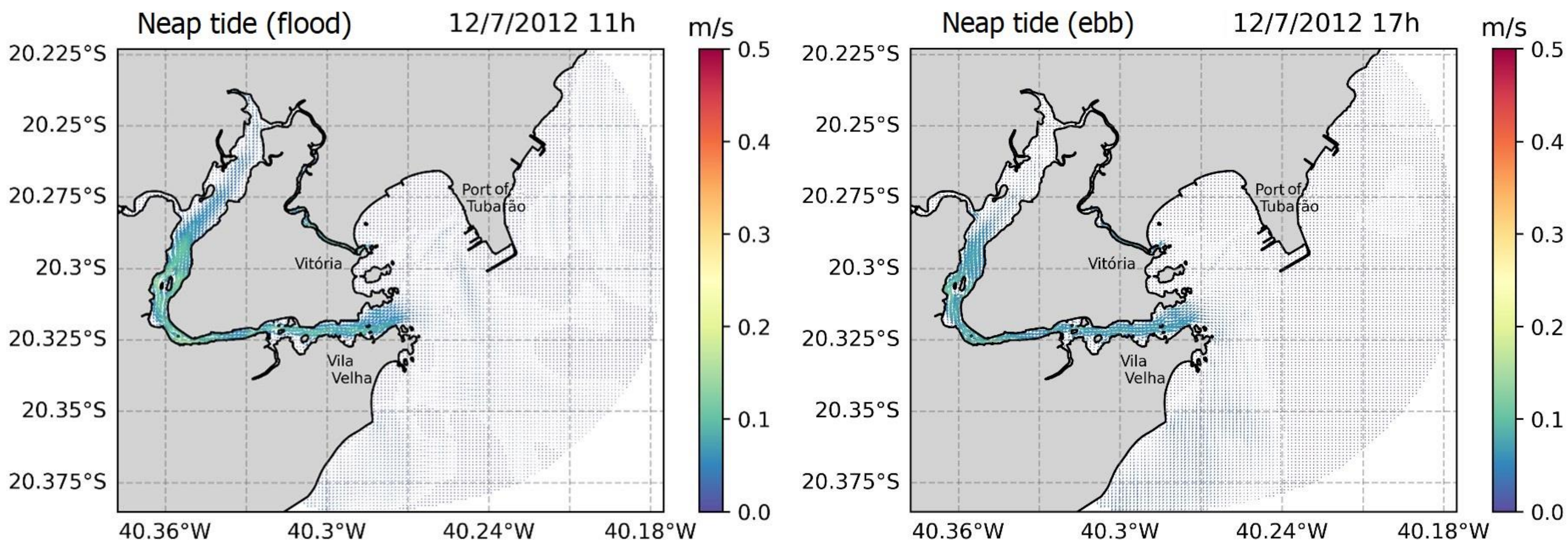


Figure 19: Current map in winter (general domain) at a time of neap tide during flood (left panel) and ebb (right panel) periods.

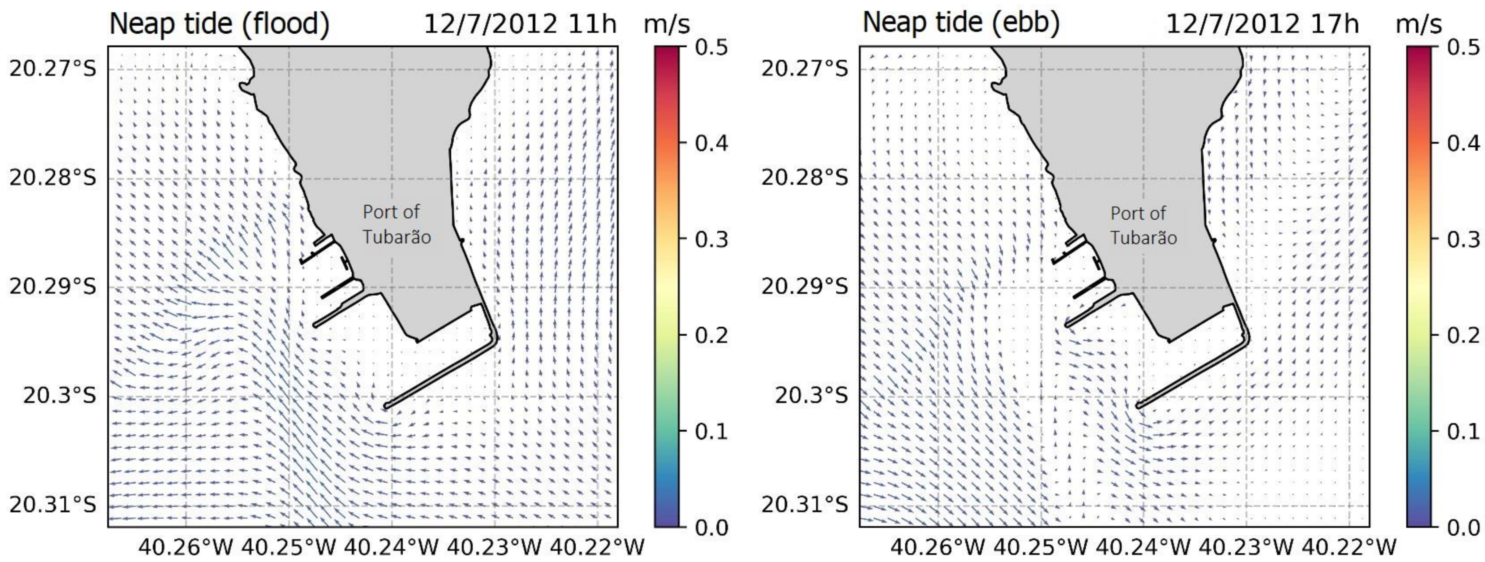


Figure 20: Current map in winter (Port of Tubarão) at a time of neap tide during flood (left panel) and ebb (right panel) periods.

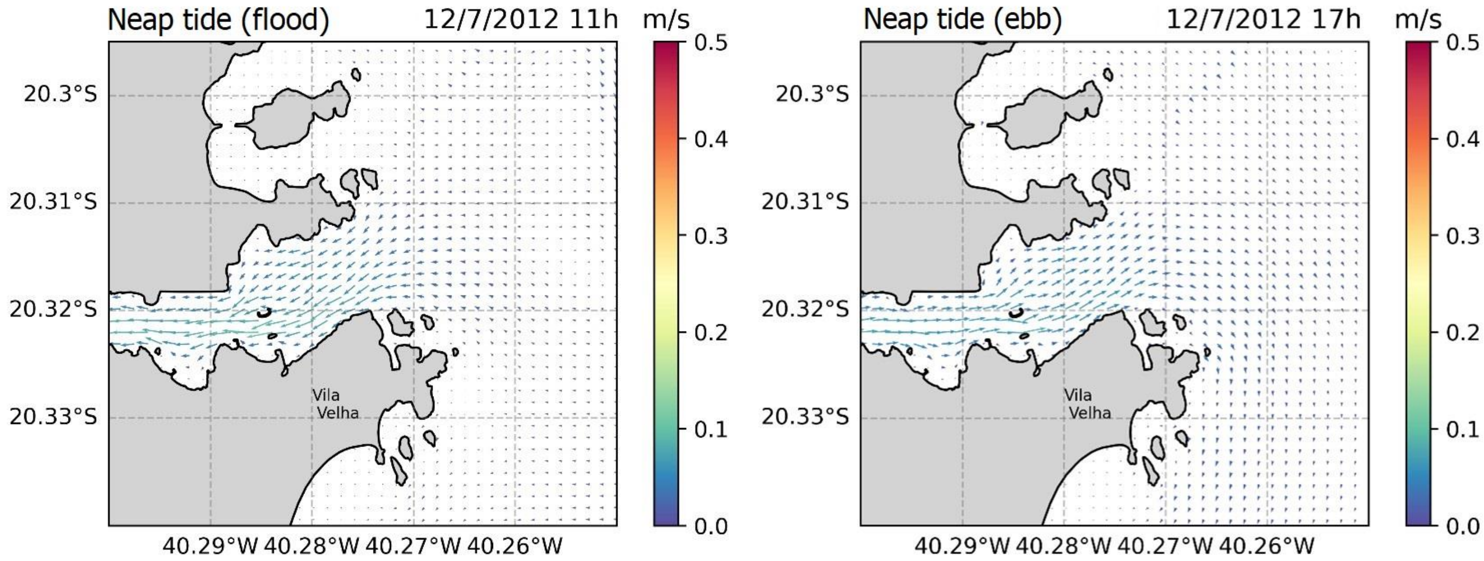


Figure 21: Current map in winter (Vila Velha) at a time of neap tide during flood (left panel) and ebb (right panel) periods.

Below is a time series of current speed, intensity versus direction and basic current statistics (Table 3) for a point located in the Port of Tubarão (Figure 22). It is observed in the current series (Figure 23) the signal of the semidiurnal tide, composed of two high tides and two low tides throughout the day, oscillating between periods of spring tide (higher amplitudes) and neap tide (lower amplitudes).

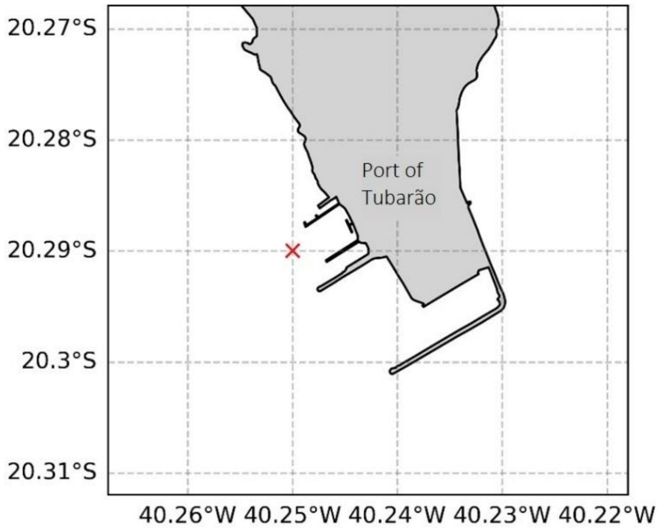


Figure 22: Location of the analysis point (red dot).

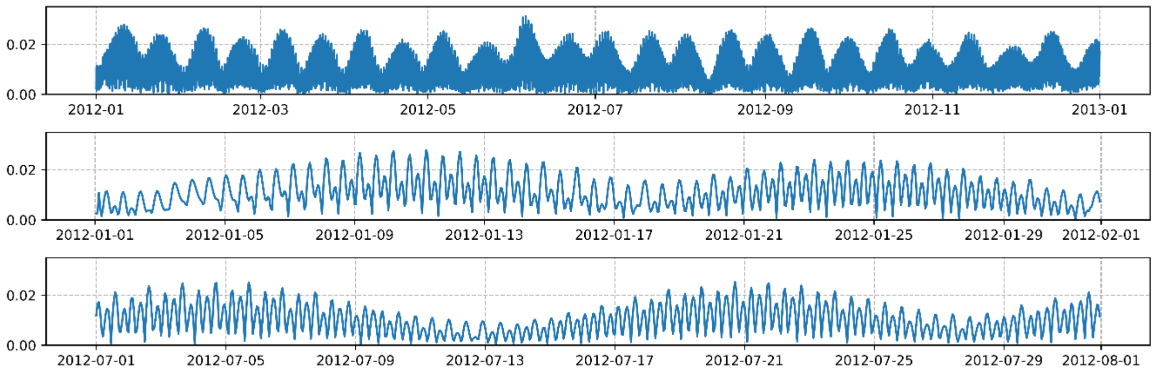


Figure 23: Time series of current velocity at the analysis point for July 2012.

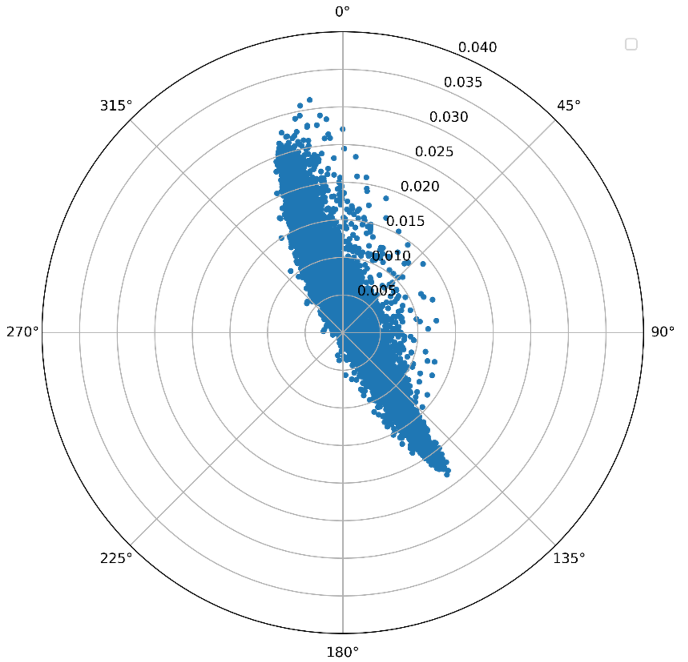


Table 3: Basic statistics of current velocity at the analysis point.

| Vel. Minimum (m/s) | Vel. Average (m/s) | Vel. Maximum (m/s) | Standard Deviation (m/s) |
|---|---|---|---|
| 0 | 0.01 | 0.32 | 0.005 |

# 3. Final Considerations

The hydrodynamic modeling performed for the Port of Tubarão region proved to be a robust and reliable tool for simulating the complex interactions between bathymetry, tides, river flow and winds. Using the Delft3D model, it was possible to accurately capture the physical phenomena that influence local coastal dynamics, providing important support for environmental management and port operations.

The main conclusions include:

→ Coastal circulation patterns: The modeling captured seasonal variations and the effects of semi-diurnal tides, oscillating between spring and neap periods. The hydrodynamic response of the system was dominated by tidal currents, with a secondary influence of winds, especially in extreme weather conditions.

→ Future Applications: The simulation provides a solid basis for future expansions of studies in the area, allowing the assessment of environmental impacts and optimization of port operations.

# 4. Bibliography

AGÊNCIA NACIONAL DE ÁGUAS (ANA), Superintendência de Informações Hidrológicas, Superintendência de Tecnologia e Capacitação, Bacias Hidrográficas do Atlântico Sul – Trecho Leste (RJ, ES, BA, SE), CD nº 4, Sistema Nacional de Informações de Recursos Hídricos (SNIRH).

DELTARES (2021). Delft3D-FLOW User Manual: Simulation of multi-dimensional hydrodynamic flows and transport phenomena, including sediments (version 3.15). Retrieved from https://www.deltares.nl/en/software/delft3d-4-suite/.

HAIDVOGEL, D. B., H. ARANGO, W. P. BUDGELL, B. D. CORNUELLE, E. CURCHISTER, E. DI LORENZO, K. FENNEL, W. R. GEYER, A. J. HERMANN, L. LANEROLLE, J. LEVIN, J. C. McWILLIANS, A. J. MILLER, A. M. MOORE, T. M. POWELL, A. F. SHCHEPETKIN, C. R. SHERWOOD, R. P. SIGNELL, J. C. WARNER, and J. WILKIN, 2008. Ocean forecasting in terrain-following coordinates: Formulation and skill assessment of the Regional Ocean Modeling System. Journal of Computational Physics, 227, 3595-3624.

INSTITUTO NACIONAL DE METEOROLOGIA – INMET. Banco de dados Climatológicas do Brasil 1981-2010. Available at: https://bdmep.inmet.gov.br/.

EGBERT, G. D.; EROFEEVA, S. Y. TPXO9-Atlas: Global Inverse Solution for Barotropic Ocean Tides. Oregon State University, College of Earth, Ocean, and Atmospheric Sciences, 2017.

MARINHA DO BRASIL, Diretoria de Hidrografia e Navegação (DHN). Carta Náutica Portos de Vitória e Tubarão - nº 1410. Rio de Janeiro: DHN, 2020. Available at: https://www.marinha.mil.br/dhn/.